Predicting estimated glomerular filtration rate slope among adult patients with IgA nephropathy in Manitoba

By

Bryce Barr

A Thesis submitted to the Faculty of Graduate and Postdoctoral Studies of

The University of Manitoba

in partial fulfillment of the requirements of the degree of

Master of Science

College of Community and Global Health

Rady Faculty of Health Sciences

University of Manitoba

Winnipeg, Manitoba

Abstract

Background: As the most common cause of glomerulonephritis worldwide, immunoglobulin A nephropathy (IgAN) represents an important cause of kidney failure. Traditional epidemiologic research and clinical trials have focused on the onset of kidney failure, or a profound decrease in the estimated glomerular filtration rate (eGFR), as a primary outcome. Over short follow up, some patients with IgAN may appear low risk, yet recent epidemiologic data suggest that few avoid kidney failure in their lifetime. The rate of decline in eGFR (eGFR slope) over a 2-year period has emerged as a surrogate endpoint in trials, and a method to identify high-risk patients earlier. However, no tools currently exist to predict eGFR slope in patients with IgAN. We aimed to develop and validate a prediction model for 2-year eGFR slope using clinical and pathological data in patients with IgAN.

Methods: Adult patients with biopsy-proven IgAN from 2002 to 2021 were identified from the Manitoba Glomerular Diseases Registry. Registry data were linked to demographic, laboratory, physician claims, and drug dispensing data from the Manitoba Population Research Data Repository. Mixed-effects linear regression models were fit to predict eGFR slope, with random intercept and slope; candidate fixed effect covariates included time, age, sex, index eGFR, proteinuria, the change in proteinuria and eGFR from biopsy to index, the time from nephrology visit to biopsy, prescription of glucocorticoids, the presence of hypertension, presence of diabetes, Oxford S, T, and C scores. Two-way interaction terms with time were tested for proteinuria, index eGFR, glucocorticoid prescription, change in eGFR from biopsy to index, and Oxford S, T, and C scores. Model performance was evaluated using marginal R^2, conditional R^2 and root mean squared error. Predictions were evaluated using calibration and Bland-Altman plots. Internal validation was performed with 10-fold cross validation.

Results: A total of 181 patients were included in the study cohort. The median age was 41 years (interquartile range, IQR 31, 54). Included patients were high risk; median eGFR at biopsy was 58 mL/min/1.73 m^2 (IQR 35-86), while median proteinuria at biopsy was 1.73 g/day (IQR 1.06, 2.95). The "parsimonious model" including fixed effects for time, age, sex, index eGFR and proteinuria, with two-way interaction terms for time with both index eGFR and proteinuria, as well as random intercept and slope for each patient, was selected as the final model. In this model, higher index proteinuria was significantly associated with faster eGFR decline (-1.47 mL/min/1.73 m^2/year, SE 0.66, p = 0.009). Model fit was excellent, with conditional R^2 of 0.95. In the development dataset, predictions were accurate, with 88% of predicted slopes within 1 mL/min/1.73 m^2/year of the observed slope. However, marginal predictions were inaccurate and poorly calibrated; only 11% of marginal predicted slopes were within 1 mL/min/1.73 m^2/year of the observed slope, with calibration slope 1.58 (95% confidence interval 0.71, 2.44). Cross-validation revealed poor generalizability, with marked deterioration in conditional predictions, while marginal predictions were more stable, but remained inaccurate.

Significance: Accurate prediction of eGFR slope could enable earlier risk stratification, facilitating earlier and more personalized treatment decisions in IgAN. Our findings highlight both the promise and the limitations of slope prediction; while models achieved excellent in-sample accuracy, they relied heavily on patient-specific random effects for accuracy, a property that does not generalize well to new patients. The results underscore the challenges of slope prediction in a heterogeneous disease and suggest that larger, more homogeneous cohorts, combined with models capable of estimating random effects using previously observed data, may improve out-of-sample predictive performance.

Table of Contents

Acknowledgements

I would like to thank the members of my committee, Drs. Lisa Lix, Navdeep Tangri, and Mark Canney for their support and mentorship through this process. Dr. Lix has been a dedicated advisor, and a strong supporter of my research career. Dr. Tangri has been instrumental in encouraging me to pursue research, create the Manitoba Glomerular Disease Registry, and complete this degree. Dr. Canney has provided me with feedback and career advice that has been invaluable and has welcomed me into the Canadian GN community. I would also like to acknowledge my clinical mentors Dr. Louis Girard, Dr. Kim Cheema, and Dr. Jeff Ma, who fostered my passion for glomerulonephritis care and whom I now consider great friends. This research would not have been possible without the support of the Section of Nephrology, and in particular my Site Lead Dr. Joe Bueti and Section Head Dr. Barry Cohen, who worked alongside me to ensure this degree could be completed while beginning my clinical career.

I wish to acknowledge my wife, Breanna, whom I cannot thank enough. She has supported me through all my clinical training and encouraged me to pursue my career to the fullest. She has been an incredible partner to me and an amazing mother to our daughters, and I am so thankful to her.

I would like to thank my parents and brother for instilling in me the value of education and how to achieve a goal. My family has been a constant in my life, and a great reminder that although it is important to work hard and do your best, there is life outside of medicine to be experienced and enjoyed.

I also wish to acknowledge the patients living with glomerular diseases in Manitoba, to whom I remain committed to delivering better care tomorrow than we do today.

Disclosure

The authors acknowledge the Manitoba Centre for Health Policy for the use of data contained in the Manitoba Population Research Data Repository under project HIPC 2020/2021–83. The results and conclusions are those of the authors and no official endorsement by the Manitoba Centre for Health Policy, Manitoba Health, or other data providers is intended or should be inferred. Data used in this study are from the Manitoba Population Research Data Repository housed at the Manitoba Centre for Health Policy, University of Manitoba and were derived from data provided by Manitoba Health, Shared Health Services of Manitoba, Shared Health Diagnostic Services of Manitoba, and Vital Statistics.

List of Figures

List of Tables

Introduction

Glomerulonephritis refers to a group of autoimmune kidney diseases characterized by inflammation of the individual filtering units within the kidney called glomeruli. This process leads to compromise of glomerular structure, followed by sclerosis and fibrosis, and ultimately loss of functional kidney tissue. Immunoglobulin A nephropathy (IgAN) is the most common primary glomerulonephritis worldwide, and leads to chronic kidney disease (CKD) and kidney failure in a significant proportion of individuals[1–3]. The diagnosis of IgAN is often prompted by the presence of microscopic or gross (visible) blood in the urine (hematuria), protein in the urine (proteinuria) or reduced kidney function, as measured by serum creatinine and the estimated glomerular filtration rate (eGFR)[4]. These findings are non-specific and can be signs of multiple forms of kidney disease. Once hematuria, proteinuria, or reduced eGFR are discovered, a kidney biopsy is typically performed to confirm the diagnosis of IgAN[5].

Until recently, treatments for IgAN were scarce and were derived from low-quality clinical trial data, focusing on kidney failure as a primary outcome, typically defined as the receipt of maintenance dialysis or kidney transplantation. Although many patients with IgAN have reduced eGFR at the time of diagnosis[6,7], it frequently takes years or decades before patients progress to kidney failure, and achieve a primary outcome in a traditional trial. This hampered the development of novel therapies and led to creation of a task force to explore more proximal clinical trial endpoints[8]. The establishment of surrogate endpoints such as 9-month change in proteinuria, and acceptance of 2-year eGFR slope as a validated surrogate endpoint by the United States Food and Drug Administration (FDA)[9], has facilitated trials with a predetermined timeline that can be met much more quickly than a trial using kidney failure (defined as eGFR <15 mL/min/1.73 m^2 or receipt of kidney replacement therapy) as a primary

outcome. A shorter timeline can reduce the cost to conduct an RCT. The result has been a profound increase in the interest of both independent investigators and pharmaceutical companies in conducting RCTs in this space and has led to regulatory approval for multiple new therapies in the past five years.

Like randomized trials, most of the epidemiologic research to date in IgAN has focused on kidney failure as a primary outcome and identification of patient factors that may influence the outcome[2,3,6,10,11]. From this research, more sophisticated prediction models have been derived and validated for use in IgAN[12], as well as CKD more generally[13]. However, these models use 50% decline in eGFR and kidney failure, respectively, as their predicted outcomes. In contrast to the robust evidence base for predictors of kidney failure, there are relatively few studies that have focused on predictors of 2-year eGFR slope, the outcome now used in most clinical trials in IgAN. Furthermore, epidemiologic research focusing on outcomes such as kidney failure or 50% decline in eGFR may under-predict long-term risk if follow up is short[2,14]; studies examining eGFR slope of participants with IgAN suggest that most patients will experience kidney failure in their lifetime if that slope is extrapolated[6]. Therefore, a tool to predict eGFR slope would be invaluable to identify patients who are likely to experience rapid eGFR decline and should be considered as candidates for therapies to reduce the risk of kidney failure. The aim of the present study was to identify the association of clinical and pathologic characteristics with rate of eGFR decline (i.e., eGFR slope) over two years of follow up in a population-based adult cohort diagnosed with biopsy-proven IgAN.

Literature Review

Glomerulonephritis is a nonspecific term to describe diseases characterized by inflammation of the individual filtering unit of the kidney called the glomerulus[15]. These diseases frequently result from autoimmunity, where the immune system inadvertently targets or causes damage to the kidney. Clinically, GNs typically present with microscopic hematuria and proteinuria, followed by declining kidney function. The treatment for most GN involves therapies that reduce the function of the immune system (immunosuppression)[5]. These treatments vary in their specificity; some therapies non-specifically reduce function of the entire immune system[16,17], while others are highly targeted at a particular part of the immune system[18,19]. Frequently, non-specific therapies have more side effects due to "off-target" actions, while targeted therapies tend to be better tolerated. Better understanding of disease pathogenesis has accelerated efforts to develop new, more targeted treatments, while improvements in risk stratification have facilitated more personalized therapeutic decision-making.

Chronic kidney disease is an irreversible abnormality of kidney structure or a reduction in function lasting at least three months[20]. Kidney function is typically measured using serum creatinine, a highly available blood test to estimate the glomerular filtration rate (eGFR), measured in millilitres per minute (mL/min), normalized to body surface area, measured in square metres (m^2). The stages of CKD are defined by five separate eGFR thresholds. Even earlier identification of CKD is possible when eGFR is still normal, through the identification of proteinuria, and more specifically albuminuria. This is measured via the urine protein-to-creatinine ratio (PCR) or urine albumin-to-creatinine ratio (ACR), respectively.

Glomerulonephritis such as IgAN leads to CKD if untreated through damage to glomeruli, eventually destroying functional kidney tissue[21]. All forms of CKD, including that

caused by IgAN, share similar pathophysiology characterized by hyperfiltration of remaining glomeruli, potentiating tubulointerstitial damage, fibrosis, and further loss of functional kidney tissue, which clinically leads to kidney failure[22]. Kidney failure is a fatal complication of CKD. To sustain life, kidney failure is treated with kidney replacement therapy, which includes dialysis and kidney transplantation. Kidney failure, even when treated with kidney replacement therapy, is associated with significant morbidity and mortality, and significant healthcare utilization and cost[23–25]. Therefore, prevention of CKD and kidney failure is of paramount importance both for patients with IgAN and healthcare systems.

Description and treatment of IgAN

IgAN is a complex autoimmune kidney disease. It is hypothesized the disease occurs because of four pathogenic "hits" that ultimately lead to kidney inflammation, scarring, and loss of function[26]. The inciting event in the development of IgAN is the formation of abnormally glycosylated galactose-deficient immunoglobulin A1 (Gd-IgA1) molecules (Hit 1)[27]; it is hypothesized this takes place in the intestinal mucosa. The immune system subsequently generates immunoglobulin G (IgG) or IgA molecules (also called antibodies) against Gd-IgA1 (Hit 2)[28]. These antibodies bind to form an immune complex (Hit 3), and these immune complexes deposit in the mesangium of the glomerulus (Hit 4)[26,29]. Immune complex deposition gives rise to mesangial cell activation, release of numerous inflammatory mediators (cytokines), and activation of a component of the innate immune system called complement[29]. This leads to progressive inflammation, which damages the glomerulus, destroying functional tissue, leading to CKD and ultimately kidney failure.

IgA nephropathy typically develops between the ages of 20 and 40 years and is more common in males than females[30,31]. Approximately 30 to 50 people are diagnosed with IgA

nephropathy in Manitoba every year, and the number of biopsy-confirmed cases is increasing[7]. The severity of disease is variable. Disease phenotypes include asymptomatic microscopic hematuria, progressive proteinuric CKD, and rapidly progressive glomerulonephritis with kidney failure; the vast majority of patients experience progressive proteinuric CKD[21].

Due to the complexity of the pathophysiology of the four-hit hypothesis, the pathophysiology of CKD, and the lifelong nature of IgAN, treatment strategies in IgA nephropathy focus on supportive therapies as well as medications that treat the immunologic disease. Treatments that mitigate the phenomenon of glomerular hyperfiltration (also called supportive therapy) include inhibitors of the renin-angiotensin system (RAASi) and sodium-glucose cotransporter 2 inhibitors (SGLT2i). Multiple RCTs have demonstrated the efficacy of these therapies in reducing CKD progression among patients with IgAN[32–36]. Kidney Disease: Improving Global Outcomes (KDIGO) is an international group responsible for the production of clinical practice guidelines. The KDIGO 2021 Clinical Practice Guideline for the Management of Glomerular Diseases recommended the prescription of maximally tolerated RAASi to target proteinuria <1 g/day, with potential to consider immunosuppressive therapy in the form of glucocorticoids if proteinuria remained >1 g/day[5]. Use of SGLT2i was not recommended, as evidence for efficacy of SGLT2i in treating CKD due to IgAN has emerged since publication of the KDIGO guidelines[35,37]. In addition, available RCT evidence for use of glucocorticoids in IgAN was equivocal when the guidelines were published[38–42]. Since 2021, multiple RCTs have demonstrated efficacy of glucocorticoids and other forms of immunosuppressive therapy in reducing proteinuria, eGFR decline, and adverse kidney outcomes such as 50% decline in eGFR or kidney failure[19,43–46]. These trials have all used consistent enrolment criteria; patients with consistent proteinuria >1 g/day despite maximal RAASi are eligible, while those with proteinuria

below that threshold are excluded. This criterion is derived from epidemiologic research suggesting a favourable prognosis for individuals below the 1 g/day threshold[2,47,48]. However, newer data suggest that such patients remain at high lifetime risk of kidney failure if the eGFR slope of these participants is extrapolated over several decades[36,49–52]. Treatment to mitigate this risk comes at a cost; trials of immunosuppressive therapy in IgAN have consistently demonstrated an increase in adverse events with immunosuppression as compared to placebo[19,41,43,45,46,53]. Therefore, accurate and comprehensive risk stratification is vital for informing therapeutic decision-making in the clinic, as well as in designing clinical trials.

Surrogate outcomes in IgA nephropathy

The development of large, high-quality clinical trials in IgAN has been difficult, owing to the relative rarity of the disease, and the long period of time typically required for the development of outcomes such as doubling of serum creatinine, 40-50% reduction in eGFR, or kidney failure (defined as eGFR <15 mL/min/1.73 m^2 or receipt of kidney replacement therapy). These outcomes lead to expensive trials requiring long-term follow-up and necessitate enrolment of only the highest risk patients to detect treatment effects on the clinical outcome. In addition, as previously discussed, such outcomes may not identify therapies which may be efficacious for individuals early in their disease course, who would not be expected to experience a 50% decline in eGFR or kidney failure during a trial. Until recently, such outcomes were required by regulatory agencies to prove efficacy of new therapies prior to regulatory approval. The US FDA has created a pathway for accelerated approval of novel therapies for diseases considered life-threatening through trials using validated surrogate endpoints[8]. A surrogate endpoint is a substitute for a direct measure of how a patient feels, functions, or survives, that predicts the direct measure[54]. Proteinuria reduction is highly associated with a reduction in the risk of kidney

failure, and as a result is accepted by the FDA as a reasonable surrogate endpoint, though they require a confirmatory trial using a validated surrogate endpoint, or an accepted clinical endpoint (such as kidney failure). Difference in eGFR slope between treatment groups has been validated as a surrogate endpoint for kidney failure in CKD trials, as well as trials in IgAN[55].

Supportive therapies used to treat both CKD and IgAN may exert acute effects on eGFR that differ from their long-term effects on eGFR. This raises the concern that simply using the index and final eGFR measurements to compute slope may ignore the time-varying effect of a treatment on eGFR slope[56,57]. Several RCTs to examine the efficacy of RAASi and SGLT2i in CKD have demonstrated acute reductions in eGFR followed by more gradual eGFR decline with these therapies compared to placebo. Measuring eGFR slope from some time after randomization (typically 3 months) to the end of follow up (typically 2-3 years) is chronic slope; this metric ignores the acute effect of therapies on eGFR[9]. The outcome that includes both the acute (typically randomization to 3 months) and chronic eGFR slope is total slope (Figure 1).

A recent meta-analysis found that the treatment effects of supportive therapies on total slope were more strongly associated with treatment effects on the clinical endpoint of doubling of serum creatinine, eGFR <15 mL/min/1.73 m^2, or kidney failure with replacement therapy than chronic slope[58]. Further, for trials of medications that acutely lower eGFR, the US FDA recommends using total slope instead of chronic slope, because total slope represents a more conservative surrogate endpoint and is therefore at lower risk of a type I error in inferential analyses[9]. It is now common in IgAN clinical trial design to employ a 9-month proteinuria endpoint to gain provisional regulatory approval, followed by a confirmatory 2-year eGFR slope endpoint to gain final approval (Figure 2).

Risk stratification of patients with IgAN

In Manitoba, a striking 45% of patients diagnosed with IgAN develop kidney failure after a median of 6 years of follow up[7]. Owing to the variability in disease presentation, identifying patient risk factors associated with disease progression and kidney failure is of critical importance in selecting patients for aggressive treatment and/or enrolment in clinical trials. Individuals at low risk of progression are unlikely to benefit from immunosuppression and may be less likely to respond to therapy. Conversely, for those at high risk of progression, the benefits of aggressive therapy and immunosuppression may outweigh the risk of side effects or toxicity of treatment[59].

Multiple factors influence the risk of developing kidney failure, including clinical factors such as elevated blood pressure (hypertension), proteinuria, decreased eGFR, and ethnicity, as well as pathologic features on kidney biopsy, such as inflammation and fibrosis, summarized by the Oxford classification. Blood pressure at the time of kidney biopsy is associated with progressive kidney disease and kidney failure[47,60–64]. In addition, uncontrolled hypertension over time is also associated with the development of kidney failure[2,61,64,65].

Proteinuria is one of the most consistent and potent predictors of kidney failure in patients with IgAN, but as proteinuria is a continuous exposure that is modified by treatment, how proteinuria is quantified is critical. Proteinuria at diagnosis is associated with kidney failure[48,60,62–64]. Both immunosuppressive therapy and supportive therapy reduce proteinuria[36,43,66]. In addition, individuals who have elevated proteinuria at diagnosis who achieve substantial reductions in proteinuria have a more favourable prognosis[2], with increasing duration of proteinuria reduction further reducing the risk of progression[67]. Finally, proteinuria over time has been demonstrated to explain more of the variability in outcome than proteinuria at

baseline[10], supporting the use of longitudinal data to evaluate the impact of proteinuria. Multiple different metrics have been proposed to account for this time-dependence. The most frequently used is time-averaged proteinuria, where all proteinuria values over the follow up period are averaged. Time-averaged proteinuria >1 gram per day (g/d) has been associated with more frequent development of kidney failure, while time-averaged proteinuria < 1g/d has been associated with a good outcome in seminal epidemiologic research arising from the Toronto Glomerulonephritis Registry[2] and other cohort studies[47,68]. Indeed, this has prompted the use of sustained proteinuria >1 g/d despite treatment with RAASi as a clinical trial enrolment criterion. Despite widespread acceptance, this threshold has been recently questioned, as multiple observational cohort studies have identified high risk of progression even among individuals with time-averaged proteinuria <1 g/d[6,49,51,69]. Furthermore, the use of time-averaged proteinuria as a metric has been questioned for multiple reasons. First, the use of a future laboratory value to predict an individual patient's outcome is flawed because that value is unknown at the time of the prediction. Second, at a given timepoint in clinical care, one does not have all the values to calculate time-averaged proteinuria (as presumably, follow-up has not ended), which limits its use in a clinical prediction model. In contrast, using time-varying proteinuria has been identified as optimal, accounting for the greatest proportion of the variability in outcome, without the methodologic concerns raised by time-averaged proteinuria[10]. Studies using time-varying proteinuria have typically shown a graded association, with increasing time-varying proteinuria leading to increased risk of kidney failure, without a threshold effect[8]. An additional time-invariant metric is the change in proteinuria over a given time period prior to the index date (typically 9 months), which predicted future differences in eGFR slope in a meta-analysis of randomized trials in IgAN[55].

While reduced eGFR has been consistently associated with a faster time to kidney failure[48,60–62,70], it is possible this association is simply a product of identifying patients who are further along their trajectory toward kidney failure and will therefore achieve it faster in a time-to-event model. A study from the Toronto Glomerulonephritis Registry identified no association between baseline eGFR and annualized decline in creatinine clearance[64]. However, multiple subsequent studies have confirmed the relationship between low eGFR and a steeper decline in eGFR[6,61], supporting its role as a predictor of both kidney failure, as well as more rapid eGFR decline.

There is substantial variability in the genetic risk, prevalence, clinical presentation, and risk of progression in IgAN among different ethnic groups. IgAN is more common among individuals with East Asian ancestry compared to white individuals[71]. While some of the increase in frequency may be explained by the presence of screening programs in East Asian countries[72], genome-wide association studies (GWAS) have demonstrated that genetic risk alleles associated with the development of IgAN are more common among Chinese than white patients[73]. Asian patients with IgAN appear to experience more aggressive disease. A study from the Toronto Glomerulonephritis Registry identified that patients of Asian ancestry with IgAN experience more rapid progression to kidney failure than non-Asian patients despite the observation that Asian patients were more frequently treated with RAASi and steroids and had better blood-pressure control[74]. Possible reasons for these differences include higher levels of Gd-IgA1 among Asians than non-Asians[75], and a more inflammatory phenotype in Asian patients[76].

Pathology features impacting risk of kidney failure and eGFR decline

Multiple early attempts were made to create pathology classes or scoring systems to describe and prognosticate biopsy findings in IgA nephropathy[77,78]. These original classification

systems were validated in small cohorts, suffered from issues with reproducibility among pathologists, and provided questionable prognostic value when added to clinical risk factors[79]. The Oxford classification, also called the MEST score, was initially developed and validated in 2008 to overcome issues with reproducibility, and to add prognostic value to clinical features[80,81]. The Oxford classification describes the presence or absence of mesangial hypercellularity (M, scored 0 or 1), endocapillary hypercellularity (E, scored 0 or 1), segmental sclerosis (S, scored 0 or 1), and tubular atrophy and interstitial fibrosis (T, scored 0, 1, or 2). Some of these lesions represent findings of inflammation in different glomerular compartments (M, E), while others represent chronic scarring (S, T). In the initial cohort, M, S, and T lesions were found to associate with the outcome of kidney failure, while E lesions were highly associated with treatment with glucocorticoids. Further to this, the prescription of glucocorticoids was associated with a reduced risk of kidney failure among those with an E lesion, thus justifying its inclusion in the initial score. The largest validation cohort of the Oxford classification, the VALIGA study[69], also did not find an association between endocapillary hypercellularity and kidney failure. Similarly, the presence of M, S, and T lesions were all significantly associated with greater eGFR decline (eGFR slope) on univariate analysis, while the E lesion was not. However, among individuals with proteinuria <0.5 g/d, who ordinarily would be excluded from clinical trials, the presence of an E lesion was associated with both the development of an increase in proteinuria to > 1g/d and >2 g/d, as well as more pronounced eGFR decline[69]. Finally, the impact of pathology lesions on kidney failure may be modified by prescribing immunosuppression/glucocorticoids. The VALIGA cohort study demonstrated that the predictive value of the MEST score was reduced among individuals who received immunosuppression[69], while additional analysis demonstrated that the benefit of glucocorticoid prescription on reducing eGFR decline was

greater among individuals with M, E, S, and T lesions, as compared to those without those lesions[82]. As a result, all four of the lesions have been included in the scoring system to inform prognosis, and possibly likelihood of response to immunosuppression, though the latter remains unproven. In fact, in the TESTING trial evaluating the efficacy of glucocorticoids in IgAN, the investigators stratified randomization on the presence or absence of the E1 lesion; there was no evidence of effect modification by baseline histology[43]. An additional inflammatory lesion, the presence of glomerular crescents, was not found to be predictive of outcome in multiple early cohort studies including the original Oxford cohort[83,84]. Subsequent studies, including a pooled cohort of over 3000 patients that included individuals with the most severe kidney dysfunction (eGFR <30 mL/min per 1.73m^2) who were excluded from the original Oxford cohort, did find an association between crescents and eGFR decline, as well as kidney failure[85,86]. Like other lesions in the Oxford classification, the impact of crescents on eGFR decline and outcome was confounded by the prescription of immunosuppression[85], and based upon these findings, an expansion of the MEST score to include crescents (C, scored 0, 1, or 2), now called MEST-C, was proposed and adopted[87]. The details of the Oxford classification are presented in Supplementary Table 6.

While the Oxford classification is informative for prognosis and the likelihood of treatment response, there are limitations. A 2023 systematic review identified moderate or poor reproducibility in reporting of the classification system[88]. Additionally, the use of a binary indicator for the E lesion does not account for whether the endocapillary hypercellularity is mild or severe. Attempts to quantify the degree of endocapillary hypercellularity using immunohistochemistry (IHC) techniques have improved the ability to identify those with an E lesion versus those without, and may assist in identifying immunosuppressive therapy response

and non-response[89]. However, IHC is not universally performed, and the Oxford (MEST-C) classification remains the dominant pathologic scoring system used in IgAN for predicting kidney failure risk. Despite this utility, pathology findings are not currently part of clinical trial enrolment criteria, and in many trials, patients have not been biopsied for many years prior to randomization[35,90]. Using the original biopsy findings as enrolment criteria may introduce misclassification, as it is possible that the pathological findings that may have been observed if a kidney biopsy had been repeated at the time of randomization would be substantially different than those observed at the time of the original biopsy.

Combining clinical and pathologic data to quantify risk in IgA nephropathy

Accurately predicting the risk of kidney failure is key to identifying patients in whom the risks of immunosuppression are outweighed by the benefits of preventing progressive kidney disease, as well as those at low risk of disease progression, where the risks of immunosuppression may not be worth the potential benefits. Attempts to quantify risk include the Kidney Failure Risk Equation (KFRE)[13], which has been validated in CKD cohorts, and the International IgAN Prediction Tool[12], developed and validated in cohorts of patients with IgAN. The KFRE predicts the probability of kidney failure at 2- and 5-year time horizons, using the clinical variables age, sex, eGFR, and urine albumin-to-creatinine ratio (ACR). The Prediction Tool predicts the probability of a 50% decline in eGFR or kidney failure at a time horizon selected by the clinician, using a combination of clinical risk factors, including eGFR, 24-hour urine protein, blood pressure, age, ethnicity, prescription of RAASi and immunosuppression, as well as the individual components of the MEST score. While these tools are highly useful, a 50% decline in eGFR or kidney failure is an event that may take years to develop, and as a result, the Prediction Tool and the KFRE may not capture the long-term or lifetime risk of a patient early in

their disease course. Recent data suggest that, of patients with time-averaged proteinuria <1 g/d, and even <0.5 g/d, extrapolating their eGFR slope over decades would indicate that few patients with IgAN avoid kidney failure in their lifetime[6]. Therefore, models to predict eGFR slope may assist in identifying patients with high lifetime kidney failure risk, even if short-term (i.e 5-year) risk is low. In addition, given recent changes in clinical trial design, identifying patients at risk of rapid eGFR decline who may be under-recognized by a clinical outcome has implications in selecting patients for trial enrolment.

Summary

Most epidemiologic research confirms a strong association between the clinical risk factors of baseline eGFR, proteinuria, ethnicity, and blood pressure with the outcome of kidney failure. The Oxford classification also aids in stratifying the risk of kidney failure. The International IgA Nephropathy Prediction Tool combines these clinical and pathological risk factors to predict a 50% decline in eGFR or kidney failure. Prediction of eGFR slope for an individual patient may provide more proximal risk stratification, especially for individuals with preserved eGFR at baseline.

Research Purpose, Objectives, Questions, and Hypotheses

Research purpose and objectives

The research purpose was to accurately predict 2-year eGFR slope among patients with biopsy-proven IgA nephropathy. The objectives were to:

1. Develop a prediction model for 2-year eGFR slope in IgA nephropathy using clinical and pathological data, and
2. Internally validate the prediction model for 2-year eGFR slope.

Research questions

1. Among adults with IgAN, can baseline eGFR, proteinuria, and Oxford classification predict 2-year eGFR slope?
2. Can a model that includes these covariates result in accurate predictions of 2-year eGFR slope?

Hypothesis

1. Baseline eGFR, proteinuria, and Oxford classification at one year post-biopsy will accurately predict 2-year eGFR slope.

Methods

Study design and data sources

We conducted a population-based, retrospective cohort study of patients with IgA nephropathy captured in the Manitoba Glomerular Diseases Registry. This Registry includes all patients aged 18 years or older who have undergone a native (i.e., not transplant) kidney biopsy as a part of routine clinical care in Manitoba[7]. Kidney biopsies are interpreted by provincial pathologists with specialty training in kidney pathology, which in concert with clinical data results in a diagnosis. All patients identified as having a glomerular disease such as IgAN are included in the Registry.

The Registry data are linkable to clinical and administrative data in the Population Research Data Repository housed in the Manitoba Centre for Health Policy (MCHP) using a unique scrambled personal health identification number (PHIN)[91]. The pathology registry housed within the Manitoba Glomerular Diseases Registry (Supplementary Table 1) were linked to the following databases within the MCHP (see also Supplementary Table 2):

1. Shared Health Diagnostic Services of Manitoba (SHDS): to access laboratory (blood and urine) data.
2. Manitoba Health Insurance Registry: to access information about patient demographics, health insurance coverage, and all-cause death (i.e., loss of health insurance coverage due to death).
3. Medical Claims/Medical Services: to access information on healthcare utilization, in particular outpatient physician visits; these visit records contain billing codes for dialysis and kidney transplantation.
4. Drug Program Information Network (DPIN): to access information on prescription drug use, in particular RAASi and glucocorticoid use.

Study population

Participants were eligible for inclusion if they underwent a kidney biopsy from January 1, 2002 to December 31, 2020. Participants with a diagnosis other than IgA nephropathy were excluded. Participants who were under age 18 years on the date of kidney biopsy, and who could not be linked to the Manitoba Health Insurance Registry were excluded; the latter was determined if the sex of a participant could not be identified. Participants with a diagnosis of IgA vasculitis based upon the clinical history provided at the time of the kidney biopsy, which was adjudicated at the time the registry was created based on the clinical history in the kidney biopsy report, were excluded. The date of cohort entry was the date of the kidney biopsy. Individuals who reached kidney failure within one year of cohort entry were excluded, and kidney failure was defined as the receipt of dialysis or kidney transplantation during the follow up period, identified using physician billing codes for dialysis and transplantation (Supplementary Table 3). Individuals with less than three years (1095 days) of follow up from cohort entry, or less than

three eGFR measurements over that follow up, were excluded; the latter criterion amended the statistical analysis plan after it was observed that individuals with two measurements frequently had extremely discordant measurements over a short term period (e.g eGFR 30 mL/min/1.73 m^2 followed by eGFR 80 mL/min/1.73 m^2 10 days later) with no other measurement, risking instability of slope estimates in the prediction model if such cases were included. The participant flow chart with inclusion and exclusion criteria is provided in Figure 1.

The index date was 365 days following the kidney biopsy. The end of follow-up was 730 days following the index date (1095 days after cohort entry), or the development of kidney failure. Individuals were censored if they died, migrated out of the province, lost provincial health coverage, or reached the study end date (December 31, 2023). The study design is summarized in Figure 3.

Covariate definitions

The covariates, their level of measurement, and their data sources are summarized in Supplementary Table 5. Age at index date was obtained from the date of birth and the date of the kidney biopsy, plus one year. Sex (male/female), defined at index date, was obtained from the Manitoba Health Insurance Registry data. The cohort entry eGFR was the closest eGFR to the kidney biopsy, and was calculated from serum creatinine measurements, using the CKD-EPI 2021 equation[92]. Values up to 90 days prior to, or 90 days after the kidney biopsy were considered. If no eGFR measurement was available in that period, the cohort entry eGFR was defined as missing. Cohort entry proteinuria was the closest 24-hour urine protein measurement, in grams per day (g/day) to the kidney biopsy. Values as early as 90 days prior to, and 90 days after the kidney biopsy were considered. When only spot urine protein-to-creatinine ratio (PCR) is available, it was converted to a 24-hour measurement using the method described by Hogan[93].

When only urine albumin-to-creatinine ratio (ACR) was available, the value was converted to PCR using a factor of 1.37[94,95], followed by a conversion to the 24-hour value. If no urine protein measurement was available within 90 days of biopsy, the cohort entry proteinuria was considered missing.

Time to kidney biopsy was measured in days, from the first nephrology contact to kidney biopsy, with first nephrology contact identified using physician billing codes arising from billing bloc 016 (Supplementary Table 3). The time from renal abnormality to biopsy was measured in days, from the first instance of urine protein >0.5 g/day or eGFR <60 mL/min/1.73 m^2 to kidney biopsy. The index eGFR was calculated as the eGFR measurement most proximal to, but not exceeding the index date. Values up to 120 days prior to the index date were considered. The index proteinuria was calculated as the 24-hour urine measurement most proximal to, but not exceeding the index date. Values up to 120 days prior to the index date were considered. When only spot urine PCR or ACR was available, conversion to 24-hour values was performed as described above. The change in proteinuria was assessed in three ways: 1) As an absolute change, calculated as the absolute difference between the index proteinuria and cohort entry proteinuria; 2) As a relative change, calculated as the ratio of index proteinuria to cohort entry proteinuria; and 3) As a qualitative indicator with three categories: stable (<30% reduction or increase from cohort entry proteinuria), improving (>30% reduction from cohort entry), worsening (>30% increase from cohort entry).

Treatment with corticosteroids, or renin-angiotensin system inhibitors (RAASi) were binary covariates, and defined as a minimum 30-day prescription for eligible medications under the Anatomic Therapeutic Chemical system[96] between the date of biopsy and the index date (Supplementary Table 4). The presence/absence of hypertension or diabetes were binary

covariates (present/absent), and obtained from Canadian Chronic Disease Surveillance System definitions[97], which employ International Classification of Diseases (ICD) version 9 and 10 codes (Supplementary Table 3).

The Oxford classification was captured (Supplementary Table 6). As the Oxford classification was only reported for biopsies performed from 2016 onward, categorical variables were created for Oxford S, Oxford T and Oxford C using the raw pathology data within the registry. These variables were defined using the same criteria as the Oxford classification. Due to a low number of patients with >25% crescents on pathology (i.e., C2), the Oxford C lesion was considered binary, with >0% crescents being assigned a value of C1.

Outcome

The primary outcome was the estimated 2-year eGFR slope, as measured in mL/min/1.73 m2/year. The slope was the annualized linear rate of decline in eGFR from the index date to the last day of follow up.

Statistical analysis

Descriptive statistics

The cohort was described using median and interquartile range (IQR) for continuous variables, and percentages for categorical variables. Descriptive statistics were reported for the overall cohort, as well as stratified by: era (2002 to 2009, 2010 to 2015, 2016 to 2021; Table 1), sex (Table 2), those who achieve kidney failure versus those who do not (Table 3), baseline CKD stage (eGFR >90, eGFR 60 to 90, eGFR 30-60, eGFR 15-30; Table 4), location of residence (Winnipeg, non-Winnipeg; Table 5), and socioeconomic status at cohort entry (Table 6).

Covariate distributions

Histograms were used to assess the distribution of continuous covariates, as well as boxplots to investigate potential outliers. Outliers were assessed for the possibility of a clerical error (i.e., age of 130 years) but were otherwise not removed. Continuous covariates were mean-centred. Frequency tables were used to examine the distribution of categorical variables. Histograms were used to plot the distribution of the number of eGFR measurements and urine protein measurements per participant. Potential associations between predictors and the number of measurements were assessed using a Spearman correlation matrix.

Missing data

For non-laboratory covariates, there were no missing values. The prevalence of missing values for cohort entry proteinuria, cohort entry eGFR, index proteinuria, and index eGFR was >10%; therefore, pattern analysis was performed to compare covariate distributions across different patterns of missingness, and to explore whether missingness may be related to observed patient factors. This process began with a frequency table to describe the proportion of missing values for each covariate, both for the whole cohort, and stratified by era (2002 to 2009, 2010 to 2015, 2016 to 2021), sex, and CKD stage at diagnosis (eGFR >90, eGFR 60 to 90, eGFR 30-60, eGFR 15-30). Missingness was then also displayed graphically to look for potential patterns; laboratory values were often missing together. Little's MCAR test, a chi-square test that tests whether the pattern of missing data depends on observed data[98], was performed and did not support MCAR. Associations between covariates and missingness were then assessed visually. Missing laboratory values appeared more common among patients from era 1 and era 3.

Five imputed datasets were then created by multiple imputation by chained equations[99]. The candidate predictors in Supplementary Table 5 were used as covariates in the imputation

model, as well as the era of diagnosis. To confirm that the imputation model was well specified, the distribution of continuous covariates in the imputed datasets was compared to the complete case dataset using density plots, and was found to be acceptable. The density plots are found in Figure 2a and 2b. We compared models fit to the multiply imputed datasets with models fit to complete cases. The fixed effect estimates from imputed-data models differed substantially from those in complete case models, indicating sensitivity of estimates to imputation assumptions. Models fit to multiple imputed datasets consistently showed inferior performance, with lower marginal and conditional R^2, higher root mean squared error, poorer calibration, and worse agreement on Bland-Altman analysis. Accordingly, complete cases were used for the primary analysis.

Model building

The following variables were considered for inclusion in the multivariable prediction model: age, sex, index proteinuria, delta-proteinuria, time to biopsy, index eGFR, delta-eGFR, treatment with glucocorticoids between biopsy and the index date, treatment with RAASi between biopsy and the index date, hypertension diagnosis, diabetes diagnosis, the presence of an Oxford M lesion, E lesion, S lesion, T lesion, and C lesion. Variable selection began by estimating correlation matrices for the candidate predictors, using the Spearman correlation for continuous and normally distributed predictors and the tetrachoric correlation for binary variables. The use of RAASi between biopsy and index was highly prevalent and therefore not included as a covariate. The delta-proteinuria covariates were highly correlated. For models including delta-proteinuria, model fit was assessed for models including absolute change, relative change, and a categorical indicator of improving/worsening/stable. Model fit and

performance metrics were best for absolute change, therefore the other measures of delta-proteinuria were discarded.

The population average eGFR slope was modeled using a fixed-effects linear regression model with time as the sole predictor. A random intercept was then added to the model, with assessment of the intraclass correlation coefficient to evaluate the proportion of the overall variability in index eGFR that is attributable to between-patient variation. A random slope was then added to account for between-patient variability in the rate of change in eGFR over time. Four multivariable models were then built, each with random intercept and random slope; they are summarized in Supplementary Table 7. The *parsimonious* model included time, age, sex, index eGFR and index proteinuria, along with two-way interactions between time and both index eGFR and index proteinuria. This structure mirrored the KFRE and was chosen to reflect a minimal set of routinely available clinical variables likely to be accessible at the time of prediction. The *treatment and trajectory* model added changes in eGFR and proteinuria from biopsy to index, as well as glucocorticoid use, to assess the extent to which pre-index disease behavior and early treatment response influence subsequent decline. The *full clinical model* further included hypertension and diabetes, two established risk factors for CKD progression, to test whether broader comorbidity adjustment improved model performance. Finally, the *full clinicopathologic model* incorporated the available Oxford classification features to evaluate whether histopathologic information provided incremental predictive value beyond clinical covariates. Pathology variables were limited to this final model to reflect real-world scenarios where biopsy tissue may be unavailable, inadequate for Oxford classification, or interpreted without access to expert renal pathology, thereby increasing the clinical applicability of the earlier models.

The variance-covariance matrix for the random effects was unstructured. Residual plots were examined to validate assumptions of normality of residuals, linearity, and homoscedasticity; assumptions appeared reasonable.

The models were compared using the Akaike Information Criterion[100] and Bayesian Information Criterion[101]. Model fit was assessed using marginal R^2 and conditional R^2[102].

As specified, the dependent variable was eGFR, for an individual at a given time, expressed in years. Each individual's predicted eGFR slope (in mL/min/1.73 m^2/year) was estimated as a linear combination of: the fixed effect of time, the fixed effect coefficients for all time-covariate interaction terms multiplied by that individual's covariate values, and the patient's random slope (obtained from the empirical Bayes estimate). We reported conditional (subject-specific) slopes, which included the random slope, and marginal (population-average) slopes, which set random effects to zero. An observed slope was also calculated for each patient using a linear model, with eGFR as the dependent variable and time as the predictor variable.

Observed and predicted slope estimates were compared using root mean squared error (RMSE), which represents the average magnitude of prediction error between observed and predicted eGFR slope[103]. Accuracy of predictions was assessed visually using calibration plots. Calibration slopes were calculated from a linear regression model of observed eGFR slope on predicted eGFR slope. Precision was evaluated using Bland–Altman plots[104], which assess agreement between observed and predicted eGFR slopes. For each patient, the mean of the observed and predicted slopes was plotted on the x-axis, and their difference on the y-axis. The plot allows visualization of systematic bias (points consistently above or below zero) and precision, reflected by the spread of differences within the 95% limits of agreement. For each model, the proportion of predictions within 1 mL/min/1.73 m^2/year was also reported.

Internal validation

The model with the best performance metrics was the parsimonious model, which was thus selected to undergo internal validation, using 10-fold cross validation[105]. The full dataset was randomly partitioned into 10 approximately equal-sized, mutually exclusive folds. Partitioning occurred at the patient level to ensure that all observations for a given patient were contained within a single fold. The partitioning process used a fixed random seed for reproducibility. The training set consisted of 9 folds, and the test set was the remaining fold. The parsimonious model was re-fit using only the training set, and included the same fixed and random effects structure as the parsimonious model fitted on the full dataset. The re-fitted model was used to generate predictions on the test set. Root mean squared error, marginal R^2, conditional R^2, and calibration slopes were calculated. This process was repeated 10 times, and the model performance metrics were pooled, with reporting of the mean and standard deviation of each metric (the cross-validated model performance). The degree of optimism for each metric was calculated, by subtracting the mean cross-validated performance the value of the metric calculated from the full dataset (apparent performance).

Sensitivity analysis

Several sensitivity analyses were performed.

- Each of the four models were re-fit with a variance component variance-covariance structure, and the standard errors of the effect estimates were compared.
- The models were re-fit with the index date set at 180 days. For this analysis, index eGFR and index proteinuria were the closest value prior to the index date, not exceeding 90 days from the index date. The performance and fit of each model were compared to the models using one-year post biopsy as the index date.

Results

Cohort characteristics

Between January 1, 2002 and December 31, 2020, we identified 458 individuals with IgAN in the Manitoba Glomerular Diseases Registry. Of those, 90 (19.7%) reached kidney failure within 1 year, 47 (10.3%) were followed for less than 3 years, and 140 (30.6%) had less than 3 eGFR measurements over the follow up period, leaving 181 patients in the final cohort (Figure 4). The baseline characteristics of the patients with two eGFR measurements are displayed in Supplementary Table 14. Patients with two measurements were more frequently male, more often from Winnipeg, with lower eGFR at both cohort entry and index.

The baseline characteristics of the overall cohort, and the cohort by era are summarized in Table 1. The number of patients diagnosed with IgAN increased over time, with 36 patients between 2002 and 2008 (Era 1), 55 between 2009 and 2014 (Era 2), and 90 between 2015 and 2020 (Era 3). The median age of the cohort was 41 years (IQR 31-54), with no substantial differences between eras. The majority were male (n = 101, 56%), and this percentage was stable between eras. Residence within Winnipeg decreased over time; 75% of patients diagnosed in Era 1 resided in Winnipeg compared to 53% of patients diagnosed in Era 3. Patients within the lowest income quintile were over-represented, with 34% of patients belonging to income quintile 1, compared to just 9.4% in quintile 5; this was stable across eras.

eGFR at cohort entry (median 67 mL/min/1.73 m^2, IQR 30-98) and index (median 66 mL/min/1.73 m^2, IQR 40-87) was highest among patients diagnosed in Era 1. Proteinuria at cohort entry was similar between eras; the median proteinuria at cohort entry for the overall cohort was 1.73 g/day (IQR 1.06-2.95), indicating a high-risk population. Patients in Era 1 had

lower median proteinuria at index (median 0.70 g/day, IQR 0.35-2.22) compared to Era 2 (median 1.08, IQR 0.47-2.00) or Era 3 (median 1.61 (IQR 0.60-2.56).

A total of 31 individuals (17%) had diabetes, while 83 (46%) had hypertension. A total of 160 patients (88%) were treated with RAASi, while 46 (25%) were treated with glucocorticoids. The prevalence of RAASi treatment remained consistent across eras, whereas glucocorticoid use was highest in Era 1 (33%, 12 patients) compared with 29% (16 patients) in Era 2 and 20% (18 patients) in Era 3. As expected, Oxford classification was not available for patients diagnosed prior to 2016, but the S, T, and C lesions could be recreated from registry data for all patients. The majority of patients had an S lesion (131 patients, 72%). The prevalence of IFTA increased across eras: in Era 1, 69% of patients had T0 and none had T2, compared with 13% with T2 in Era 2 and 26% in Era 3. Conversely, crescents were more common in Era 1: 42% of patients had crescents in Era 1, compared to 29% in Era 2 and 20% in Era 3. Kidney failure occurred in 33 individuals (18%), while 26 (14%) died. Death and kidney failure were most common in Era 1, perhaps reflecting the longer period of follow up.

When examining the cohort by sex (Table 2), 33 female patients (41%) belonged to the lowest income quintile, compared to 29 (29%) of male patients. Female patients had higher proteinuria than males at both cohort entry (median 1.92 g/day, IQR 1.26-3.44 versus 1.56 g/day IQR 0.97-2.67) and index (1.56 g/day, IQR 0.60-2.94 versus 1.08 g/day, IQR 0.50-1.94). Diabetes was more common among females (21%) than males (14%). Treatment, pathology characteristics, and outcomes were otherwise similar between males and females.

Patients who progressed to kidney failure were more often in the lowest income quintile (52% vs. 30% among non-progressors) and had substantially lower eGFR at both cohort entry (median 34 mL/min/1.73 m^2, IQR 23–46 vs. 64 mL/min/1.73 m^2, IQR 42–91) and index (17

mL/min/1.73 m², IQR 11–29 vs. 61 mL/min/1.73 m², IQR 40–86). Glucocorticoid use was more frequent among progressors (36%, 12 patients) compared with non-progressors (23%, 34 patients), whereas RAASi use was less common (79%, 26 patients vs. 91%, 134 patients). Advanced IFTA (T2) was also more prevalent among progressors (36%, 12 patients) than non-progressors (12%, 18 patients). The cohort characteristics by kidney failure status are summarized in Table 3.

Patients with more advanced CKD at cohort entry were older (median 57 years, IQR 43-64 for CKD 4 versus median 29, IQR 23-37 for CKD 1). The time from nephrology consultation to biopsy was shortest for those with CKD 4 (median 23 days, IQR 6-119) and longest for those with CKD 1 (median 98 days, IQR 27-354). The prevalence of hypertension increased with worsening CKD stage, from 27% in CKD 1 to 35% in CKD 2, 60% in CKD 3, and 73% in CKD 4. RAASi use was consistently high across CKD 1–3 (89–95%) and glucocorticoid use remained similar (20–24%), whereas in CKD 4 glucocorticoid prescription was more frequent (50%) and RAASi use less common (73%). The presence of T1 and T2 lesions increased with worsening CKD stage, while the presence of crescents was approximately similar across stages. Table 4 summarizes the baseline characteristics by CKD stage at cohort entry.

Patients living outside of Winnipeg were more often in the lowest income quintile (32 patients, 44%) compared to those living in Winnipeg (30 patients, 28%). The clinical, treatment, and pathology characteristics were otherwise similar by residence (Table 5). However, mortality was higher among rural patients (21%, 15 patients) than among those in Winnipeg (10%, 11 patients).

Patients in the highest income quintile had the lowest eGFR at cohort entry (median 43 mL/min/1.73 m^2, IQR 33-62) and index (median 41 mL/min/1.73 m^2, IQR 32-77). No clear

income related trends were observed in the baseline, treatment, or pathology characteristics (Table 6). Kidney failure occurred most frequently in income quintiles 1 (27%), and 5 (24%).

Missing data

Of the 181 patients in the final cohort, 47 (26%) had one or more missing data values. eGFR at cohort entry was missing in 13 individuals (7.2%) and proteinuria at cohort entry in 14 (7.7%). At index, eGFR and proteinuria were missing in 26 (14%) and 33 (18%), respectively. Missingness was most pronounced in Era 1 (Table 1). In Era 3, missing cohort entry values were rare, but index eGFR and proteinuria were missing in 17% and 20%, respectively; missingness was less common in Era 2. Missing data were more frequent in females than males, but were not clearly associated with kidney failure status (Table 3), location of residence (Table 4), or socioeconomic status (Table 5). Patients missing index values were almost always missing both eGFR and proteinuria. As missingness appeared related to era and sex, multiple imputation was performed using all candidate covariates in the imputation model. Density plots (Figures 5, 6) comparing imputed and observed distributions demonstrated close alignment, supporting that the imputation model was well-specified. The performance characteristics of models using imputed data were inferior to those using complete cases, therefore complete cases were used for the main analysis. The baseline characteristics of complete cases are found in Supplementary Tables 8 through 13.

Regression models

Model coefficients and performance

Four mixed-effects linear regression models for eGFR were fit using complete cases; the coefficients, standard errors (SEs), and model performance characteristics for each model are found in Tables 7-10.

Parsimonious model

The parsimonious model included time, index eGFR, index proteinuria, age, sex, and interaction terms for index eGFR and proteinuria with time. The marginal intercept was 54.67 (SE 1.71, p <0.001), indicating that for a male patient with age, index eGFR, and index proteinuria measurements equal to the population average, the expected eGFR at index would be approximately 54 mL/min/1.73 m^2. Age was associated with lower eGFR (-0.096, SE 0.040, p = 0.018). The interaction term between index proteinuria and time was statistically significant (-1.47 mL/min/1.73 m^2/year for each 1 g/day above the population mean, SE 0.66, p <0.001), suggesting increasing proteinuria was associated with an accelerated rate of eGFR decline. The interaction term between eGFR and time was not significant, suggesting no relationship between the initial eGFR and the subsequent rate of change. Model performance was excellent, with marginal R^2 0.81, conditional R^2 0.95, and RMSE 7.25.

Treatment and trajectory model

This model added change in proteinuria, change in eGFR, time to biopsy, and glucocorticoid exposure, with a two-way interaction term between glucocorticoid exposure and time. The marginal intercept was 53.63 (SE 1.85, p <0.001). The coefficient for time to kidney biopsy was statistically significant (0.0016, SE 0.00075, p = 0.030). However, the magnitude of the coefficient suggests a clinically negligible effect of time to biopsy on initial eGFR. The interaction term between index proteinuria and time remained statistically significant in this model (-1.72 mL/min/1.73 m^2/year for each 1 g/day above the population mean, SE 0.72, p = 0.016). Conversely, the interaction term between glucocorticoid prescription and time was not significant, suggesting no modification of eGFR slope with glucocorticoid prescription in this model. Model performance was unchanged, with marginal R^2 0.81, conditional R^2 0.95, and

RMSE 7.31, indicating that added covariates did not account for additional between-patient or within-patient variability beyond that captured by the parsimonious model. A slight improvement in model fit was observed compared to the parsimonious model (AIC 145082 vs 145534, BIC 145217 vs 145629).

Full clinical model

This model added the presence of hypertension and diabetes to the model, along with an interaction term between the change in eGFR and time. The marginal intercept was 52.9 (SE 2.00, p <0.001), while the marginal effect of time was -5.29 mL/min/1.73 m^2/year (SE 1.42, p <0.001). Duration of time to biopsy was again statistically significantly associated with initial eGFR (0.0018, SE 0.00077, p = 0.021). The interaction term between proteinuria and time remained statistically significant (-1.92 mL/min/1.73 m^2/year for each 1 g/day above the population mean, SE 0.74, p = 0.009). All other interaction terms were not significant. Model performance was unchanged from previous models, with marginal R^2 0.80, conditional R^2 0.95, and RMSE 7.31. No improvement in model fit was noted between the treatment and trajectory model and the full clinical model (AIC 145082 vs 145084, BIC 145217 vs 145243).

Full clinicopathologic model

The addition of pathology characteristics resulted in substantial changes in some effect estimates. The marginal intercept was 51.38 (SE 2.53, p <0.001), while the marginal effect of time was no longer significant (β -1.66, SE 2.41, p = 0.491). The interaction between proteinuria and time remained significant with a similar magnitude to the prior models (-1.78 mL/min/1.73 m^2/year for each 1 g/day above the population mean, SE 0.74, p = 0.016). The interaction between crescents and proteinuria was statistically significant (-4.61 mL/min/1.73 m^2/year, SE 2.32, p = 0.047), suggesting the presence of crescents was associated with a significantly faster

rate of eGFR decline. Other interactions between pathology characteristics, such as S and T lesions, and time had negative coefficients but did not reach statistical significance. Model performance and fit were not significantly different from the parsimonious model, or any of the other models (marginal R^2 0.80, conditional R^2 0.95, RMSE 7.31, AIC 145063 and BIC 145286).

Model coefficients by era

To examine for possible era effects in model results, two models were re-fit after partitioning the datasets into the three previously defined eras. Due to its performance characteristics and parsimony, the parsimonious model was selected. Due to the significant changes in pathology characteristics that were observed over time in the descriptive statistics, the full clinicopathologic model was also selected.

In the parsimonious model (Table 11), the marginal effect of time was significant in all eras, with a higher magnitude of eGFR decline in Era 1 (-7.30 mL/min/1.73 m^2/year, SE 1.36) compared to Eras 2 and 3 (-3.56 mL/min/1.73 m^2/year, SE 1.26 and -3.37 mL/min/1.73 m^2/year, SE 1.62, respectively). The remainder of fixed-effect coefficients were consistent across eras, with the notable exception of the proteinuria–time interaction. In Eras 1 and 3, higher proteinuria was significantly associated with faster eGFR decline (–3.14 mL/min/1.73 m^2/year, SE 1.06 in Era 1; –2.32 mL/min/1.73 m^2/year, SE 1.18 in Era 3), whereas in Era 2 the interaction was not significant (–0.74 mL/min/1.73 m^2/year, SE 0.90). The variability of the random slope for time increased over eras (SD 5.15 in Era 1, 7.99 in Era 2, and 12.31 in Era 3), accompanied by a decline in marginal R^2 (0.92, 0.80, and 0.77, respectively) while conditional R^2 remained stable. This pattern suggests that in more recent eras, a greater share of variability was attributable to between-patient differences.

In the full clinicopathologic model (Table 12), the main effect of time was not significant in any era, with wide standard errors, though the point estimates suggested modest decline in Eras 1 and 3 (–1.90 mL/min/1.73 m² per year, SE 3.00 in Era 1; –3.12, SE 5.02 in Era 3) and a near-null estimate in Era 2 (0.48, SE 2.95). The interaction between proteinuria and time was significant in Era 3 (–2.79, SE 1.26), indicating that higher proteinuria was associated with faster decline in recent years, while smaller, non-significant effects were seen in Eras 1 and 2 (–1.49, SE 1.24 and –0.82, SE 1.09, respectively). Other covariate-time interactions were imprecise, with wide confidence intervals, and pathology terms did not consistently modify slope across eras. It should be noted that the presence of crescents was strongly associated with more rapid eGFR decline in Era 1 (-8.82, SE 2.34), an era where almost half the cohort had crescents on kidney biopsy. Random slope variability increased markedly from Era 1 (SD 3.56) to Era 3 (SD 12.76), suggesting greater heterogeneity in eGFR decline in more recent cohorts. RMSE rose from 5.80 in Era 2 to 8.40 in Era 3, consistent with less precise prediction in the most recent era.

Overall, these findings suggest an increase in heterogeneity with time. The effect estimates of the parsimonious model were generally stable with time, while differences were observed in the effect of pathology on eGFR slope between eras, perhaps reflecting differences in the prevalence of different pathology findings over time.

Model using imputed data

We elected to fit two models to the imputed datasets, the parsimonious model, and the full clinicopathologic model. Coefficients and standard errors from the parsimonious model were similar to those from the complete case analysis (Table 13). However, the marginal R^2 was lower in the imputed datasets, indicating that the fixed effects explained less variability in eGFR compared with the complete case model. The variability of the random effects was substantially

greater in the imputed datasets, with a random intercept SD of 11.11 and a random slope SD of 10.05. Together with the lower marginal R^2, this suggests less of the variability in eGFR was explained by the fixed effects, with a greater proportion instead captured by the random effects.

In the full clinicopathologic model fit to the imputed dataset (Table 14), the marginal effect of time was not significant (–0.19 mL/min/1.73 m²/year, SE 2.15, p = 0.928), consistent with the complete case analysis. The interaction between index proteinuria and time was also similar to the complete case model (–1.39 mL/min/1.73 m²/year, SE 0.63, p = 0.028). However, unlike the complete case analysis, the Oxford S–time interaction reached statistical significance (–3.76, SE 1.84, p = 0.041), while the Oxford C–time interaction was no longer significant (–1.97, SE 2.05, p = 0.338). Model performance was poorer, with a lower marginal R^2 compared to the complete case analysis (0.70 vs. 0.80), although the conditional R^2 remained stable. The random slope SD was similar across models, but the random intercept SD was higher in the imputed dataset (10.89), again suggesting that more between-patient variability was captured by the random effects when using imputed data.

Evaluating eGFR slope predictions

The observed and conditional predicted slopes for the parsimonious model are presented in Table 15. The apparent predictive performance of each of the models in predicting eGFR slope is presented in Table 16.

Parsimonious model

The RMSE of conditional predicted eGFR slopes was 6.41. Pearson correlation between predicted and observed eGFR slope was 0.88. While predicted values were similar to observed values (Figure 7), the slope of the calibration line (1.15, 95% CI 1.04, 1.26) deviated from 1.0, indicating some miscalibration. Specifically, the model tended to overestimate decline among

patients with observed eGFR slopes greater than 0, and underestimate decline in those with rapid progression**.** Predictions were well calibrated when observed eGFR slopes were close to the population average. Predicted eGFR slope was within 1 mL/min/1.73 m^2/year of observed slope 88% of the time. Bland Altman plots comparing conditional predicted and observed eGFR slopes demonstrated good overall agreement between predicted and observed slopes, with differences centred on zero, and few predictions falling outside the 95% limits of agreement (Figure 8). With the exception of patients with large negative mean slopes, no systematic trend in the difference between predicted and observed slope was found across the range of slopes.

The RMSE of marginal predicted eGFR slopes was 12.31. Correlation between predicted and observed eGFR slope was 0.30. Calibration was poor (calibration slope 1.58, 95% CI 0.71, 2.44), and predictions often deviated markedly from observed values across all observed values of eGFR (Figure 9). Marginal predicted eGFR slope was within 1 mL/min/1.73 m^2/year of observed slope only 11% of the time. Unlike the conditional predictions, Bland Altman plots of marginal predicted versus observed eGFR slopes demonstrated a negative proportional bias (Figure 10), suggesting the marginal parsimonious model underestimates eGFR slope for patients with the most negative eGFR slope (i.e it predicts a less negative slope), and overestimates eGFR slope for patients with observed slopes close to or greater than 0 (i.e it predicts decline when it doesn't occur). The limits of agreement were also much wider than the plot of conditional predictions, indicating greater prediction error. Examination of density plots (Figure 11) demonstrate the distribution of predicted and observed slopes was broad, reflecting the heterogeneity of observed patient trajectories. Conversely, marginal predicted slopes were narrowly centred around the population average, substantially underestimating the variability seen in the observed data.

Overall, the findings suggest that inclusion of the random effects was critical for accurate prediction of individual eGFR slopes, and support that between-patient variability may be a barrier to accurate prediction of eGFR slope in this cohort.

Treatment and trajectory model

The RMSE of conditional predicted eGFR slopes was 6.54. Correlation between predicted and observed eGFR slope was 0.88. While predictions generally tracked observed values (Figure 12), the slope of the calibration line (1.14, 95% CI 1.03, 1.26) deviated from 1.0, indicating miscalibration. Similar to the parsimonious model, the model tended to overestimate decline among patients with observed eGFR slopes greater than 0, and underestimate decline in those with rapid progression**.** Predictions were well calibrated when observed eGFR slopes were close to the population average. Predicted eGFR slope was within 1 mL/min/1.73 m^2/year of observed slope 83% of the time. Bland Altman analysis comparing conditional predicted and observed eGFR slopes demonstrated good overall agreement between predicted and observed slopes, with most differences centred on zero, and few predictions falling outside the 95% limits of agreement (Figure 13), which were similar to the conditional predictions of the parsimonious model. With the exception of patients with very negative mean slopes, no systematic trend in the difference between predicted and observed slope was found across the range of slopes.

Examination of marginal predictions from the treatment and trajectory model revealed similar issues to the marginal predictions arising from the parsimonious model. The RMSE of marginal predicted eGFR slopes was 12.69. Correlation between marginal predicted and observed eGFR slope was 0.28. Calibration was poor, (calibration slope 1.55, 95% CI 0.60, 2.51); predictions deviated from observed values markedly and unpredictably (Figure 14). Only 10% of marginal predicted eGFR slopes were within 1 mL/min/1.73 m^2/year of observed slope.

Bland-Altman plots comparing marginal predicted and observed eGFR slopes demonstrated a negative proportional bias with wider limits of agreement than the plot of conditional predictions (Figure 15), similar to that observed in the marginal parsimonious model. The density plot of observed, conditional, and marginal predicted eGFR slope (Figure 16) revealed distributions very similar to the parsimonious model, with conditional and observed slopes closely overlapping, and marginal slopes centred around the population average with much less variability.

The findings are very similar to the parsimonious model. The results suggest that when patient-specific slopes can be included, slope can be accurately predicted, and that slope is difficult to predict without accounting for between-patient variability.

Full clinical model

The RMSE of conditional predicted eGFR slopes was 6.31. Correlation between predicted and observed eGFR slope was 0.88. The calibration slope (1.14, 95% CI 1.04, 1.25) deviated from 1.0, indicating miscalibration. Consistent with prior models, the model tended to overestimate decline among patients with observed eGFR slopes greater than 0. While the calibration slope and loess line of the calibration plot (Figure 17) suggest underestimation of decline among patients with very rapid progression, visual inspection shows that most observed slopes lie above the line of identity, indicating that across the spectrum, observed slopes were generally less negative than predicted. Predicted eGFR slope was within 1 mL/min/1.73 m^2/year of observed slope 69% of the time. Bland Altman plots comparing conditional predicted and observed eGFR slopes demonstrated good overall agreement between predicted and observed slopes, with the mean difference centred on zero (Figure 18). However, unlike prior models, visual inspection of the plot reveals a large number of differences below zero, suggesting over-prediction of eGFR decline (the model predicts a more negative eGFR slope than is observed).

This is consistent with the findings of the calibration plot. Few predictions fell outside the 95% limits of agreement, which were similar to the conditional predictions of the prior models. With the exception of patients with very negative mean slopes, no systematic trend in the difference between predicted and observed slope was found across the range of slopes.

Examination of marginal predictions from the full clinical model revealed similar issues to the marginal predictions arising from the prior models. The RMSE of marginal predicted eGFR slopes was 12.65. Correlation between marginal predicted and observed eGFR slope was 0.28. Calibration was poor, (calibration slope 1.39, 95% CI 0.54, 2.25); predictions deviated from observed values markedly and unpredictably (Figure 19). Only 14% of marginal predicted eGFR slopes were within 1 mL/min/1.73 m^2/year of observed slope. Bland-Altman plots comparing marginal predicted and observed eGFR slopes demonstrated a negative proportional bias with wider limits of agreement than the plot of conditional predictions (Figure 20), similar to that observed in the prior marginal models.

The findings suggest that the addition of clinical features such as hypertension, diabetes, and an interaction term for the change in eGFR with time may lead to systematic over-prediction of eGFR decline (i.e., more negative slope prediction than what is observed).

Full clinicopathologic model

The RMSE of conditional predicted eGFR slopes from the full clinicopathologic model was 6.93. Correlation between predicted and observed eGFR slope was 0.87. The calibration slope (1.14, 95% CI 1.02, 1.26) deviated from 1.0, indicating miscalibration. Examination of the calibration plot (Figure 22) revealed many observed slopes along the line of identity. However, for some patients, the model tended to underestimate eGFR decline. As in prior models, several outliers with profoundly rapid observed decline were noted; the model underpredicted their rate

of decline. eGFR slope was within 1 mL/min/1.73 m^2/year of observed slope 74% of the time. Bland Altman analysis comparing conditional predicted and observed eGFR slopes showed that most differences centred on zero (Figure 23). Visual inspection, however, revealed a number of points above zero, with the mean difference line also above zero, indicating that the model tended to under-predict eGFR decline (i.e., predicted slopes were less negative than is observed). This finding was consistent with the calibration plot. Few predictions fell outside the 95% limits of agreement, comparable to prior conditional models. Apart from several outliers, no systematic trend in the differences was evident the range of slopes.

As in prior marginal models, predictions from the marginal full clinicopathologic model were inaccurate. The RMSE of marginal predicted eGFR slopes was 12.60. Correlation between marginal predicted and observed eGFR slope was 0.31. Calibration was poor, (calibration slope 1.19, 95% CI 0.54, 1.84), with predicted values deviating substantially and inconsistently from observed slopes (Figure 24). Only 10% of marginal predicted eGFR slopes were within 1 mL/min/1.73 m^2/year of observed slope. Bland-Altman plots comparing marginal predicted and observed eGFR slopes (Figure 25) demonstrated a similar negative proportional bias observed in prior marginal models, but with greater dispersion around the mean difference line, suggesting an increase in the variability of predictions with no improvement in model bias.

Models using imputed datasets

The apparent performance metrics for eGFR slope from the models fit to imputed datasets are found in Table 17. For the conditional parsimonious model fit to the imputed datasets, the RMSE was 8.96 and the correlation with observed slopes was 0.79. The calibration slope (1.15, 95% CI 1.02–1.28) was similar to the complete case analysis, but the calibration plot (Figure 27) demonstrated substantial variability, with many predictions deviating markedly

above or below the line of identity. Overall, 77% of predicted slopes were within 1 mL/min/1.73 m²/year of the observed slope. Bland–Altman plots (Figure 28) showed that the mean difference between predicted and observed slopes was centered on zero, indicating no systematic bias. However, the limits of agreement were wider than in the complete case analysis, and numerous observations lay well outside these bounds, reflecting poorer agreement and greater error dispersion when imputed data were used.

For the conditional full clinicopathologic model fit to the imputed datasets, the RMSE was 11.20, and the correlation with observed slopes was 0.79. Calibration was poorer than the complete case analysis (calibration slope 1.33, 95% CI 1.18, 1.49). The calibration plot (Figure 30) showed that although many observed slopes lay along the line of identity, the model tended to under-predict decline among rapid progressors. Overall, 78% of predicted slopes were within 1 mL/min/1.73 m^2/year of the observed slope. Bland Altman analysis (Figure 31) showed that most differences were centred around zero, but limits of agreement were wider than in the complete case analysis, with numerous data points deviating substantially from the zero line. The marginal predictions from the full clinicopathologic model were also inaccurate.

These findings highlight that although imputation preserved covariate distributions, model performance and prediction accuracy was inferior to the complete case models, with greater variability and miscalibration.

Internal validation

On the basis of its simplicity and performance characteristics, the parsimonious model was selected for internal validation. The apparent and cross-validated performance metrics of the parsimonious model are presented in Tables 18 and 19. For the conditional eGFR slope predictions, the pooled cross-validated RMSE was 12.11 (SD 5.40), with an optimism estimate

of 5.70. The cross-validated correlation between observed and predicted eGFR slope was -0.15 (SD 0.24), with optimism of 1.03. The cross-validated calibration slope was 0.79 (SD 21.92), with optimism of 0.35.

For the marginal eGFR slope predictions, the pooled cross-validated RMSE was 11.98 (SD 4.69), with an optimism estimate of 0.33. The cross-validated correlation between observed and predicted eGFR slope was 0.24 (SD 0.46), with optimism of 0.06. The cross-validated calibration slope was 1.89 (SD 3.88), with optimism of 0.31.

Internal validation demonstrated substantial performance degradation for conditional predictions, with high RMSE, near-zero correlation, and unstable calibration. Marginal predictions showed better stability, with lower optimism, though predictions generated in the validation datasets remained poorly calibrated and widely variable. This pattern suggests that the apparent accuracy of conditional predictions was heavily driven by the random effects, as expected when accounting for subject-specific variation, underscoring their critical role in capturing patient-specific heterogeneity and improving individual predictions.

Sensitivity analyses

Two sensitivity analyses were performed. First, the parsimonious model was re-fit using a variance components variance-covariance structure (Table 20). Coefficients and standard errors were nearly identical to those obtained with the unstructured variance-covariance structure, and model performance was also comparable.

Second, the parsimonious model was re-fit, using 180 days post-kidney biopsy as the index date (Table 21). In this model, the marginal effect of time was -4.80 mL/min/1.73 m^2/year (SE 0.84, $p < 0.001$), which represented a slightly larger decline than in the original analysis. Higher index proteinuria was associated with a lower index eGFR (-1.01, SE 0.34, $p = 0.004$),

while the interaction between proteinuria and time was similar to the original model (-1.70 mL/min/1.73 m^2/year, SE 0.51, p = 0.001). Model performance was similar, with marginal R^2 0.82 and conditional R^2 0.93, although accuracy was lower, with an RMSE of 9.12.

Taken together, these sensitivity analyses support that the results were robust to changes in the variance-covariance structure, and to redefining the index date. However, predictive performance declined when the index date was shifted to 180 days post-biopsy, possibly reflecting that covariates such as proteinuria or eGFR remain in flux at this earlier time point due to the effect of treatment initiation and titration.

Discussion

Summary of findings

In this population-based retrospective cohort study of 181 adults (137 complete cases) with biopsy-proven IgA nephropathy diagnosed in Manitoba, mixed-effects linear regression models were used to predict the 2-year rate of change in eGFR (eGFR slope) using clinical and pathological predictors. The models demonstrated strong apparent performance within the development dataset but limited generalizability when tested through cross-validation. This study represents, to our knowledge, the first attempt to predict eGFR slope in a real-world IgA nephropathy cohort using linked administrative and registry data.

Across all model specifications, apparent model performance was similar, with high conditional R^2 values, and the vast majority of conditional (subject-specific) predictions closely approximating observed patient slopes. However, when random effects were removed to generate marginal (population-level) predictions, calibration and accuracy declined substantially. Marginal predictions systematically over- or underestimated observed slopes, and calibration plots demonstrated severe miscalibration. Cross-validation further revealed that the strong apparent performance of the conditional models did not generalize to unseen data, with notable deterioration in calibration and precision. Together, these findings indicate that the models relied heavily on patient-specific random effects to maintain apparent accuracy, limiting their utility for predicting outcomes in new patients.

Among fixed effects, higher proteinuria at the index date, one-year post biopsy, was consistently associated with faster eGFR decline, regardless of the model structure. The addition of pathology features did not improve predictions, though interpretation of the effects of

pathologic lesions on eGFR slope are limited by imprecision of the estimates, and the availability of data within the registry.

Interpretation of model performance

To our knowledge, this is the first study to develop and validate a prediction model for eGFR slope in IgAN. We demonstrated the feasibility of building a model that is accurate when the random effects can be precisely estimated from available data. We also demonstrated the challenges associated with applying such a model to unseen data or a new patient who lacks historical eGFR data, and the importance of making accurate marginal predictions to maximize clinical utility of the model in such a context.

Comparisons of observed and predicted eGFR slopes provided insight into the nature of prediction error. In the marginal models, negative proportional bias was observed. For patients with steeply declining eGFR, the model systematically predicted a less negative slope, while for patients with stable or improving eGFR, the model predicted decline. This pattern reflects regression to the mean[106], in which predictions are biased toward the population average. Because the random effects in mixed models capture patient-specific deviations from the mean trajectory, their exclusion in marginal predictions leaves only the fixed effects to explain individual differences. When the covariates included in the model are only weakly associated with the change in eGFR over time, as was seen in this study, patient-specific predictions cluster tightly around the population mean. This may reflect the limited strength of association between the available predictors and true disease progression in this cohort, or insufficient sample size to detect those associations with adequate precision. Interestingly, although the marginal predictions were systematically biased toward the population mean, their cross-validated

performance showed minimal optimism, suggesting that while the marginal models lacked precision, they were stable and not overfitted.

The inclusion of comorbidities, treatment characteristics, and pathology features did not meaningfully improve the predictive accuracy or calibration of the eGFR slope models. There are several possible reasons. First, the combination of a small sample size and multiple covariates increased the likelihood of overfitting, limiting the precision of estimates beyond the strongest predictor variable, proteinuria. In mixed-effects models, random intercepts and slopes already absorb much of the within-patient variability, and adding numerous fixed effects with weak or inconsistent associations (whether real or because the sample is small), can inflate variance without improving predictive performance. Second, IgAN is a widely variable disease in its rate of progression, and it has been demonstrated that clinical and pathological risk factors account for a small amount of variability in kidney disease progression[12,64]. This likely reflects the influence of unmeasured factors, including genetic susceptibility[107], ancestry or ethnicity[74], environmental exposures[108], and immune or molecular disease signatures[109], that were not captured in this dataset but may substantially affect disease trajectory. As an example, the International IgA Nephropathy Prediction Tool models had R^2 values of 0.25 to 0.35 in the derivation and validation cohorts, which comprised research cohorts collected in expert centres[12]. As a population-based cohort, the Manitoba Glomerular Diseases Registry may capture even greater variability in disease presentation, treatment, and progression than selected research cohorts, which may further limit the predictive value of population-level covariates, and the ability of the model to make accurate out-of-sample predictions. The weak or imprecise associations observed in the model coefficients in this study would support this notion. Third, patients entered the cohort at differing points in their disease trajectory. Proteinuria, eGFR, and

the time from nephrology contact to kidney biopsy were highly variable, and we were unable to capture the indication for kidney biopsy, along with pre-biopsy disease behaviour that may have influenced subsequent eGFR slope. This heterogeneity introduces noise into the model and may attenuate our ability to accurately model the impact of a given covariate on eGFR slope for a given patient at a given timepoint in their disease. Finally, the nature of the data sources and imprecisions in the covariate definitions could explain their limited contribution to model performance, despite being biologically important. Glucocorticoid exposure in this study was defined as a binary variable**,** coded as present if a prescription for any glucocorticoid was dispensed for at least 30 days. This approach may have resulted in misclassification bias, which typically results more imprecise estimates that are biased toward the null[110]. Under this definition, a patient could have completed six months of treatment as per the reduced-dose TESTING protocol which has demonstrated therapeutic benefit[43], whereas another patient could have filled the same prescription and never taken the medication, yet both would be categorized as "exposed." Such heterogeneity in dose, adherence, and duration within a binary exposure variable could have obscured any true association between glucocorticoid use and eGFR decline, contributing to the absence of improvement in predictive accuracy when treatment variables were added to the model.

Clinical implications of the findings

The results reaffirm the importance of proteinuria in predicting eGFR decline. Patients with higher proteinuria at one year post-biopsy experienced substantially faster eGFR loss after adjusting for other covariates. The estimated effect size, approximately 1.5 mL/min/1.73 m^2/year faster decline per 1 g/day higher proteinuria, emphasizes the critical importance of lowering proteinuria to prevent CKD progression and kidney failure that has been demonstrated in

randomized trials[55]. The landmark nature of our analysis is also unique and expands the available literature regarding how proteinuria predicts kidney outcomes in IgAN. It is well-established that increasing baseline[48,60,62–64], time-averaged[47,68], and time-varying proteinuria[10] are all associated with kidney disease progression, and our study adds to that literature by demonstrating that the degree of proteinuria at one-year is also prognostic. Interestingly, we did not find an association between the change in proteinuria from baseline to one year and subsequent kidney function decline. This is consistent with data from the Toronto GN Registry, which demonstrate that patients with >3 g/day of proteinuria at baseline who achieved a significant reduction in proteinuria to <1 g/day had similar outcomes to patients who had <1 g/day persistently[2]. This supports that achieving the lowest proteinuria possible, likely at any timepoint, is the most important treatment goal in IgAN.

However, contrary to prior publications, we did not observe an association between eGFR and subsequent kidney function decline. An early epidemiologic study including patients from Canada, Finland, and Australia demonstrated and association between lower baseline kidney function and accelerated kidney function decline[61]. This study modeled the association of covariates with subsequent observed decline using linear regression, without accounting for patient-specific variability as in a mixed-effects model. Our model estimated slope from the coefficients of the covariate-time interaction terms and included patient-specific random effects to model between-patient variability in both baseline and slope. Thus, it is possible that prior findings using simple linear regression may reflect a spurious association that is no longer present after proper portioning of within- and between-person differences.

In this cohort, the number of patients diagnosed with IgAN increased with time. This is consistent with prior work which demonstrated an almost threefold increase in the incidence of

kidney biopsy in Manitoba over the study period[7]. This increase is at least partially attributable to increases in the availability of biopsy, and the increasingly recognized importance of kidney biopsy in management of GN and kidney disease more broadly. It is not clear if the incidence of IgAN is actually increasing in Manitoba. We found that patients belonging to the lowest SES quintile were over-represented; this is consistent with prior literature showing a higher incidence of IgAN in patients of low SES, the reasons for which are not clear[111,112].

Era effects

A number of interesting era effects were observed, both in the characteristics of the cohort and in the performance of the models. Patients diagnosed in the earliest era were slightly younger, had higher eGFR, and lower proteinuria at the index date, despite similar proteinuria at cohort entry. They also had a higher prevalence of crescents, less IFTA, and were more likely to receive glucocorticoids compared with those in later eras. Although definitive conclusions cannot be drawn, these findings collectively suggest that patients biopsied in Era 1 may have had earlier or more treatment-responsive disease. Consistent with this interpretation, diabetes and hypertension were less prevalent in the earliest era. Because these conditions can independently cause chronic kidney disease, their increasing prevalence over time may partly explain the greater IFTA, lower eGFR, and higher proteinuria observed in later eras. These temporal shifts in disease characteristics and comorbidity burden may also underlie the increase in the variability of the random slopes with time, reflecting an increase in the heterogeneity of disease behaviour across eras. It is possible that these changes reflect evolving biopsy practices, rather than true shifts in disease biology; patients biopsied in Era 1 may have represented a more specific clinical phenotype prompting a biopsy, whereas in later eras, greater biopsy availability, and broader indications for kidney biopsy may have captured a more heterogeneous population. Finally, the

growing heterogeneity in patient characteristics and biopsy indications over time likely mirrors secular changes in treatment paradigms and physician practice patterns**,** which may have influenced both who was biopsied and how aggressively patients were treated, introducing treatment-by-era interactions that were not formally modeled in this analysis.

Strengths and limitations

This study has several strengths. By leveraging a population-based registry capturing all patients diagnosed with IgAN in our province, the cohort is not subject to the selection bias inherent to research cohorts with specific enrolment criteria[6] or those derived from expert centres[2,69]. Because the registry dates back to 2002, it also enabled the identification of important era effects which may have influenced patient characteristics, biopsy practices, and treatment patterns over time. In addition, linkage with the Manitoba Centre for Health Policy (MCHP) databases allowed for comprehensive capture of administrative, clinical, and medication data, which are known to be of high quality[91]. Finally, as the first study to develop prediction models for eGFR slope in IgA nephropathy, this analysis makes a methodological contribution to the literature by demonstrating the importance of appropriately estimating random effects to balance apparent accuracy in the derivation dataset with generalizability to new patients. This is discussed in greater detail in a future section.

However, this analysis also has many limitations. First, missing data were prevalent, and data completeness varied by era, sex, and clinical severity. While the multiple imputation approach produced covariate distributions that closely resembled those in the complete-case analysis, model performance and prediction accuracy was worse when applied to the imputed datasets, which is common when using imputed data[113]. However, one important contributor to this decline in performance may derive from the fact that index eGFR was one of the covariates

where missingness was prevalent and therefore imputed. As the measure from which future trajectory is measured, by imputing index eGFR we are partially imputing the outcome trajectory, since slope is defined relative to this baseline value. If the imputed value deviates even slightly from the true baseline value, this error is then propagated to the predicted slope, introducing noise. Accordingly, although imputation preserved the distribution of the covariates, the predictive accuracy of the model was degraded. Thus, the need to use only complete cases led to a significant decrease in sample size, and reduction in power as previously discussed.

Second, closely related to the issue of missingness was the availability of data from which to accurately model eGFR slopes in this population. A total of 140 patients were excluded because they had fewer than three eGFR measurements available for analysis. This decision reflected a trade-off between maximizing sample size, and preserving the reliability of slope estimation. With only two measurements, the estimated trajectory for an individual is fully determined by a single difference, and is therefore highly sensitive to measurement error or transient fluctuations in kidney function. Indeed, empirical examination of some individual eGFR plots showed implausibly discordant eGFR measurements over short intervals, producing unstable and clinically illogical slopes. Including such patients would have inflated residual variance and undermined both model calibration and predictive validity. Still, excluding them likely introduced selection bias, as it is probable that individuals with close follow up may be systematically different from those with sparse follow up, though observed differences in characteristics and outcomes appeared minor. Ultimately, although the decision to exclude these patients reduced sample size and statistical power, the reliability and interpretability of the mixed-effects estimates were likely strengthened.

Third, there was potential for temporal misalignment between covariate measurement and the period over which eGFR slope was estimated. Pathology features were measured at the time of biopsy, whereas treatments and comorbidities reflected the period preceding the one-year index date. Because eGFR slope was modeled beginning at that index date, these predictors were not necessarily synchronized with the time frame over which decline was estimated, potentially attenuating their apparent predictive strength. For example, the presence of crescents at biopsy may have influenced treatment decisions, with some patients receiving prompt immunosuppression that mitigated subsequent decline, while others remained untreated and continued to progress. In this context, the effect of crescents on post–one-year slope may be partly mediated or modified by treatment**,** blunting any direct association observed in the model. The study was not designed to account for such treatment-by-pathology interactions or mediation effects, which may have further contributed to the weak or inconsistent associations between biopsy findings and subsequent eGFR decline. Aside from pathology characteristics which are inherently time-invariant, the decision to exclude time-varying treatment or clinical covariates was intentional, as the goal was to develop a prediction model based solely on information available at the time of prediction; while time-varying measures such as proteinuria during follow-up may be explanatory, they would not be known at the point when a prediction is made.

Fourth, covariate definitions may have limited their utility as predictors in the models. For example, although hypertension was included as a comorbidity, the actual measured blood pressures, which have been found to associate with kidney function decline in IgAN[2], were not available to be included. Therefore, a patient with a previous diagnosis of hypertension, who is considered exposed, could have well-controlled blood pressure at index, while another patient without a pre-existing diagnosis of hypertension, who is therefore considered unexposed, could

have elevated blood pressure at index. This potential misclassification bias could result in imprecise estimates that were biased toward the null. Like hypertension, diabetes was defined using diagnostic codes rather than contemporaneous glycemic measurements, which may not perfectly reflect the presence or severity of disease. Proteinuria values were obtained from a combination of 24-hour urine collections, spot urine PCRs, and ACRs. Conversion of spot measurements to 24-hour equivalents may have introduced measurement error, particularly at higher levels of proteinuria, where the correlation between spot measurements and 24-hour values is known to weaken[93].

Fifth, variable selection was guided by clinical relevance and prior literature rather than data-driven statistical procedures. While this approach aligns with current best practices for prediction modeling[114] and helps prevent overfitting, it may have limited the identification of additional empirically informative predictors within this dataset. A hybrid strategy incorporating penalization methods such as least absolute shrinkage and selection operator (LASSO), which adds a penalty term to coefficient values and shrinks unimportant predictors' coefficients to zero[115], could provide a useful balance between theoretical interpretability and data-driven optimization in future work.

Finally, our modeling approach assumed the change in eGFR to be linear with time. In reality, kidney function decline in IgA nephropathy may be non-linear, with periods of stability interspersed with acute declines related to disease activity and flares, or treatment. Although defining the index date at one year post-biopsy was intended to minimize the acute effects of early therapy, the analytic framework could not capture short-term or nonlinear changes in kidney function that may have prognostic importance.

Implications for future research

Our findings provide several insights that may improve the development and validation of models to predict eGFR slope in IgAN. In our modeling framework, random effects were estimated using the best linear unbiased predictors (BLUPs) to quantify each patient's deviation from the population mean, conditional on all observed eGFR measurements for that patient. Though this approach is widely accepted and statistically sound[116], in clinical practice, or in a validation dataset, these data are not available, as only previously collected eGFR values are known, if any are available at all. A potential extension of this analysis would be to estimate random effects from a patient's baseline and historical eGFR values to generate conditional, individualized predictions. This approach has been applied successfully in models predicting eGFR trajectories in diabetes[117] and lung function decline in chronic obstructive pulmonary disease[118]. These models employ a conditional prediction framework derived from the joint multivariate normal distribution of all possible values for an individual. Rather than explicitly estimating the random effects from the observed data, the covariance structure of the mixed model is used to update predictions dynamically as soon as one or more past measurements are available. Studies using this approach have demonstrated feasibility in generating predictions that are robust in cross-validation or external validation settings, and it is possible this approach could be utilized to build an accurate, generalizable prediction model for eGFR slope in IgAN.

A potential source of bias in the slope predictions relates to informative dropout. In this study, eGFR values only contributed to slope estimates if they were measured prior to the development of kidney failure. As the mixed-effects framework assumes that missing outcome data are missing at random and that dropout is ignorable, failure to account for informative dropout may bias mean slopes. More specifically, individual patient slopes may be associated

with the time-to-dropout, with the most negative slopes being associated with shorter time-to-dropout. If this phenomenon is not appropriately accounted for, mean slope estimates can be biased upward (i.e less negative). This has been demonstrated previously in an analysis of the Modified Diet in Renal Disease trial[119]. One approach to address this issue is shared-parameter modeling, in which the eGFR slope and time-to-dropout (kidney failure) are modeled jointly via a shared set of random effects[56]. Shared-parameter models have been demonstrated to provide less biased estimates of slope, but are computationally intensive, and were beyond the scope of this work. However, future studies focusing on slope prediction in IgAN should include a shared-parameter model as a sensitivity analysis to examine the degree to which slope estimates are biased by informative dropout due to kidney failure.

Conclusion

In summary, this study highlights the challenges of accurately predicting short-term eGFR decline in IgA nephropathy using routinely collected clinical and pathological data. While mixed-effects models reproduced individual trajectories well when all patient data were available, their predictive accuracy deteriorated substantially when applied to new patients or when random effects could not be reliably estimated. These findings underscore the central importance of the methods used to estimate and apply random effects, as they strongly influence both apparent model performance and true generalizability. Beyond these methodological insights, the study reinforces the dominant prognostic role of proteinuria and illustrates how data completeness, temporal alignment, and evolving biopsy and treatment practices shape the performance of longitudinal prediction models. Future research should focus on developing dynamic, externally validated frameworks that can update predictions as new eGFR data accrue

and more fully account for treatment effects and informative dropout, to move slope-based prediction closer to clinical applicability in IgA nephropathy.

Table 1. Baseline characteristics of patients with IgA nephropathy by era

Characteristic	Overall (n = 181)[1]	2002 to 2008 (n = 36)[1]	2009 to 2014 (n = 55)[1]	2015 to 2020 (n = 90)[1]
Age at cohort entry (years)	41 (31, 54)	38 (26, 47)	44 (32, 58)	42 (31, 56)
Sex				
Male	101 (56%)	21 (58%)	31 (56%)	49 (54%)
Female	80 (44%)	15 (42%)	24 (44%)	41 (46%)
Location of Residence				
Winnipeg	108 (60%)	27 (75%)	33 (60%)	48 (53%)
Outside of Winnipeg	73 (40%)	9 (25%)	22 (40%)	42 (47%)
SES Quintile				
1	62 (34%)	9 (25%)	19 (35%)	34 (38%)
2	36 (20%)	6 (17%)	13 (24%)	17 (19%)
3	30 (17%)	6 (17%)	7 (13%)	17 (19%)
4	36 (20%)	s	s	13 (14%)
5	17 (9.4%)	s	s	9 (10%)
eGFR at cohort entry (mL/min/1.73 m^2)	58 (35, 86)	67 (30, 98)	52 (31, 80)	58 (39, 87)
Missing	13 (7.2%)	8 (22%)	s	s
Proteinuria at cohort entry (g/day)	1.73 (1.06, 2.95)	1.71 (0.88, 2.85)	1.73 (1.04, 3.52)	1.77 (1.08, 2.61)
Missing	14 (7.7 %)	9 (25%)	s	s
Index eGFR (mL/min/1.73 m^2)	51 (31, 81)	66 (40, 87)	43 (27, 71)	55 (33, 84)
Missing	26 (14%)	7 (19%)	s	15 (17%)
Index proteinuria (g/day)	1.19 (0.53, 2.27)	0.70 (0.35, 2.22)	1.08 (0.47, 2.00)	1.61 (0.60, 2.56)
Missing	33 (18%)	8 (22%)	7 (13%)	18 (20%)
Nephrology consult to biopsy (days)	49 (8, 210)	38 (-16, 144)	62 (-7, 274)	49 (16, 233)
Diabetes	31 (17%)	s	10 (18%)	18 (20%)
Hypertension	83 (46%)	12 (33%)	25 (45%)	46 (51%)
RAASi treatment	160 (88%)	s	48 (87%)	78 (87%)
Glucocorticoid treatment	46 (25%)	12 (33%)	16 (29%)	18 (20%)
Oxford S				
0	50 (28%)	12 (33%)	16 (29%)	22 (24%)
1	131 (72%)	24 (67%)	39 (71%)	68 (76%)
Oxford T				
0	94 (52%)	25 (69%)	24 (44%)	45 (50%)
1	57 (31%)	11 (31%)	24 (44%)	22 (24%)
2	30 (17%)	0 (0%)	7 (13%)	23 (26%)
Oxford C (binary)				
0	132 (73%)	21 (58%)	39 (71%)	72 (80%)
1	49 (27%)	15 (42%)	16 (29%)	18 (20%)
Kidney failure status				
No kidney failure	148 (82%)	27 (75%)	46 (84%)	75 (83%)
Kidney failure	33 (18%)	9 (25%)	9 (16%)	15 (17%)
Vital status				

Alive	155 (86%)	28 (78%)	45 (82%)	82 (91%)
Dead	26 (14%)	8 (22%)	10 (18%)	8 (8.9%)
Follow up time (years)	8.2 (5.2, 12.6)	15.7 (14.5, 17.5)	10.7 (9.2, 12.8)	5.8 (4.2, 7.4)

[1]Median (Q1, Q3) are reported for continuous variables

SES, socioeconomic status; eGFR, estimated glomerular filtration rate; RAASi, renin-angiotensin-aldosterone system inhibitor; s, suppressed (cell size 5 or less)

Table 2. Baseline characteristics of patients with IgA nephropathy by sex

Characteristic	Male (n = 101)	Female (n = 80)
Age at cohort entry (years)	42 (32, 56)	41 (30, 52)
Location of Residence		
Winnipeg	58 (57%)	50 (63%)
Outside of Winnipeg	43 (43%)	30 (38%)
SES Quintile		
1	29 (29%)	33 (41%)
2	18 (18%)	18 (23%)
3	19 (19%)	11 (14%)
4	22 (22%)	s
5	13 (13%)	s
eGFR at cohort entry (mL/min/1.73 m^2)	58 (40, 81)	57 (32, 94)
Missing	s	8 (10%)
Proteinuria at cohort entry (g/day)	1.56 (0.97, 2.67)	1.92 (1.26, 3.44)
Missing	s	9 (11%)
Index eGFR (mL/min/1.73 m^2)	50 (30, 77)	54 (32, 84)
Missing	11 (11%)	15 (19%)
Index proteinuria (g/day)	1.08 (0.50, 1.94)	1.56 (0.60, 2.94)
Missing	15 (15%)	18 (23%)
Nephrology consult to biopsy (days)	38 (6, 206)	63 (11, 281)
Diabetes	14 (14%)	17 (21%)
Hypertension	48 (48%)	35 (44%)
RAASi treatment	89 (88%)	71 (89%)
Glucocorticoid treatment	23 (23%)	23 (29%)
Oxford S		
0	26 (26%)	24 (30%)
1	75 (74%)	56 (70%)
Oxford T		
0	45 (45%)	49 (61%)
1	38 (38%)	19 (24%)
2	18 (18%)	12 (15%)
Oxford C (binary)		
0	76 (75%)	56 (70%)
1	25 (25%)	24 (30%)
Kidney failure status		
No kidney failure	82 (81%)	66 (83%)
Kidney failure	19 (19%)	14 (18%)
Vital status		
Alive	84 (83%)	71 (89%)
Dead	17 (17%)	9 (11%)
Follow up time (years)	7.9 (4.9, 13.6)	8.4 (5.7, 11.9)

Results are reported as median (Q1, Q3) for continuous variables, and n (%) for categorical variables
SES, socioeconomic status; eGFR, estimated glomerular filtration rate; RAASi, renin-angiotensin-aldosterone system inhibitor; s, suppressed (cell size 5 or less)

Table 3. Baseline characteristics of patients with IgA nephropathy by kidney failure status over follow up

Characteristic	No kidney failure (n = 141)	Kidney failure (n = 33)
Age at cohort entry (years)	42 (30, 56)	40 (32, 49)
Sex		
Male	82 (55%)	19 (58%)
Female	66 (45%)	14 (42%)
Location of Residence		
Winnipeg	88 (59%)	20 (61%)
Outside of Winnipeg	60 (41%)	13 (39%)
SES Quintile		
1	45 (30%)	17 (52%)
2	33 (22%)	S
3	24 (16%)	6 (18%)
4	33 (22%)	s
5	13 (8.8%)	s
eGFR at cohort entry (mL/min/1.73 m^2)	64 (42, 91)	34 (23, 46)
Missing	12 (8.1%)	s
Proteinuria at cohort entry (g/day)	1.62 (1.03, 2.52)	2.41 (1.33, 3.44)
Missing	11 (7.4%)	s
Index eGFR (mL/min/1.73 m^2)	61 (40, 86)	17 (11, 29)
Missing	20 (14%)	6 (18%)
Index proteinuria (g/day)	0.82 (0.45, 1.82)	2.65 (2.02, 3.82)
Missing	26 (18%)	7 (21%)
Nephrology consult to biopsy (days)	49 (8, 163)	69 (-4, 287)
Diabetes	25 (17%)	6 (18%)
Hypertension	64 (43%)	19 (58%)
RAASi treatment	134 (91%)	26 (79%)
Glucocorticoid treatment	34 (23%)	12 (36%)
Oxford S		
0	38 (30%)	s
1	103 (70%)	s
Oxford T		
0	87 (59%)	7 (21%)
1	43 (29%)	14 (42%)
2	18 (12%)	12 (36%)
Oxford C (binary)		
0	111 (75%)	21 (64%)
1	37 (25%)	12 (36%)
Vital status		
Alive	131 (89%)	24 (73%)
Dead	17 (11%)	9 (27%)
Follow up time (years)	8.2 (5.0, 12.5)	8.2 (5.8, 13.9)

Results are reported as median (Q1, Q3) for continuous variables, and n (%) for categorical variables
SES, socioeconomic status; eGFR, estimated glomerular filtration rate; RAASi, renin-angiotensin-aldosterone system inhibitor; s, suppressed (cell size 5 or less)

Table 4. Baseline characteristics of patients with IgA nephropathy by CKD stage at cohort entry

Characteristic	CKD 1 (n = 37)	CKD 2 (n = 44)	CKD 3 (n = 60)	CKD 4 (n = 22)
Age at cohort entry (years)	29 (23, 37)	41 (30, 48)	45 (37, 55)	57 (43, 64)
Sex				
Male	16 (43%)	30 (68%)	37 (62%)	12 (55%)
Female	21 (57%)	14 (32%)	23 (38%)	10 (45%)
Location of Residence				
Winnipeg	23 (62%)	25 (57%)	37 (62%)	12 (55%)
Outside of Winnipeg	14 (38%)	19 (43%)	23 (38%)	10 (45%)
SES Quintile				
1	16 (43%)	13 (30%)	18 (30%)	9 (41%)
2	9 (24%)	10 (23%)	9 (15%)	s
3	s	10 (23%)	12 (20%)	s
4	6 (16%)	s	11 (18%)	s
5	s	s	10 (17%)	s
eGFR at cohort entry (mL/min/1.73 m^2)	108 (100, 116)	76 (65, 82)	44 (35, 48)	23 (21, 26)
Missing	s	s	s	s
Proteinuria at cohort entry (g/day)	1.86 (0.97, 2.41)	1.66 (1.02, 2.31)	1.75 (1.08, 3.09)	1.61 (1.16, 3.69)
Missing	s	s	s	s
Index eGFR (mL/min/1.73 m^2)	108 (87, 117)	67 (60, 74)	38 (29, 50)	21 (14, 35)
Missing	s	s	s	s
Index proteinuria (g/day)	1.06 (0.50, 2.22)	1.49 (0.66, 2.05)	1.48 (0.63, 2.44)	0.55 (0.38, 2.20)
Missing	s	9 (20%)	7 (12%)	s
Nephrology consult to biopsy (days)	98 (27, 354)	89 (15, 247)	41 (1, 162)	23 (6, 119)
Diabetes	s	7 (16%)	15 (25%)	s
Hypertension	10 (27%)	15 (34%)	36 (60%)	16 (73%)
RAASi treatment	33 (89%)	40 (91%)	57 (95%)	15 (68%)
Glucocorticoid treatment	9 (24%)	9 (20%)	14 (23%)	11 (50%)
Oxford S				
0	7 (19%)	13 (30%)	16 (27%)	s
1	30 (81%)	31 (70%)	44 (73%)	s
Oxford T				
0	35 (95%)	26 (59%)	16 (27%)	6 (27%)
1	s	s	31 (52%)	7 (32%)
2	s	s	13 (22%)	9 (41%)
Oxford C (binary)				
0	27 (73%)	34 (77%)	45 (75%)	15 (68%)
1	10 (27%)	10 (23%)	15 (25%)	7 (32%)
Kidney failure status				
No kidney failure	s	s	44 (73%)	12 (55%)
Kidney failure	s	s	16 (27%)	10 (45%)
Vital status				

Alive	s	s	53 (88%)	14 (64%)
Dead	s	s	7 (12%)	8 (36%)
Follow up time (years)	8.4 (6.2, 13.6)	7.8 (4.7, 10.8)	7.3 (4.9, 10.7)	8.1 (4.0, 12.0)

Results are reported as median (Q1, Q3) for continuous variables, and n (%) for categorical variables
SES, socioeconomic status; eGFR, estimated glomerular filtration rate; RAASi, renin-angiotensin-aldosterone system inhibitor; s, suppressed (cell size 5 or less)

Table 5. Baseline characteristics of patients with IgA nephropathy by location of residence at cohort entry

Characteristic	Out of Winnipeg (n = 73)	Winnipeg (n = 108)
Age at cohort entry (years)	41 (31, 58)	42 (31, 52)
Sex		
Male	43 (59%)	58 (54%)
Female	30 (41%)	50 (46%)
SES Quintile		
1	32 (44%)	30 (28%)
2	13 (18%)	23 (21%)
3	9 (12%)	21 (19%)
4	9 (12%)	27 (25%)
5	10 (14%)	7 (6.5%)
eGFR at cohort entry (mL/min/1.73 m^2)	58 (31, 84)	58 (37, 87)
Missing	9 (8.3%)	s
Proteinuria at cohort entry (g/day)	1.62 (1.03, 2.86)	1.76 (1.10, 2.95)
Missing	11 (10%)	s
Index eGFR (mL/min/1.73 m^2)	54 (31, 82)	50 (31, 81)
Missing	19 (18%)	7 (9.6%)
Index proteinuria (g/day)	1.15 (0.50, 2.02)	1.23 (0.55, 2.44)
Missing	18 (17%)	15 (21%)
Nephrology consult to biopsy (days)	50 (8, 255)	48 (8, 191)
Diabetes	12 (16%)	19 (18%)
Hypertension	34 (47%)	49 (45%)
RAASi treatment	62 (85%)	98 (91%)
Glucocorticoid treatment	18 (25%)	28 (26%)
Oxford S		
0	16 (22%)	34 (31%)
1	57 (78%)	74 (69%)
Oxford T		
0	37 (51%)	57 (53%)
1	21 (29%)	36 (33%)
2	15 (21%)	15 (14%)
Oxford C (binary)		
0	52 (71%)	80 (74%)
1	21 (29%)	28 (26%)
Kidney failure status		
No kidney failure	60 (82%)	88 (81%)
Kidney failure	13 (18%)	20 (19%)
Vital status		
Alive	58 (79%)	97 (90%)
Dead	15 (21%)	11 (10%)
Follow up time (years)	7.4 (4.5, 9.9)	9.1 (5.7, 13.8)

Results are reported as median (Q1, Q3) for continuous variables, and n (%) for categorical variables
SES, socioeconomic status; eGFR, estimated glomerular filtration rate; RAASi, renin-angiotensin-aldosterone system inhibitor; s, suppressed (cell size 5 or less)

Table 6. Baseline characteristics of patients with IgA nephropathy by SES quintile at cohort entry

Characteristic	1 (n = 62)	2 (n = 36)	3 (n = 30)	4 (n = 36)	5 (n = 17)
Age at cohort entry (years)	39 (29, 52)	44 (32, 58)	42 (34, 54)	46 (33, 54)	39 (29, 57)
Sex					
Male	29 (47%)	18 (50%)	19 (63%)	22 (61%)	s
Female	33 (53%)	18 (50%)	11 (37%)	14 (39%)	s
Location of Residence					
Winnipeg	32 (52%)	13 (36%)	9 (30%)	9 (25%)	10 (59%)
Outside of Winnipeg	30 (48%)	23 (64%)	21 (70%)	27 (75%)	7 (41%)
eGFR at cohort entry (mL/min/1.73 m^2)	59 (31, 91)	66 (43, 91)	58 (45, 80)	47 (30, 79)	43 (33, 62)
Missing	s	s	s	s	s
Proteinuria at cohort entry (g/day)	1.92 (1.17, 3.32)	1.84 (1.10, 2.63)	1.57 (1.06, 2.26)	1.75 (0.87, 4.39)	1.48 (0.97, 1.95)
Missing	s	s	s	s	s
Index eGFR (mL/min/1.73 m^2)	52 (25, 86)	50 (32, 92)	58 (30, 71)	62 (34, 80)	41 (32, 77)
Missing	8 (13%)	s	s	s	s
Index proteinuria (g/day)	1.48 (0.55, 2.67)	1.63 (0.74, 2.24)	1.10 (0.45, 2.09)	0.66 (0.29, 2.05)	1.36 (0.60, 1.67)
Missing	13 (21%)	s	s	s	s
Nephrology consult to biopsy (days)	38 (9, 175)	48 (3, 421)	96 (13, 214)	52 (8, 312)	41 (-4, 171)
Diabetes	13 (21%)	7 (19%)	15 (25%)	s	s
Hypertension	32 (52%)	13 (36%)	15 (50%)	15 (42%)	8 (47%)
RAASi treatment	51 (82%)	32 (89%)	26 (87%)	35 (97%)	16 (94%)
Glucocorticoid treatment	18 (29%)	7 (19%)	s	12 (33%)	s
Oxford S					
0	15 (24%)	15 (42%)	8 (27%)	9 (25%)	s
1	47 (76%)	21 (58%)	22 (73%)	27 (75%)	s
Oxford T					
0	34 (55%)	21 (58%)	16 (53%)	18 (50%)	s
1	14 (23%)	11 (31%)	11 (37%)	14 (39%)	7 (41%)
2	14 (23%)	s	s	s	s
Oxford C (binary)					
0	47 (76%)	25 (69%)	21 (70%)	24 (67%)	s
1	15 (24%)	11 (31%)	9 (30%)	12 (33%)	s
Kidney failure status					
No kidney failure	45 (73%)	s	24 (80%)	s	s
Kidney failure	17 (27%)	s	6 (20%)	s	s
Vital status					
Alive	52 (84%)	29 (81%)	s	s	s
Dead	10 (16%)	7 (19%)	s	s	s
Follow up time (years)	7.6 (5.2, 10.6)	7.8 (4.4, 11.2)	8.0 (5.7, 13.9)	11.0 (5.5, 15.4)	8.4 (5.7, 12.7)

Results are reported as median (Q1, Q3) for continuous variables, and n (%) for categorical variables
SES, socioeconomic status; eGFR, estimated glomerular filtration rate; RAASi, renin-angiotensin-aldosterone system inhibitor; s, suppressed (cell size 5 or less)

Table 7. Coefficients and standard errors from parsimonious mixed-effects linear regression model for eGFR.

Predictor	Coefficient	Standard error	95% CI	p-value
Marginal Intercept	**54.67**	**1.71**	**51.32, 58.02**	**<0.001**
Time	**-4.08**	**0.90**	**-5.84, -2.32**	**<0.001**
Index eGFR	**0.96**	**0.019**	**0.92, 1.00**	**<0.001**
Index Proteinuria	-0.50	0.43	-1.34, 0.34	0.251
Age	**-0.096**	**0.040**	**-0.17, -0.018**	**0.018**
Sex	-0.20	1.16	-2.47, 2.07	0.860
Index proteinuria*time	**-1.47**	**0.66**	**-2.76, -0.18**	**0.009**
Index eGFR*time	-0.0090	0.027	-0.062, 0.044	0.743
SD(Intercept|Patient)	6.21			
SD(Time|Patient)	9.86			
SD(Observations)	7.29			
AIC				145534
BIC				145629
Marginal R^2				0.81
Conditional R^2				0.95
RMSE				7.25

Values that are statistically significant at $\alpha = .05$ are presented in bold
Continuous covariates are mean-centred

Table 8. Coefficients and standard errors from treatment and trajectory mixed-effects linear regression model for eGFR.

Predictor	Coefficient	Standard error	95% CI	p-value
Marginal Intercept	**53.63**	**1.85**	**50.00, 57.26**	**<0.001**
Time	**-4.43**	**1.18**	**-6.74, -2.12**	**<0.001**
Index eGFR	**0.96**	**0.021**	**0.92, 1.00**	**<0.001**
Index Proteinuria	-0.73	0.48	-1.67, 0.21	0.134
Age	-0.078	0.043	-0.16, 0.01	0.071
Sex	-0.32	1.23	-2.73, 2.09	0.793
Delta-proteinuria	0.092	0.24	-0.38, 0.56	0.698
Delta-eGFR	0.057	0.043	-0.027, 0.14	0.191
Duration of time to biopsy (days)	**0.0016**	**0.00075**	**-0.00013, 0.0031**	**0.030**
Corticosteroids	1.73	1.33	-0.88, 4.34	0.195
Index proteinuria*time	**-1.72**	**0.72**	**-3.13, -0.31**	**0.016**
Index eGFR*time	-0.011	0.030	-0.070, 0.048	0.709
Steroids*time	0.86	2.04	-3.14, 4.86	0.674
SD(Intercept|Patient)	6.08			
SD(Time|Patient)	11.236			
SD(Observations)	7.31			
AIC				145082
BIC				145217
Marginal R^2				0.81
Conditional R^2				0.95
RMSE				7.31

Values that are statistically significant at $\alpha = .05$ are presented in bold
Continuous covariates are mean-centred

Table 9. Coefficients and standard errors from full clinical mixed-effects linear regression model for eGFR.

Predictor	Coefficient	Standard error	95% CI	p-value
Marginal Intercept	**52.90**	**2.00**	**48.98, 56.82**	**<0.001**
Time	**-5.29**	**1.42**	**-8.07, -2.51**	**<0.001**
Index eGFR	**0.96**	**0.021**	**0.92, 1.00**	**<0.001**
Index Proteinuria	-0.86	0.50	-1.84, 0.12	0.090
Age	-0.086	0.046	-0.18, 0.004	0.065
Sex	-0.35	1.24	-2.78, 2.08	0.781
Delta-proteinuria	0.10	0.24	-0.37, 0.57	0.673
Delta-eGFR	0.076	0.046	-0.014, 0.17	0.101
Duration of time to biopsy (days)	**0.0018**	**0.00077**	**0.00029, 0.0033**	**0.021**
Corticosteroids	1.60	1.35	-1.05, 4.25	0.238
Hypertension	1.38	1.32	-1.21, 3.97	0.298
Diabetes	-0.70	1.73	-4.09, 2.69	0.688
Index proteinuria*time	**-1.92**	**0.74**	**-3.37, -0.47**	**0.009**
Index eGFR*time	-0.013	0.030	-0.072, 0.046	0.661
Delta-eGFR*time	-0.073	0.067	-0.20, 0.059	0.274
Steroids*time	0.12	2.15	-4.09, 4.33	0.954
SD(Intercept|Patient)	6.31			
SD(Time|Patient)	10.24			
SD(Observations)	7.35			
AIC				145084
BIC				145243
Marginal R^2				0.80
Conditional R^2				0.95
RMSE				7.31

Values that are statistically significant at $\alpha = .05$ are presented in bold
Continuous covariates are mean-centred

Table 10. Coefficients and standard errors from full clinicopathological mixed-effects linear regression model for eGFR.

Predictor	Coefficient	Standard error	95% CI	p-value
Marginal Intercept	**51.38**	**2.53**	**46.42, 56.34**	**<0.001**
Time	-1.66	2.41	-6.38, 3.06	0.491
Index eGFR	**0.96**	**0.024**	**0.91, 1.00**	**<0.001**
Index Proteinuria	-0.97	0.50	-1.95, 0.01	0.058
Age	-0.079	0.046	-0.17, 0.011	0.092
Sex	-0.39	1.26	-2.86, 2.08	0.755
Delta-proteinuria	0.044	0.24	-0.43, 0.51	0.856
Delta-eGFR	0.076	0.048	-0.018, 0.17	0.115
Duration of time to biopsy (days)	**0.0019**	**0.00079**	**0.00035, 0.0034**	**0.020**
Corticosteroids	1.48	1.44	-1.34, 4.30	0.305
Hypertension	1.54	1.33	-1.07, 4.15	0.249
Diabetes	-0.85	1.84	-4.46, 2.76	0.646
Oxford S	2.59	1.40	-0.15, 5.33	0.066
Oxford T1	-0.37	1.52	-3.35, 2.61	0.810
Oxford T2	-0.69	1.93	-4.47, 3.09	0.736
Oxford C1 or 2	-0.37	1.54	-3.39, 2.65	0.813
Index proteinuria*time	**-1.78**	**0.74**	**-3.23, -0.33**	**0.016**
Index eGFR*time	-0.028	0.033	-0.093, 0.037	0.404
Steroids*time	1.84	2.25	-2.57, 6.25	0.414
Delta-eGFR*time	0.087	0.069	-0.048, 0.22	0.207
Oxford S*time	-2.35	2.17	-6.60, 1.90	0.279
Oxford T1*time	-1.34	2.26	-5.77, 3.09	0.553
Oxford T2*time	-4.38	2.98	-10.22, 1.46	0.142
Oxford C*time	**-4.61**	**2.32**	**-9.16, -0.063**	**0.047**
SD(Intercept|Patient)	6.31			
SD(Time|Patient)	10.05			
SD(Observations)	7.35			
AIC				145063
BIC				145286
Marginal R^2				0.80
Conditional R^2				0.95
RMSE				7.31

Values that are statistically significant at $\alpha = .05$ are presented in bold
Continuous covariates are mean-centred

Table 11. Coefficients and standard errors from parsimonious mixed-effects linear regression model for eGFR by era.

Predictor	Era 1 (2002 to 2008)	Era 2 (2009 to 2014)	Era 3 (2015 to 2020)
Marginal Intercept	**52.24** **(3.98)**	**55.60** **(3.28)**	**53.67** **(2.80)**
Time	**-7.30** **(1.36)**	**-3.56** **(1.26)**	**-3.37** **(1.62)**
Index eGFR	**0.99** **(0.040)**	**0.96** **(0.041)**	**0.96** **(0.028)**
Index Proteinuria	-1.74 (1.22)	-0.29 (0.76)	-0.49 (0.65)
Age	-0.059 (0.091)	-0.104 (0.078)	-0.091 (0.062)
Sex	0.343 (2.67)	-0.72 (2.16)	0.74 (1.88)
Index proteinuria*time	**-3.14** **(1.06)**	-0.74 (0.90)	**-2.32** **(1.18)**
Index eGFR*time	0.027 (0.035)	0.015 (0.045)	-0.028 (0.048)
SD(Intercept|Patient)	5.30	6.70	6.46
SD(Time|Patient)	5.15	7.99	12.31
SD(Observations)	6.42	5.85	8.37
AIC	22841	48133	78328
BIC	22915	48216	78415
Marginal R^2	0.92	0.80	0.77
Conditional R^2	0.96	0.96	0.94
RMSE	6.37	5.81	8.32

Data are presented as coefficient (standard error)
Values that are statistically significant at $\alpha = .05$ are presented in bold
Continuous covariates are mean-centred

Table 12. Coefficients and standard errors from full clinicopathological mixed-effects linear regression model for eGFR by era.

Predictor	Era 1 (2002 to 2008)	Era 2 (2009 to 2014)	Era 3 (2015 to 2020)
Marginal Intercept	**42.56 (10.27)**	**47.84 (4.95)**	**52.53 (3.95)**
Time	-1.90 (3.00)	0.48 (2.95)	-3.12 (5.02)
Index eGFR	**0.92 (0.11)**	**0.96 (0.051)**	**0.94 (0.031)**
Index Proteinuria	-7.01 (3.77)	-1.28 (0.99)	-1.083 (0.68)
Age	-0.25 (0.19)	-0.082 (0.096)	-0.098 (0.063)
Sex	3.64 (7.04)	0.22 (2.31)	-0.66 (1.91)
Delta-proteinuria	2.11 (1.67)	0.056 (0.30)	1.09 (0.59)
Delta-eGFR	-0.053 (0.12)	**0.29 (0.092)**	-0.014 (0.074)
Duration of time to biopsy (days)	0.003 (0.003)	0.001 (0.001)	**0.005 (0.001)**
Corticosteroids	4.08 (4.70)	3.58 (2.65)	2.06 (2.29)
Hypertension	-9.18 (6.57)	0.51 (2.51)	2.13 (1.90)
Diabetes	15.54 (10.99)	0.12 (3.29)	1.14 (2.64)
Oxford S	5.48 (5.09)	0.28 (2.67)	2.64 (2.19)
Oxford T1	9.57 (8.87)	1.33 (2.98)	0.46 (2.29)
Oxford T2	-	4.37 (4.96)	-0.69 (4.72)
Oxford C1 or 2	-3.20 (4.45)	-3.40 (2.95)	1.49 (2.41)
Index proteinuria*time	-1.49 (1.24)	-0.82 (1.09)	**-2.79 (1.26)**
Index eGFR*time	0.009 (0.044)	-0.010 (0.054)	-0.046 (0.057)
Steroids*time	2.98 (2.23)	-2.23 (2.97)	4.61 (4.58)
Delta-eGFR*time	-0.066 (0.060)	0.081 (0.098)	0.13 (0.14)
Oxford S*time	-0.14 (2.74)	-2.76 (3.07)	1.59 (4.36)
Oxford T1*time	-1.45 (2.47)	-3.17 (3.34)	1.30 (4.26)
Oxford T2*time	-	**-12.64 (5.44)**	-3.76 (4.72)

Oxford C*time	**-8.82 (2.34)**	-0.75 (3.48)	-5.04 (4.28)
SD(Intercept|Patient)	5.79	6.57	6.14
SD(Time|Patient)	3.56	7.86	12.76
SD(Observations)	6.44	5.84	8.45
AIC	20545	46948	76304
BIC	20702	47141	76508
Marginal R^2		0.80	0.74
Conditional R^2		0.96	0.94
RMSE	6.40	5.80	8.40

Data are presented as coefficient (standard error)
Values that are statistically significant at $\alpha = .05$ are presented in bold
Continuous covariates are mean-centred
Note that no patients in Era 1 have IFTA = 2

Table 13. Coefficients and standard errors from parsimonious mixed-effects linear regression model for eGFR using imputed datasets.

Predictor	Coefficient	Standard error	95% CI	p-value
Marginal Intercept	**54.97**	**1.14**	**52.74, 57.20**	**<0.001**
Time	**-4.13**	**0.79**	**-5.68, -2.58**	**<0.001**
Index eGFR	**0.94**	**0.029**	**0.88, 1.00**	**<0.001**
Index Proteinuria	0.22	0.65	-1.05, 1.49	0.73
Age	0.008	0.064	-0.12, 0.13	0.90
Sex	-1.33	1.74	-4.74, 2.08	0.45
Index proteinuria*time	**-1.42**	**0.57**	**-2.54, -0.30**	**0.01**
Index eGFR*time	0.0046	0.024	-0.042, 0.052	0.85
SD(Intercept|Patient)	11.11			
SD(Time|Patient)	10.05			
SD(Observations)	7.07			
AIC				171685
BIC				171782
Marginal R^2				0.74
Conditional R^2				0.95
RMSE				7.02

Values that are statistically significant at $\alpha = .05$ are presented in bold
Continuous covariates are mean-centred

Table 14. Coefficients and standard errors from full clinicopathological mixed-effects linear regression model for eGFR using imputed datasets.

Predictor	Coefficient	Standard error	95% CI	p-value
Marginal Intercept	**54.80**	**3.69**	**47.57, 62.03**	**<0.001**
Time	-0.19	2.15	-4.40, 4.02	0.928
Index eGFR	**0.92**	**0.034**	**0.85, 0.99**	**<0.001**
Index Proteinuria	-0.48	0.73	-1.91, 0.95	0.514
Age	-0.053	0.068	-0.19, 0.080	0.432
Sex	-1.28	1.75	-4.71. 2.15	0.466
Delta-proteinuria	0.28	0.37	-0.45, 1.00	0.455
Delta-eGFR	-0.0076	0.069	-0.14, 0.13	0.913
Duration of time to biopsy (days)	0.00043	0.00087	-0.0013, 0.0021	0.618
Corticosteroids	1.49	2.15	-2.72, 5.70	0.488
Hypertension	1.94	1.86	-1.71, 5.59	0.300
Diabetes	1.41	2.40	-3.29, 6.11	0.557
Oxford S	0.26	1.99	-3.64, 4.16	0.896
Oxford T1	-1.53	2.21	-5.86, 2.80	0.491
Oxford T2	-2.87	2.78	-8.32, 2.58	0.304
Oxford C1 or 2	2.42	2.23	-1.95, 6.79	0.280
Index proteinuria*time	**-1.39**	**0.63**	**-2.62, -0.16**	**0.028**
Index eGFR*time	-0.047	0.029	-0.10, 0.0098	0.104
Steroids*time	1.84	2.03	-2.14, 5.82	0.366
Delta-eGFR*time	0.0052	0.062	-0.12, 0.13	0.933
Oxford S*time	**-3.76**	**1.84**	**-7.37, -0.15**	**0.041**
Oxford T1*time	-2.01	2.05	-6.03, 2.01	0.327
Oxford T2*time	-4.89	2.65	-10.08, 0.30	0.065
Oxford C*time	-1.97	2.05	-5.99, 2.05	0.338
SD(Intercept|Patient)	10.89			
SD(Time|Patient)	10.35			
SD(Observations)	7.07			
AIC				171097
BIC				171325
Marginal R^2				0.70
Conditional R^2				0.95
RMSE				7.03

Values that are statistically significant at $\alpha = .05$ are presented in bold
Continuous covariates are mean-centred

Table 15. Summary of observed and predicted eGFR slopes

Statistic	Conditional predicted (n = 137)	Marginal predicted (n = 137)	Overall observed (n = 181)	Era 1 observed (n = 36)	Era 2 observed (n = 55)	Era 3 observed (n = 90)
Mean (SD)	-3.93 (10.01)	-3.99 (2.39)	-5.07 (12.70)	-4.68 (8.82)	-5.15 (11.50)	-5.18 (14.60)
Median (IQR)	-3.87 (-8.88, 1.17)	-3.41 (-5.16, -2.21)	-4.04 (-10.10, 1.14)	-4.04 (-10.60, 0.49)	-4.74 (-9.41, 0.77)	-2.88 (-9.39, 1.50)
Range	-44.31, 33.44	-14.93, -1.13	-69.0, 35.1	-23.0, 21.6	-50.8, 15.2	-69.0, 35.1

SD, standard deviation; IQR, interquartile range

Table 16. Apparent performance metrics for eGFR slope predictions generated from each model.

Metric	Parsimonious	Treatment and trajectory	Full Clinical	Full Clinicopathologic
Conditional				
RMSE	6.41	6.54	6.31	6.93
Correlation	0.88	0.88	0.88	0.87
Calibration slope (95% CI)	1.15 (1.04, 1.26)	1.14 (1.03, 1.26)	1.14 (1.04, 1.25)	1.14 (1.02, 1.26)
Within 1 mL/min/year	88%	83%	69%	74%
Marginal				
RMSE	12.31	12.69	12.65	12.60
Correlation	0.30	0.28	0.28	0.31
Calibration slope (95% CI)	1.58 (0.71, 2.44)	1.55 (0.60, 2.51)	1.39 (0.54, 2.25)	1.19 (0.54, 1.84)
Within 1 mL/min/year	11%	10%	14%	10%

RMSE, root mean squared error; CI, confidence interval

Table 17. Apparent performance metrics for eGFR slope predictions generated from each model using imputed datasets.

Metric	Parsimonious	Full Clinicopathologic
Conditional		
RMSE	8.96	11.20
Correlation	0.79	0.79
Calibration slope (95% CI)	1.15 (1.02, 1.28)	1.33 (1.18, 1.49)
Within 1	77%	78%
Marginal		
RMSE	14.09	17.11
Correlation	0.18	0.14

Calibration slope (95% CI)	1.23 (0.24, 2.24)	1.03 (-0.04, 2.10)
Within 1	11%	11%

RMSE, root mean squared error; CI, confidence interval

Table 18. Apparent and cross-validated performance metrics of eGFR slope prediction model (parsimonious model, conditional predictions)

Performance metric	Apparent performance	Standard error	Cross-validated performance	Standard deviation	Optimism
RMSE	6.41		12.11	5.40	5.70
Pearson correlation	0.88		-0.15	0.24	1.03
Calibration slope	1.14	0.11	0.79	21.92	0.35

RMSE, root mean squared error

Table 19. Apparent and cross-validated performance metrics of eGFR slope prediction model (parsimonious model, marginal predictions)

Performance metric	Apparent performance	Standard error	Cross-validated performance	Standard deviation	Optimism
RMSE	12.31		11.98	4.69	0.33
Pearson correlation	0.30		0.24	0.46	0.06
Calibration slope	1.58	0.44	1.89	3.88	0.31

RMSE, root mean squared error

Table 20. Coefficients and standard errors from parsimonious mixed-effects linear regression model for eGFR fit with variance components variance-covariance structure.

Predictor	Coefficient	Standard error	95% CI	p-value
Marginal Intercept	**54.44**	**1.71**	**51.09, 57.79**	**<0.001**
Time	**-4.07**	**0.90**	**-5.83, -2.31**	**<0.001**
Index eGFR	**0.96**	**0.019**	**0.92, 1.00**	**<0.001**
Index Proteinuria	-0.49	0.43	-1.33, 0.35	0.251
Age	**-0.092**	**0.040**	**-0.17, -0.014**	**0.018**
Sex	-0.038	1.16	-2.31, 2.24	0.860
Index proteinuria*time	**-1.73**	**0.67**	**-3.04, -0.42**	**0.009**
Index eGFR*time	-0.0093	0.028	-0.064, 0.046	0.743
SD(Intercept|Patient)	6.21			
SD(Time|Patient)	9.88			
SD(Observations)	7.29			
AIC				150469
BIC				150558
Marginal R^2				0.81
Conditional R^2				0.95
RMSE				7.25

Values that are statistically significant at α = .05 are presented in bold

Table 21. Coefficients and standard errors from parsimonious mixed-effects linear regression model for eGFR fit with index date set at 180 days post-kidney biopsy.

Predictor	Coefficient	Standard error	95% CI	p-value
Marginal Intercept	**56.98**	**1.66**	**53.73, 60.23**	**<0.001**
Time	**-4.80**	**0.84**	**-6.45, -3.15**	**<0.001**
Index eGFR	**0.97**	**0.019**	**0.93, 1.00**	**<0.001**
Index Proteinuria	**-1.01**	**0.34**	**-1.68, -0.34**	**0.004**
Age	**0.057**	0.039	-0.019, 0.13	0.147
Sex	0.29	1.12	-1.91, 2.49	0.798
Index proteinuria*time	**-1.70**	**0.51**	**-2.70, -0.70**	**0.001**
Index eGFR*time	-0.012	0.025	-0.061, 0.037	0.637
SD(Intercept|Patient)	6.34			
SD(Time|Patient)	10.01			
SD(Observations)	9.16			
AIC				205910
BIC				206009
Marginal R^2				0.82
Conditional R^2				0.93
RMSE				9.12

Values that are statistically significant at α = .05 are presented in bold

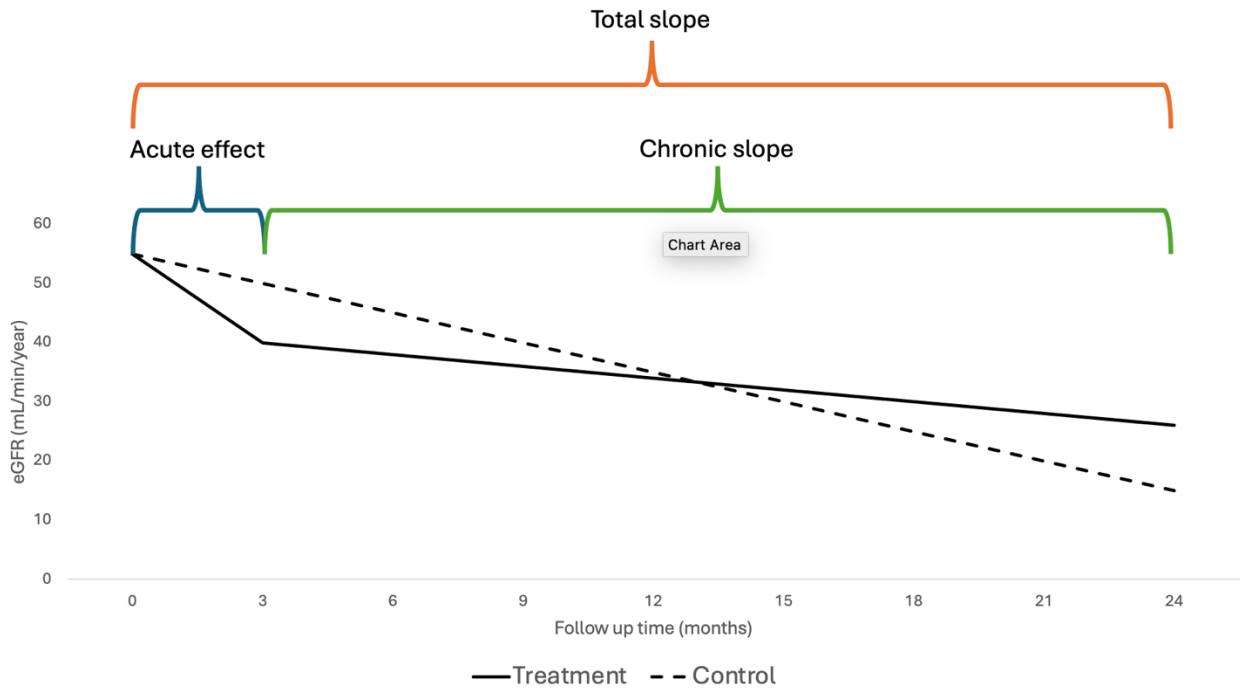

Figure 1. Total versus chronic slope in IgA nephropathy

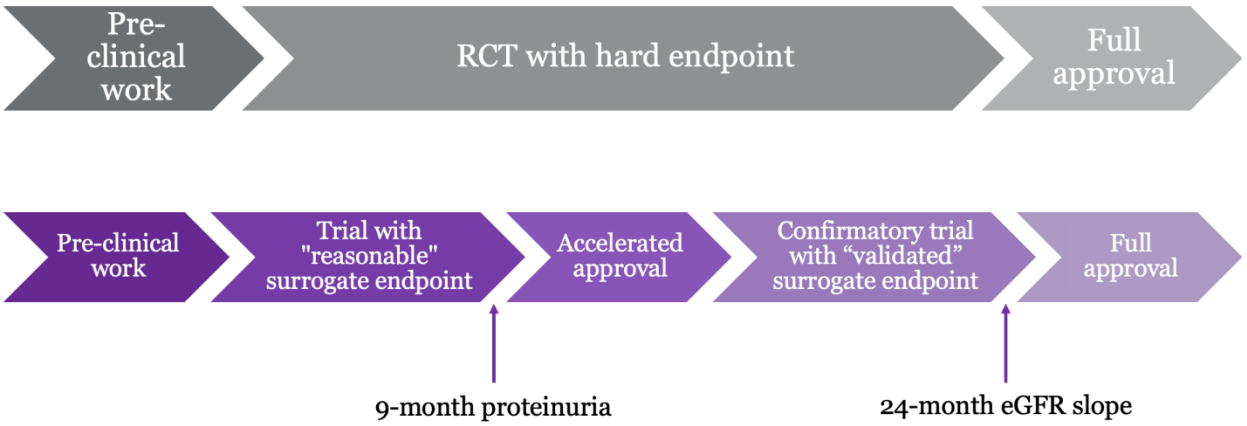

Figure 2. Surrogate outcomes in IgA nephropathy

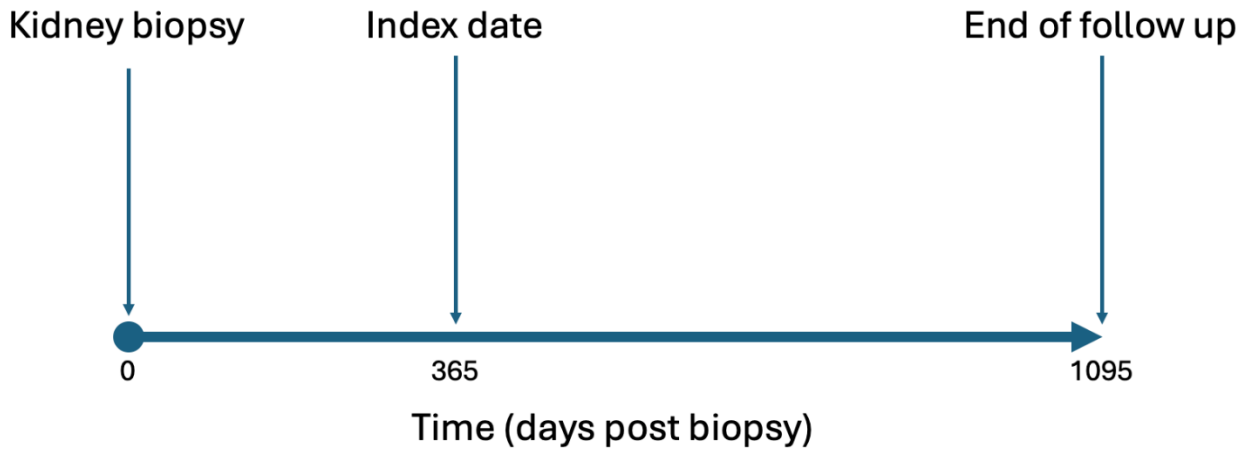

Figure 3. Overview of study design

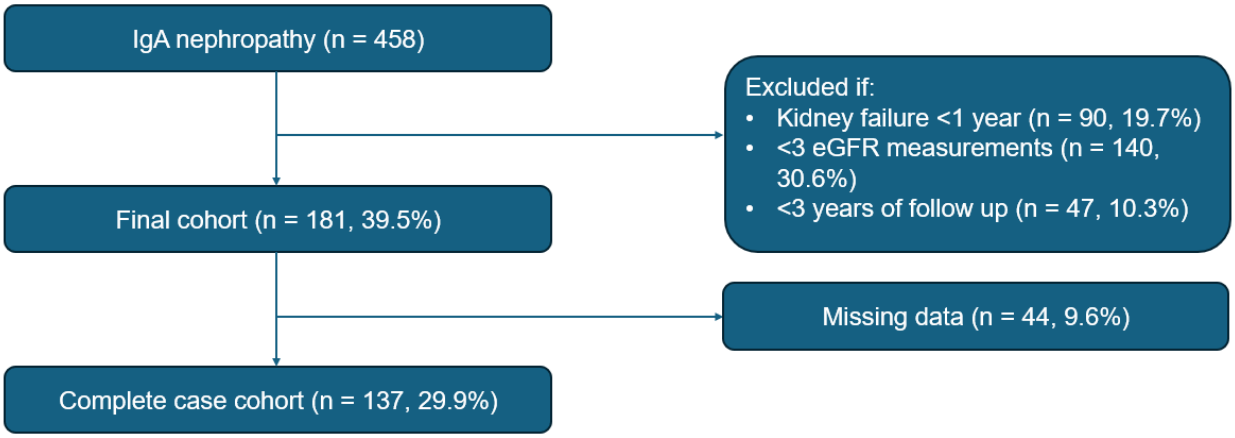

Figure 4. Cohort Flow Diagram

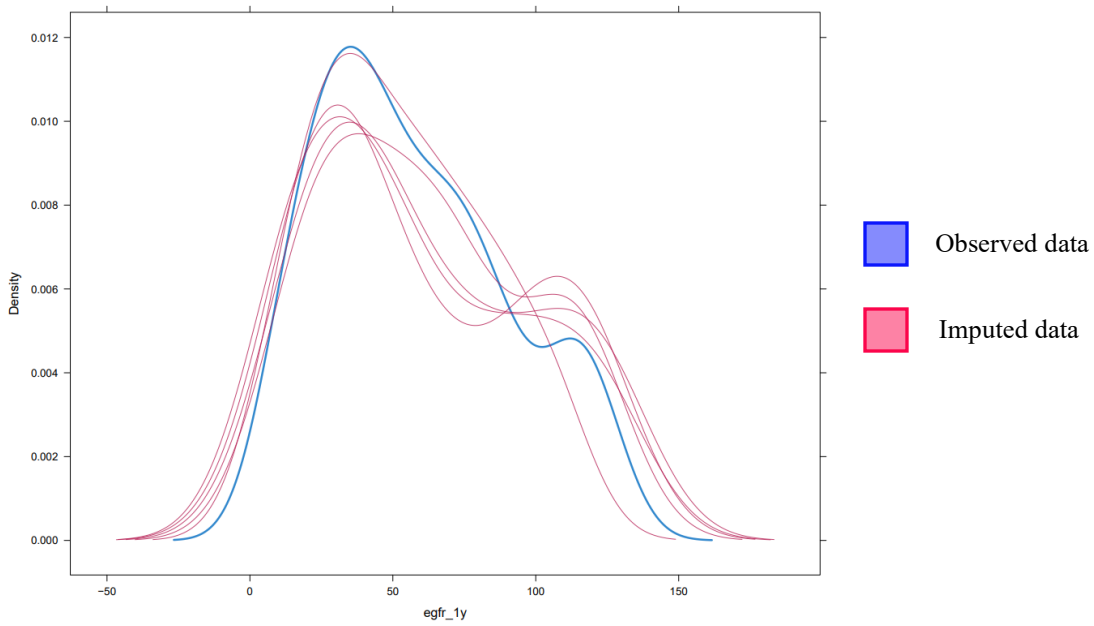

Figure 5. Density distribution of observed and imputed index eGFR values

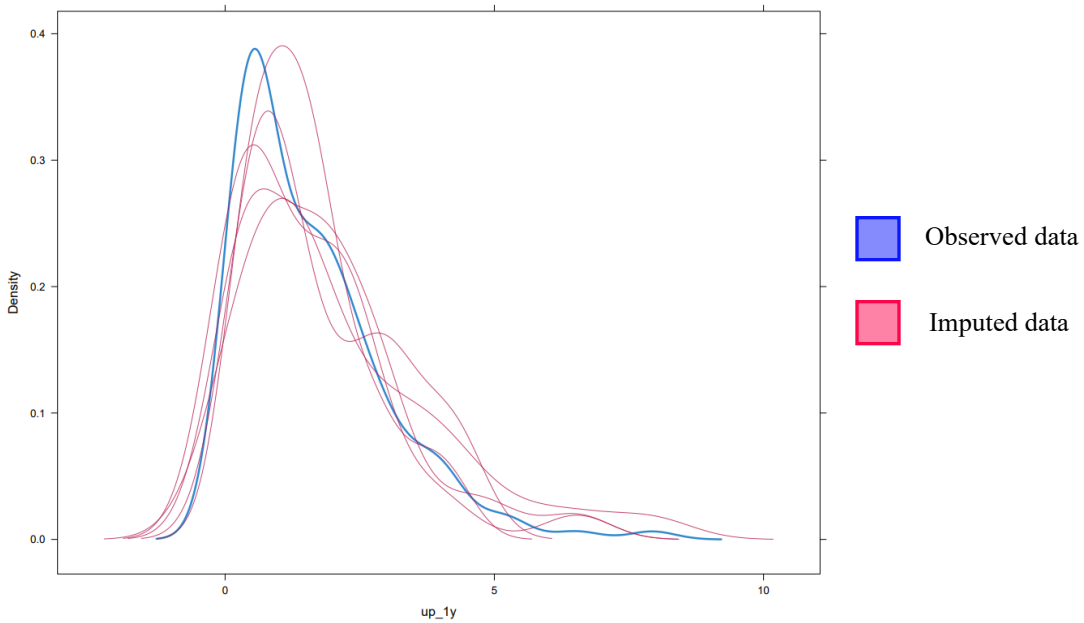

Figure 6. Density distribution of observed and imputed index proteinuria values

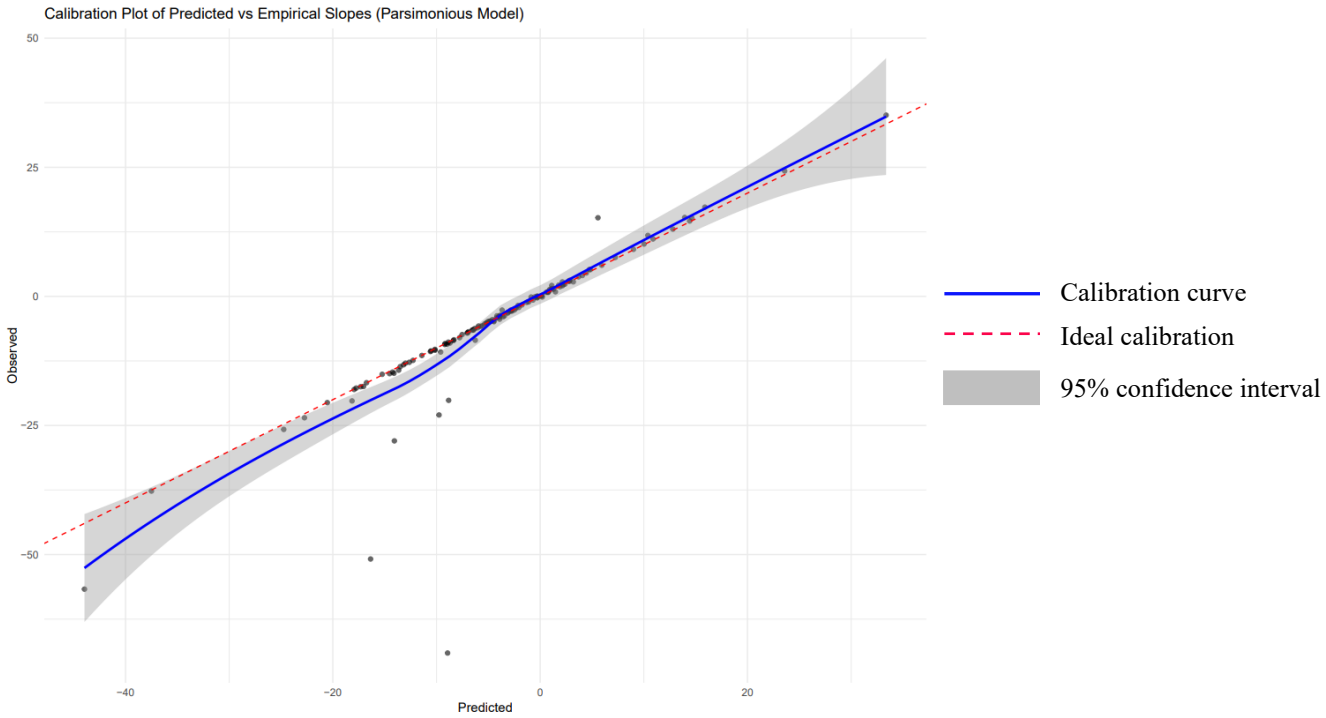

Figure 7. Calibration plot of conditional predicted versus observed eGFR slopes from the Parsimonious Model

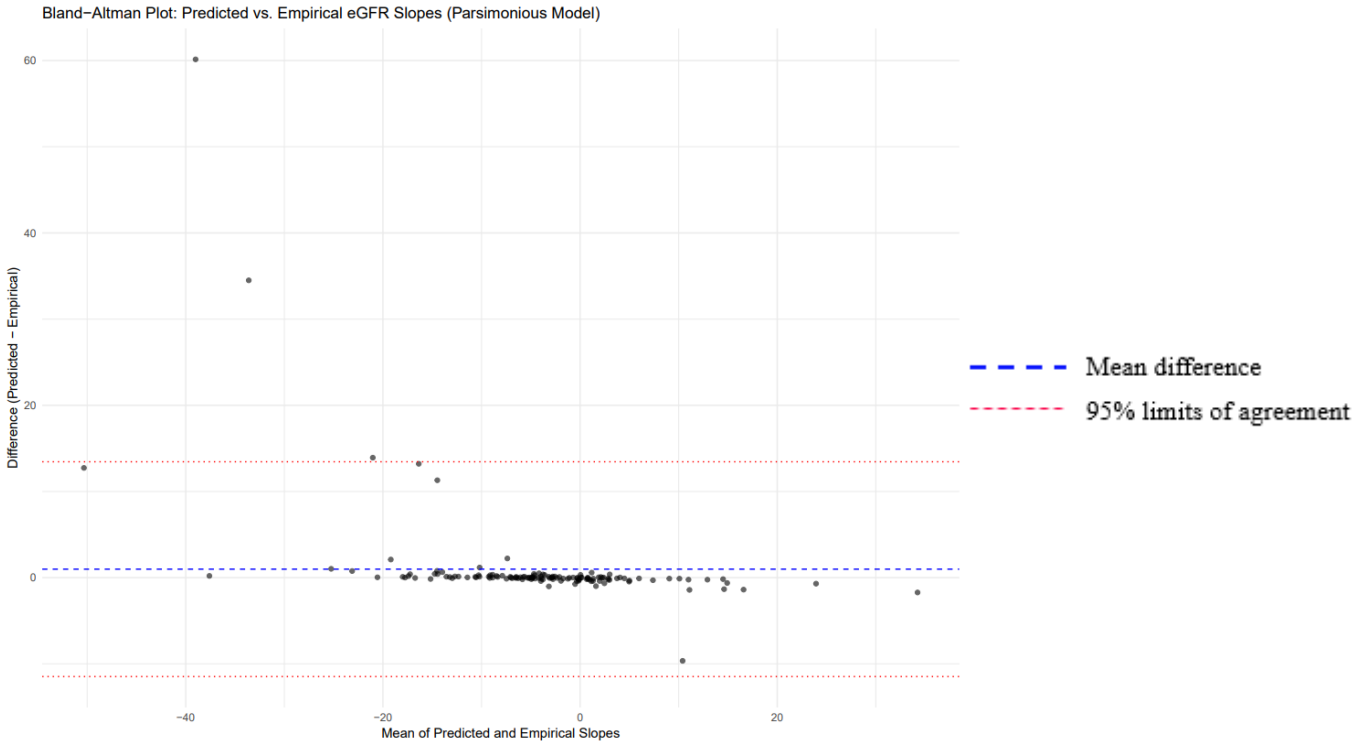

Figure 8. Bland–Altman analysis of conditional predicted versus observed eGFR slopes (Parsimonious Model)

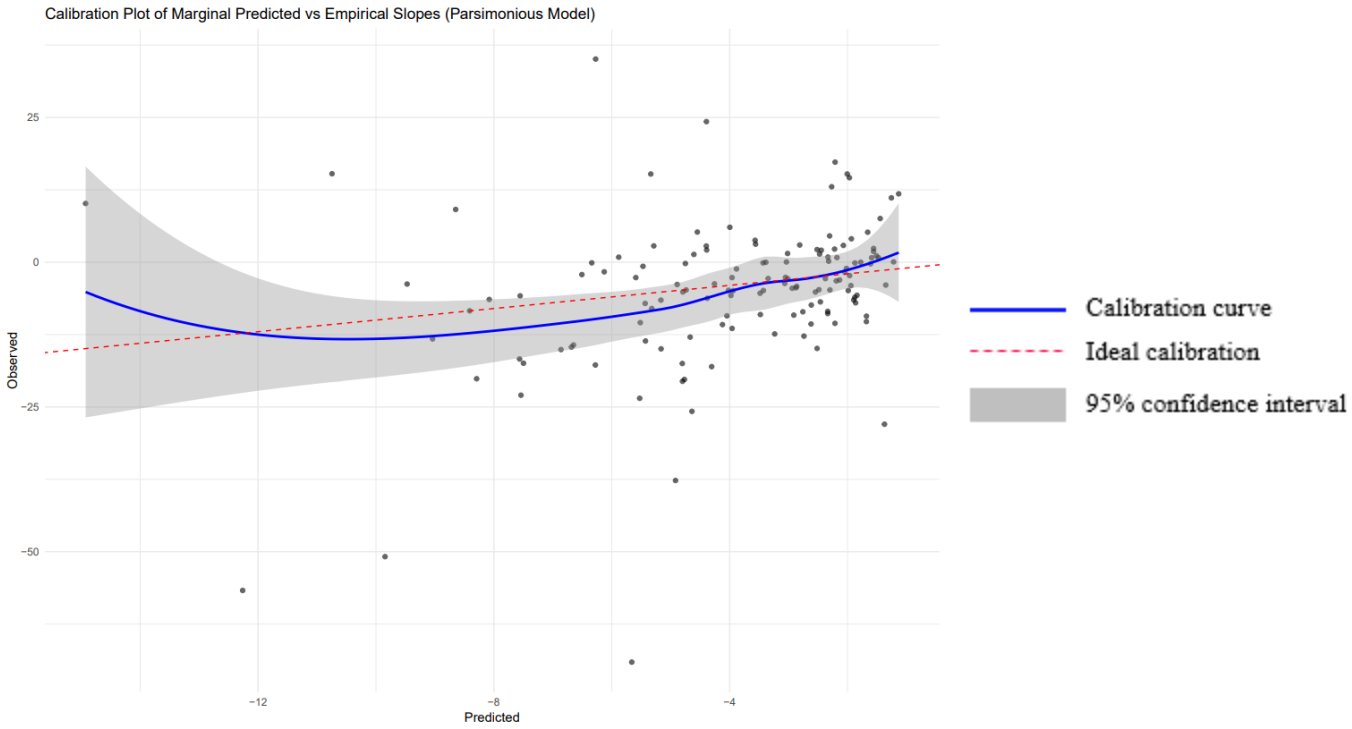

Figure 9. Calibration plot of marginal predicted versus observed eGFR slopes from the Parsimonious Model

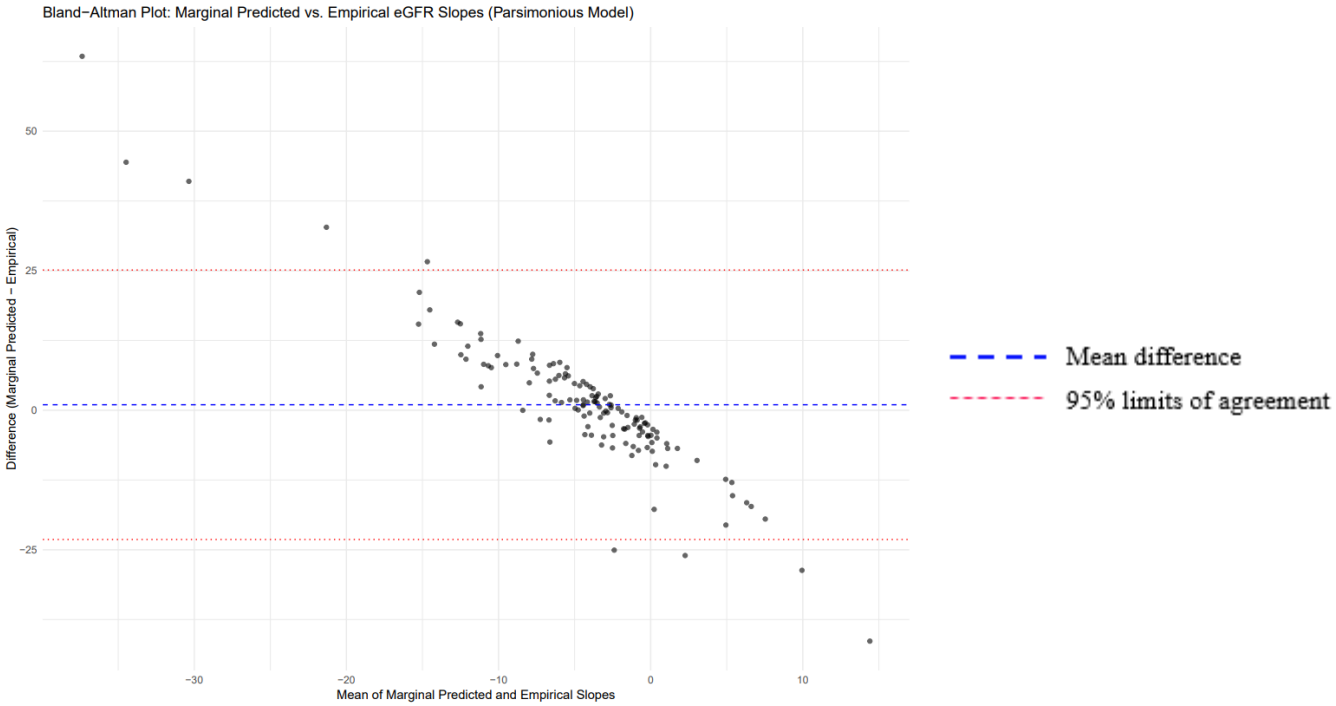

Figure 10. Bland–Altman analysis of marginal predicted versus observed eGFR slopes (Parsimonious Model)

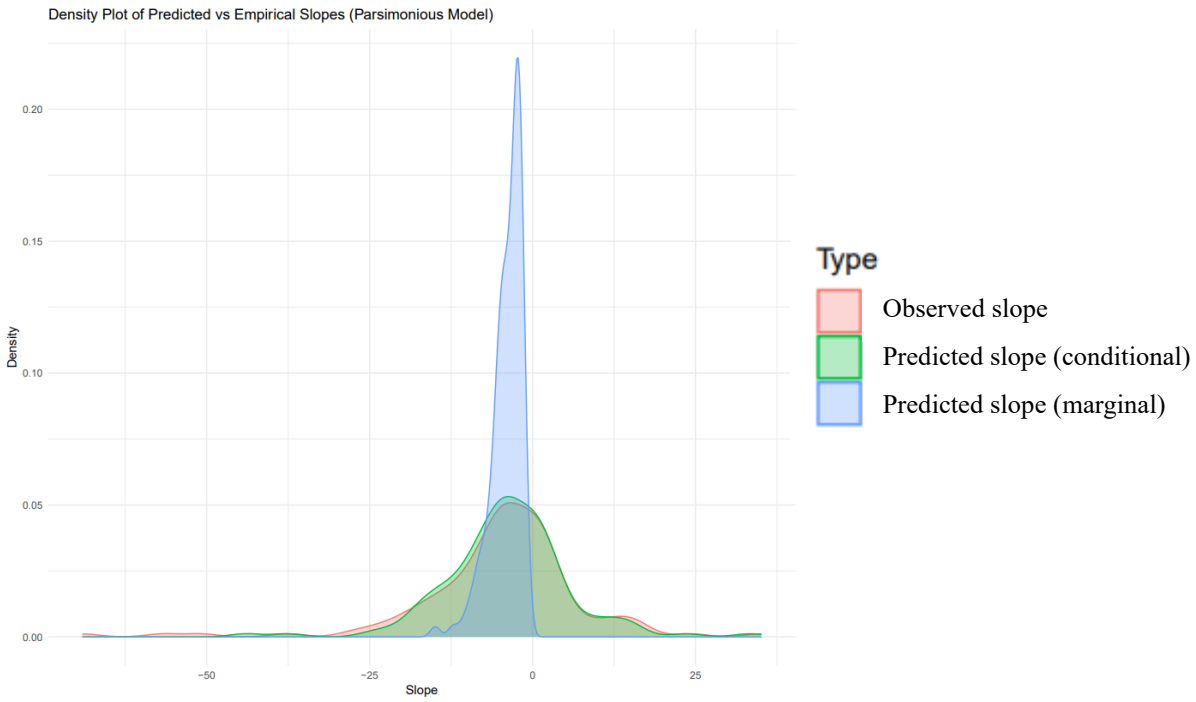

Figure 11. Density plot of conditional and marginal predicted versus observed eGFR slopes from Parsimonious Model

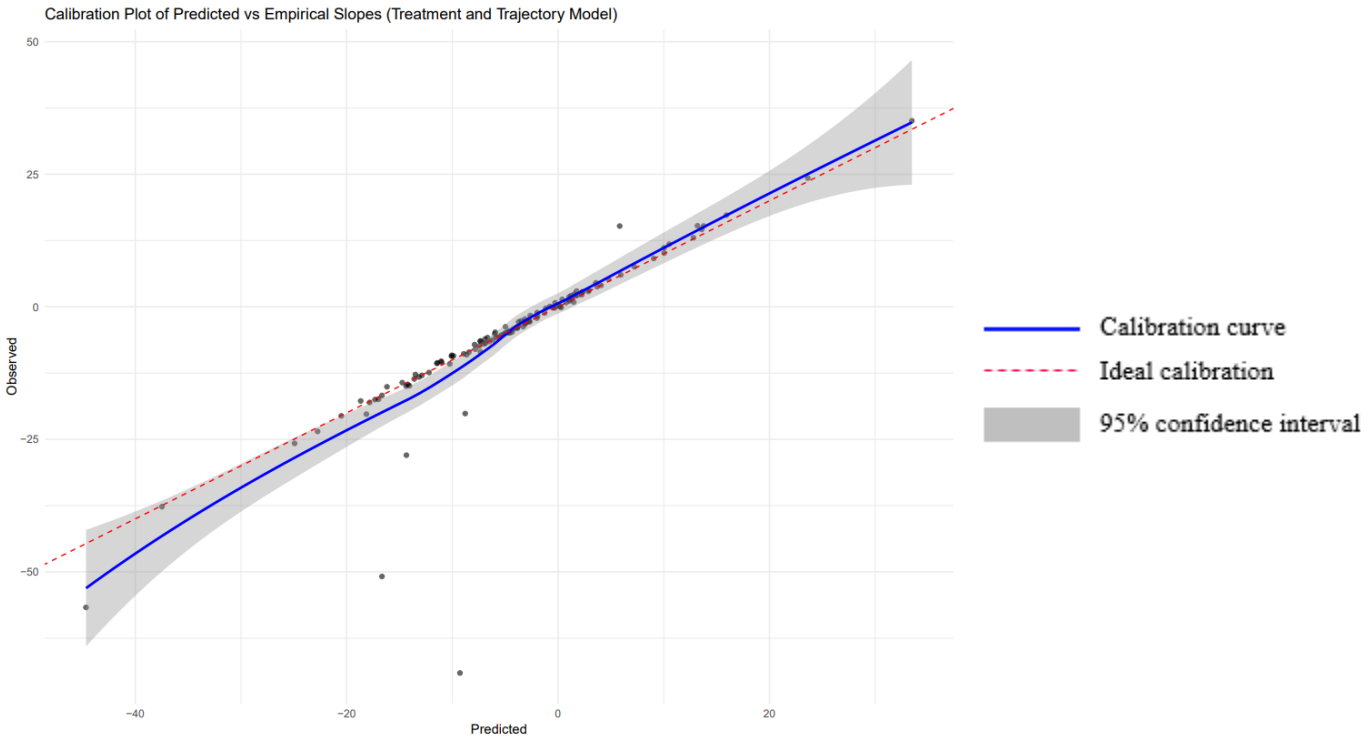

Figure 12. Calibration plot of conditional predicted versus observed eGFR slopes from the Treatment and Trajectory Model

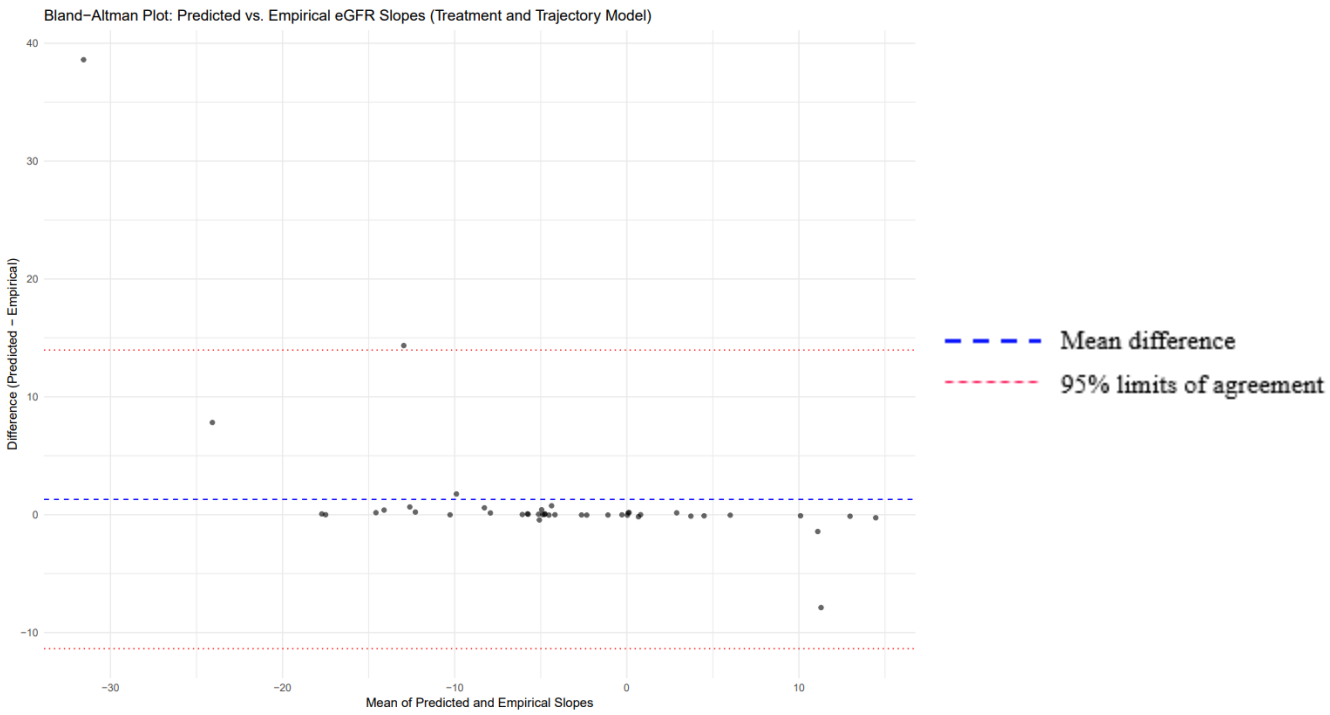

Figure 13. Bland–Altman analysis of conditional predicted versus observed eGFR slopes (Treatment and Trajectory Model)

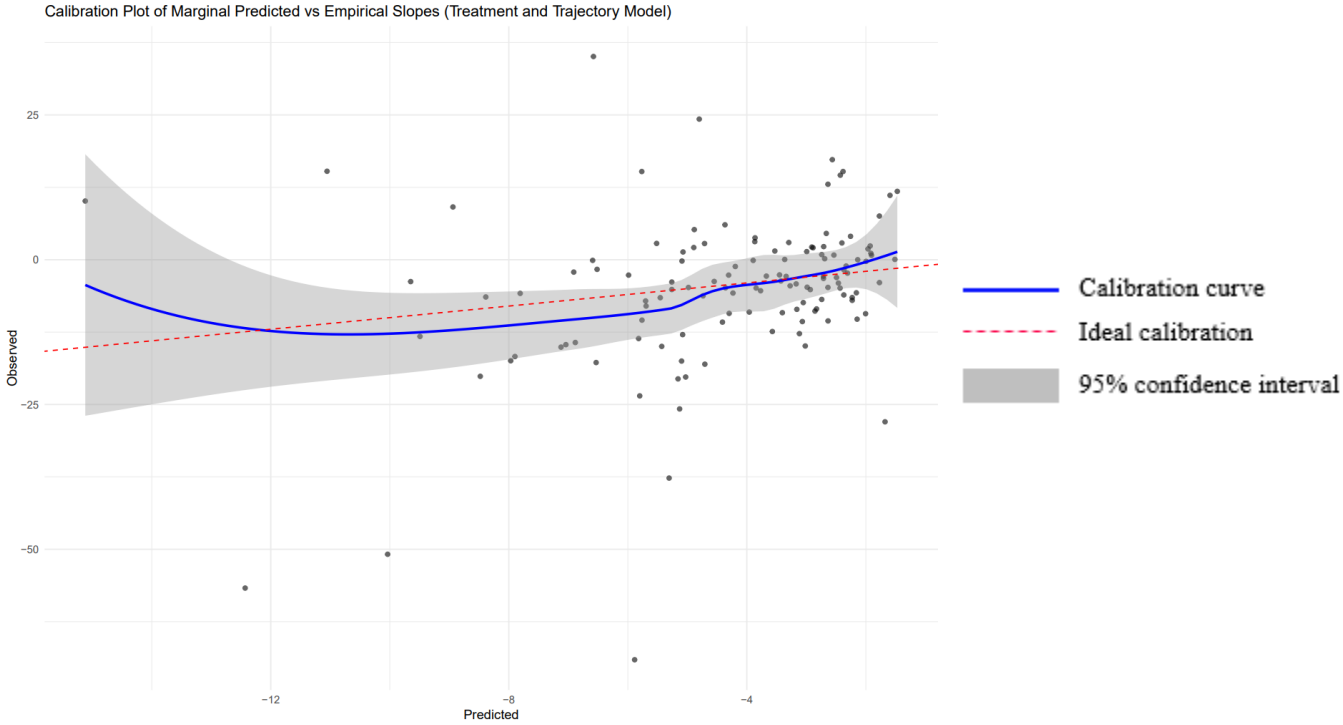

Figure 14. Calibration plot of marginal predicted versus observed eGFR slopes from the Treatment and Trajectory Model

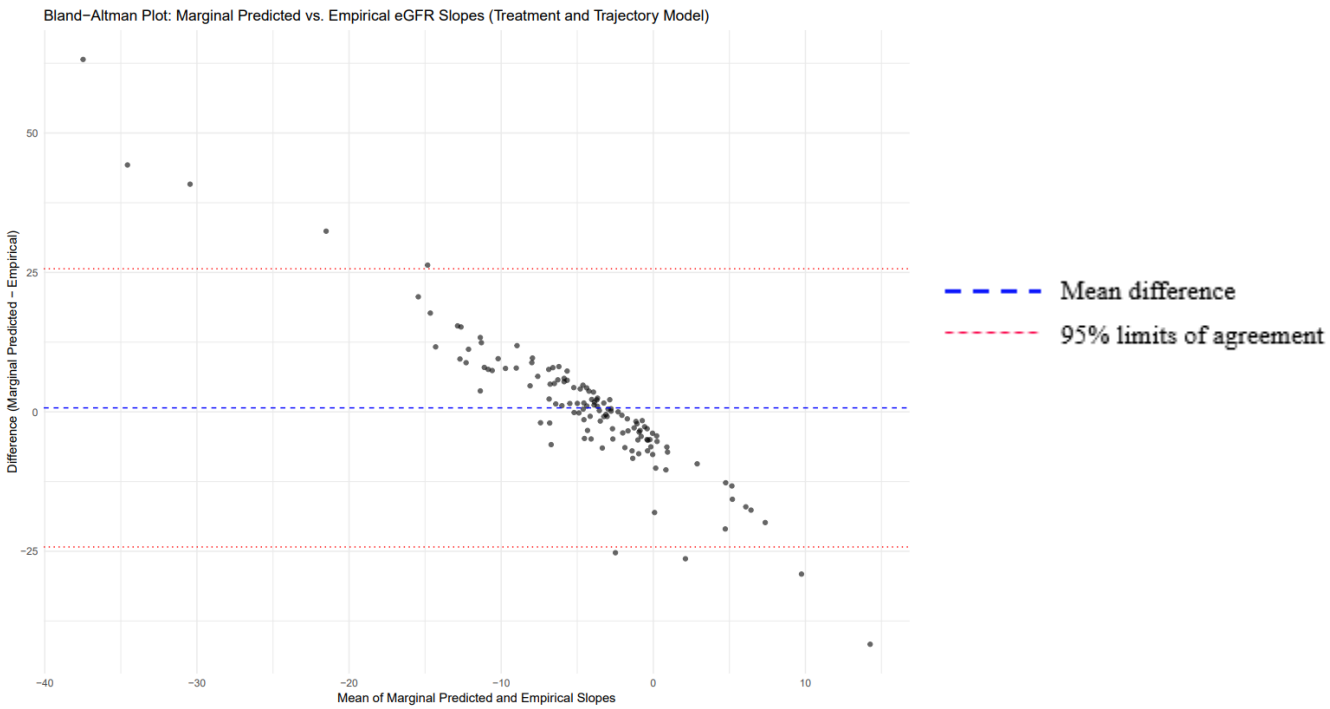

Figure 15. Bland–Altman analysis of marginal predicted versus observed eGFR slopes (Treatment and Trajectory Model)

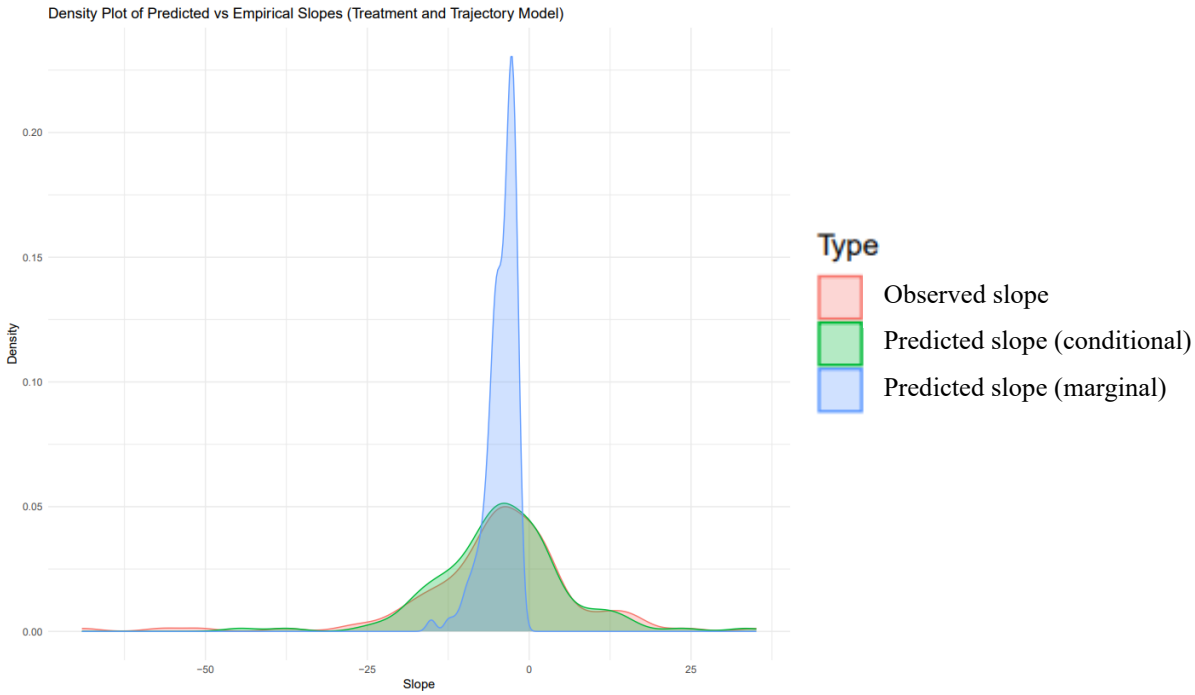

Figure 16. Density plot of conditional and marginal predicted versus observed eGFR slopes from Treatment and Trajectory Model (complete cases)

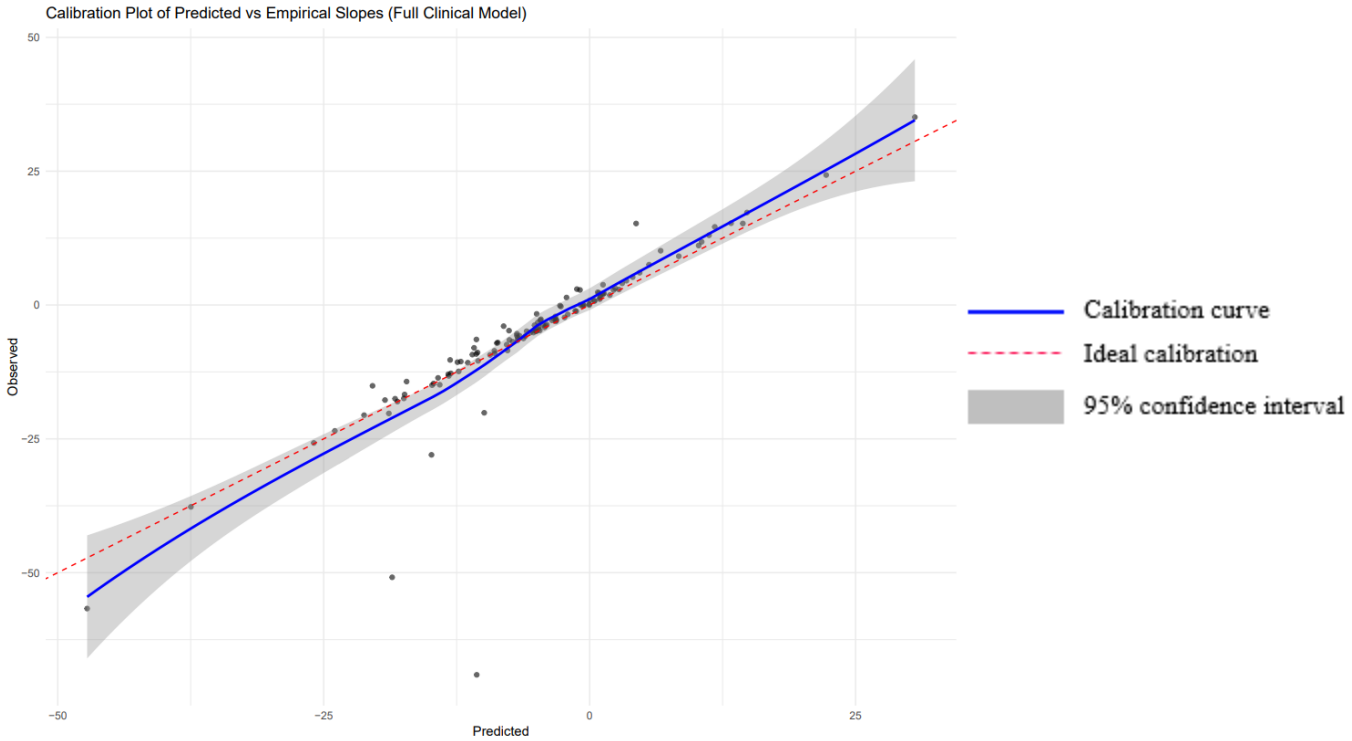

Figure 17. Calibration plot of conditional predicted versus observed eGFR slopes from the Full Clinical Model

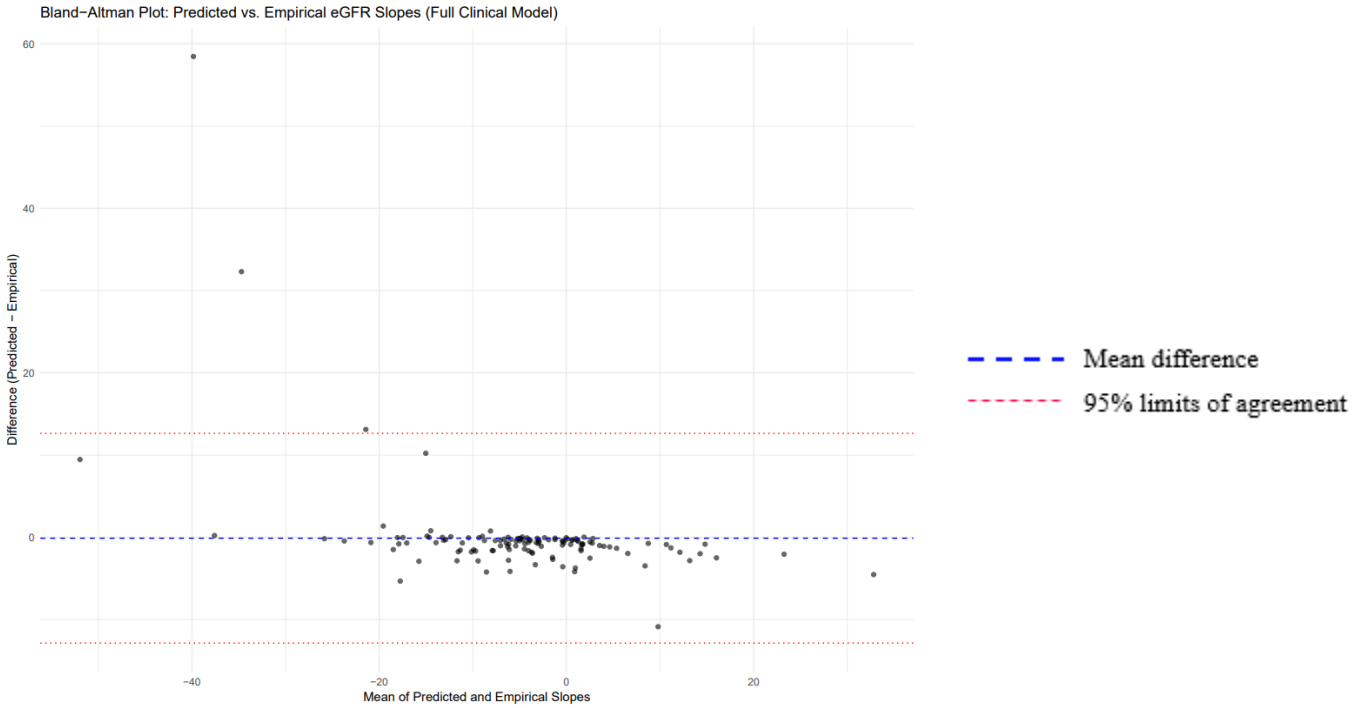

Figure 18. Bland–Altman analysis of conditional predicted versus observed eGFR slopes (Full Clinical Model)

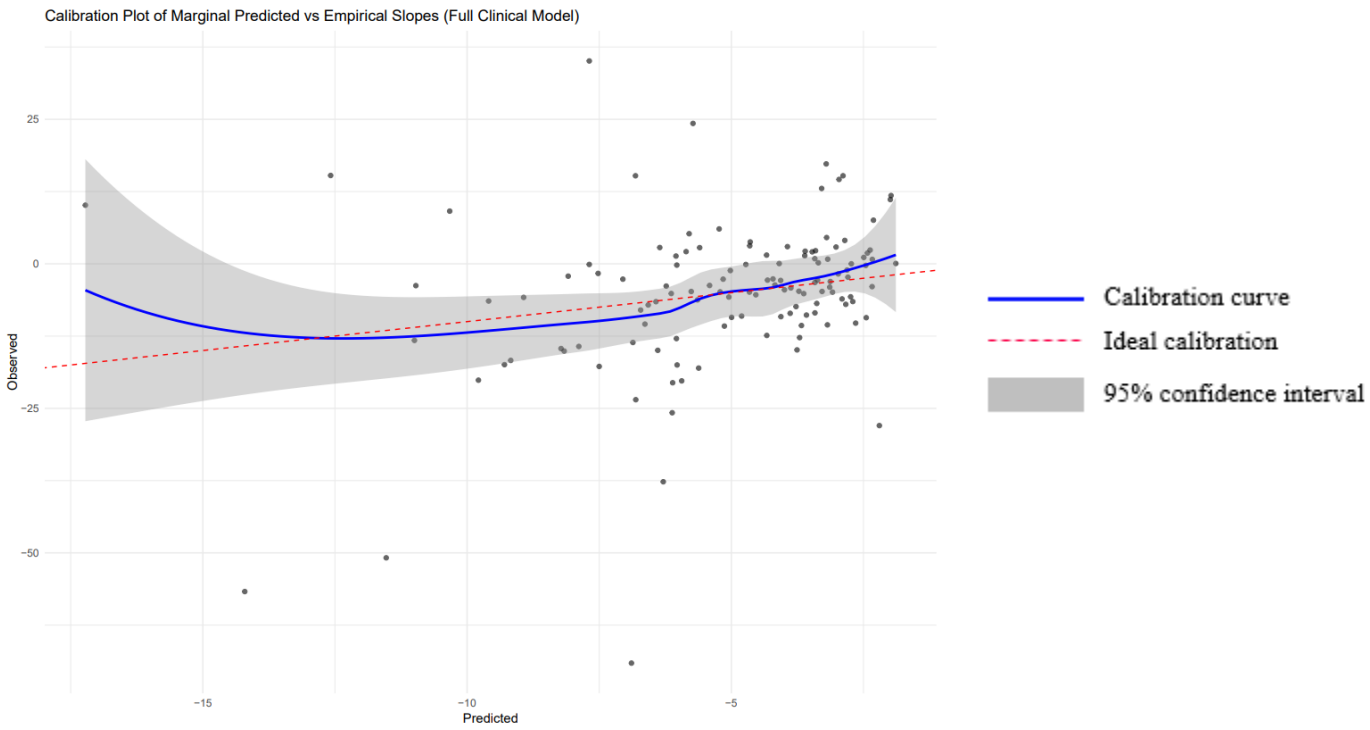

Figure 19. Calibration plot of marginal predicted versus observed eGFR slopes from the Full Clinical Model

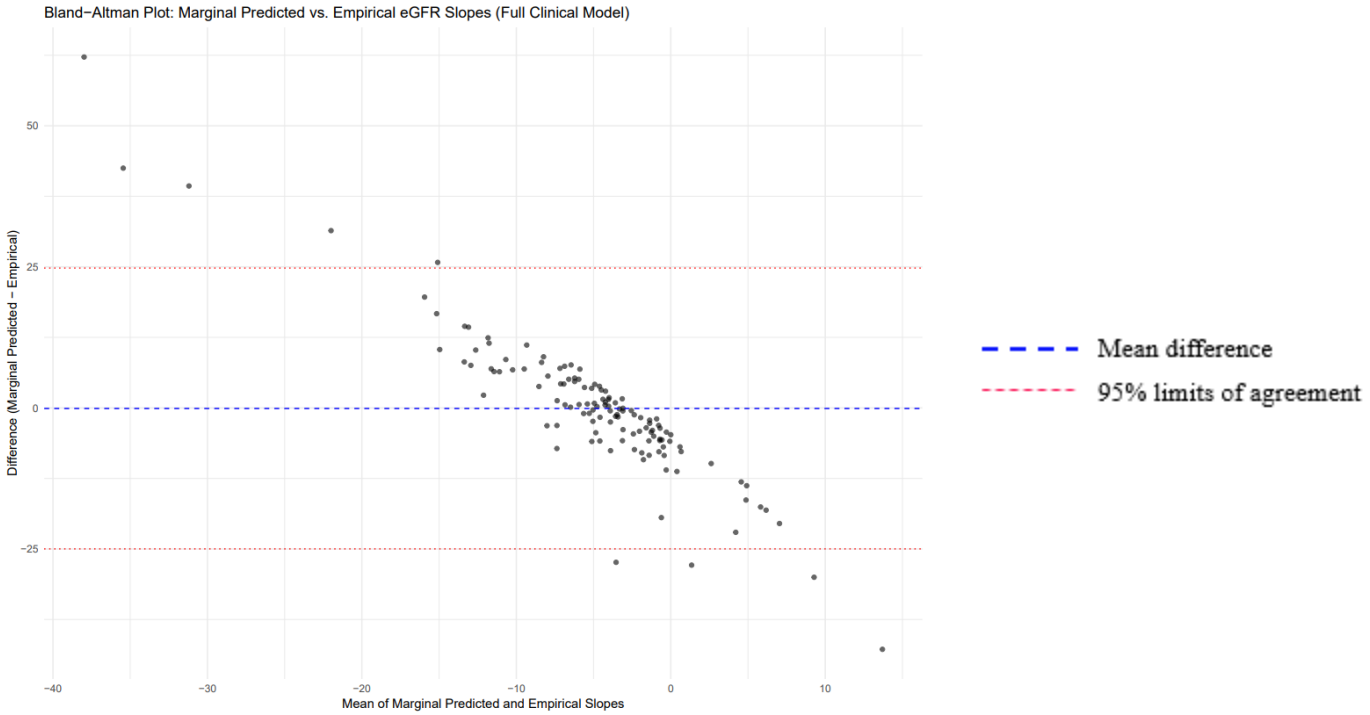

Figure 20. Bland–Altman analysis of marginal predicted versus observed eGFR slopes (Full Clinical Model)

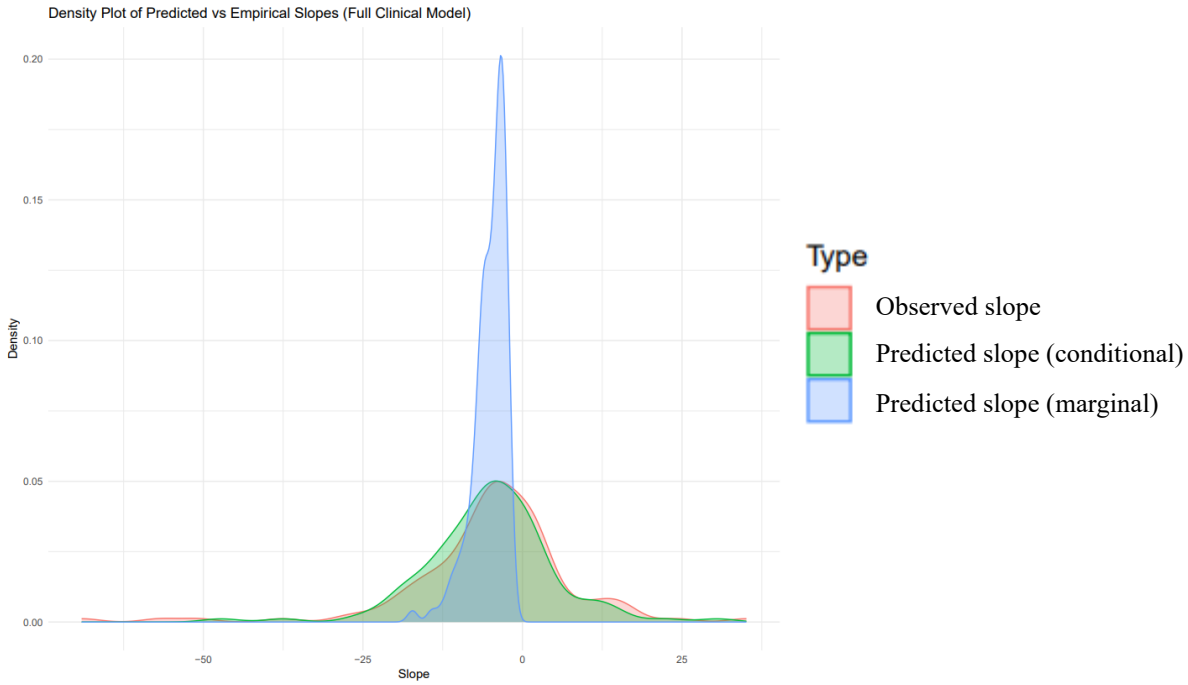

Figure 21. Density plot of conditional and marginal predicted versus observed eGFR slopes from Full Clinical Model (complete cases)

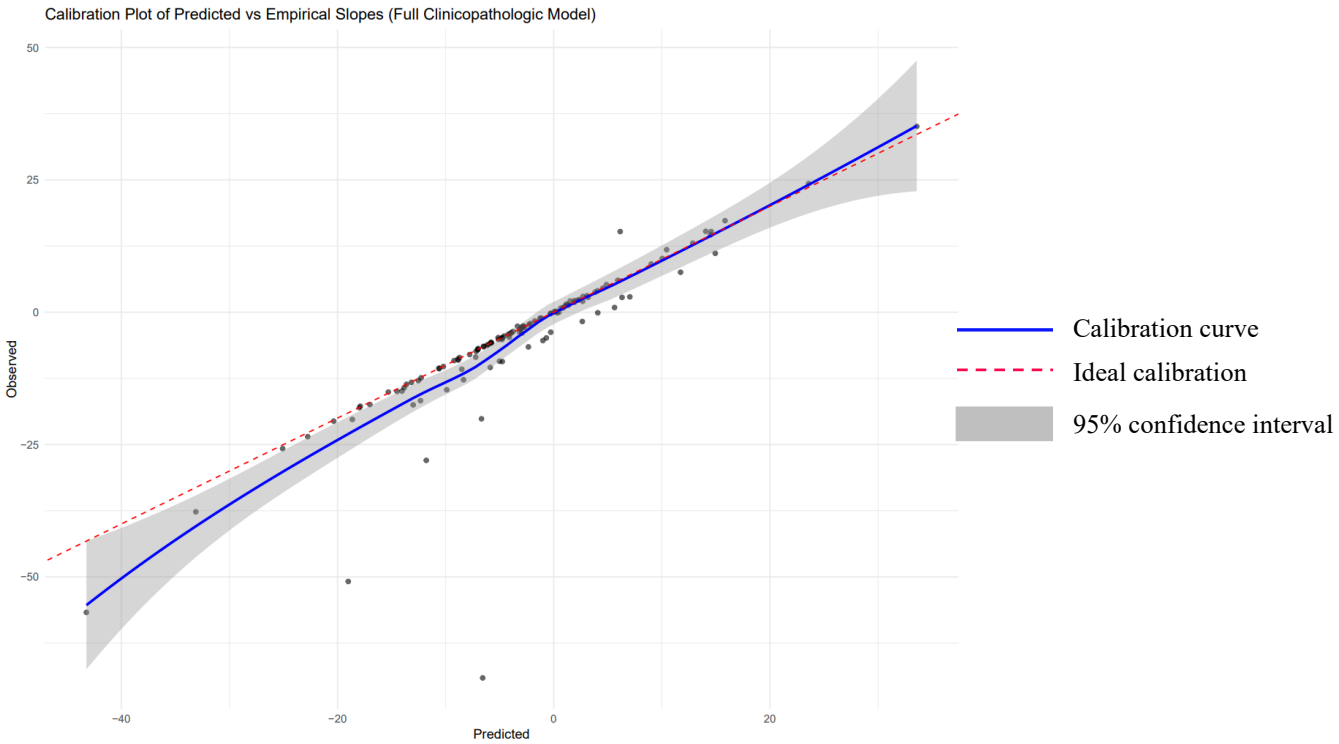

Figure 22. Calibration plot of conditional predicted versus observed eGFR slopes from the Full Clinicopathologic Model

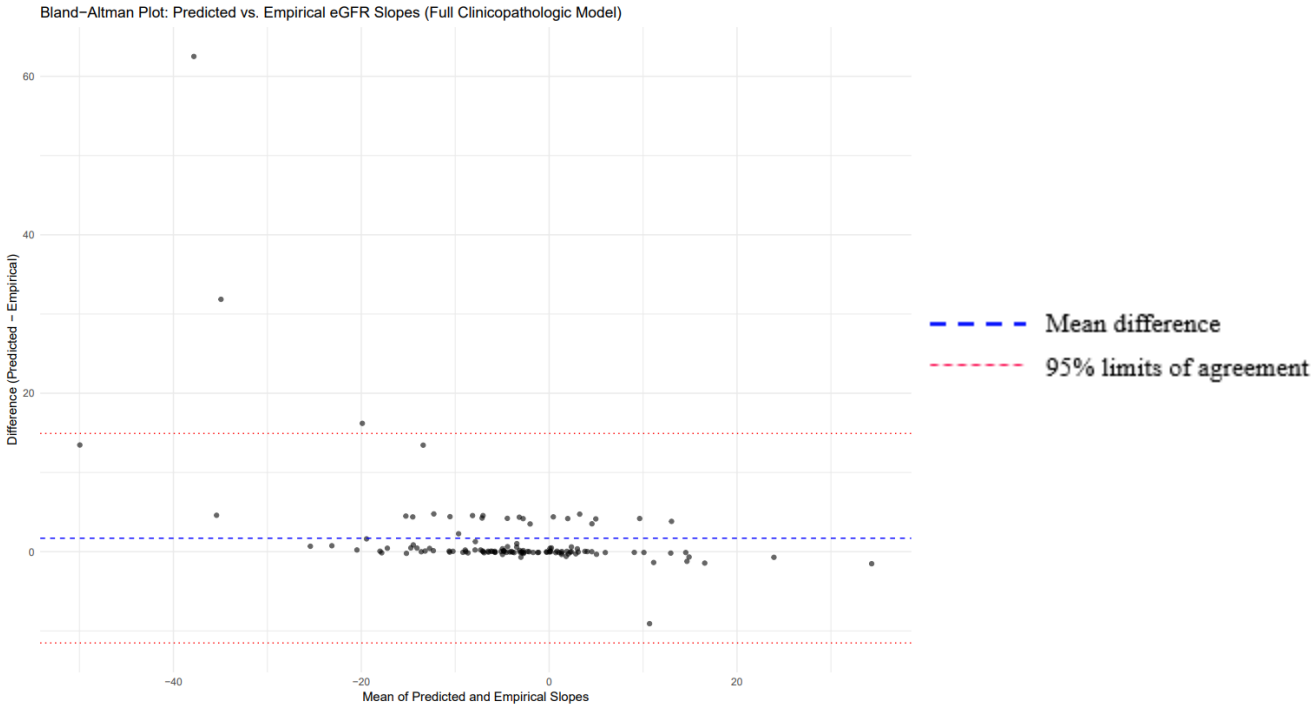

Figure 23. Bland–Altman analysis of conditional predicted versus observed eGFR slopes (Full Clinicopathologic Model)

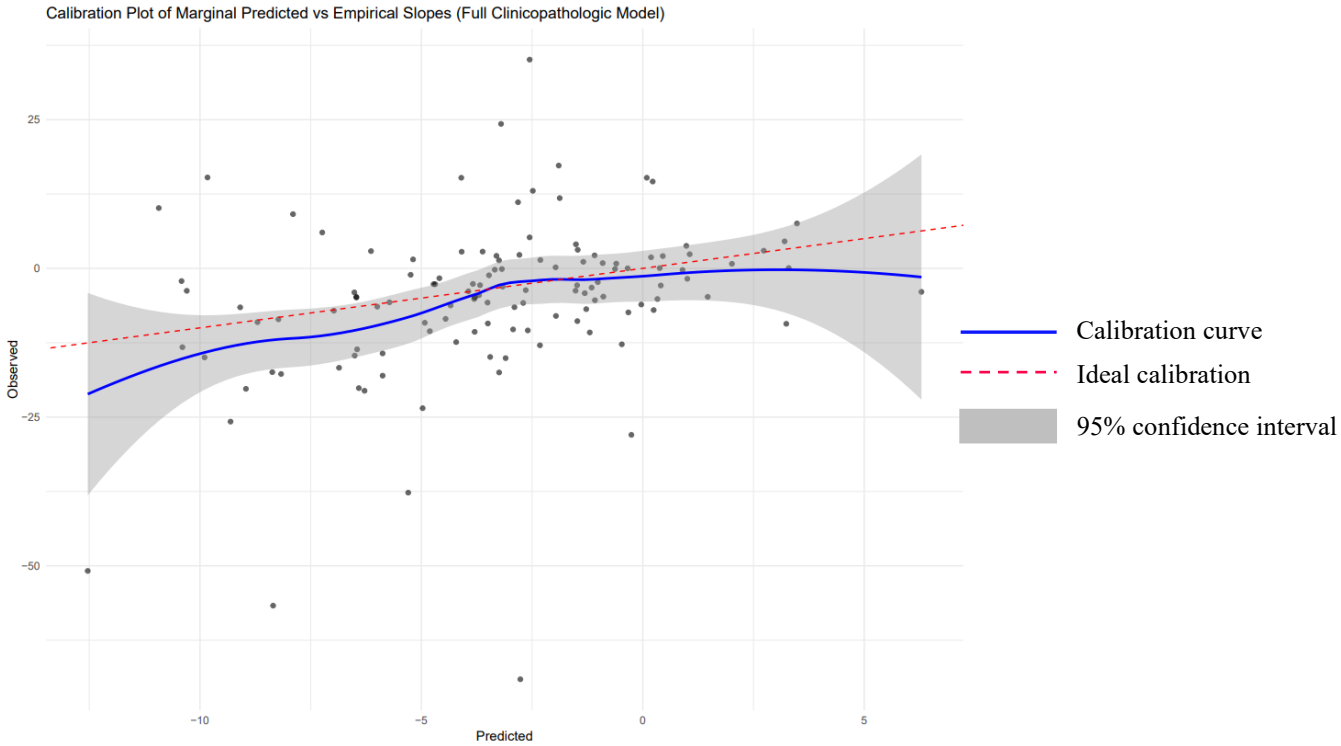

Figure 24. Calibration plot of marginal predicted versus observed eGFR slopes from the Full Clinicopathologic Model

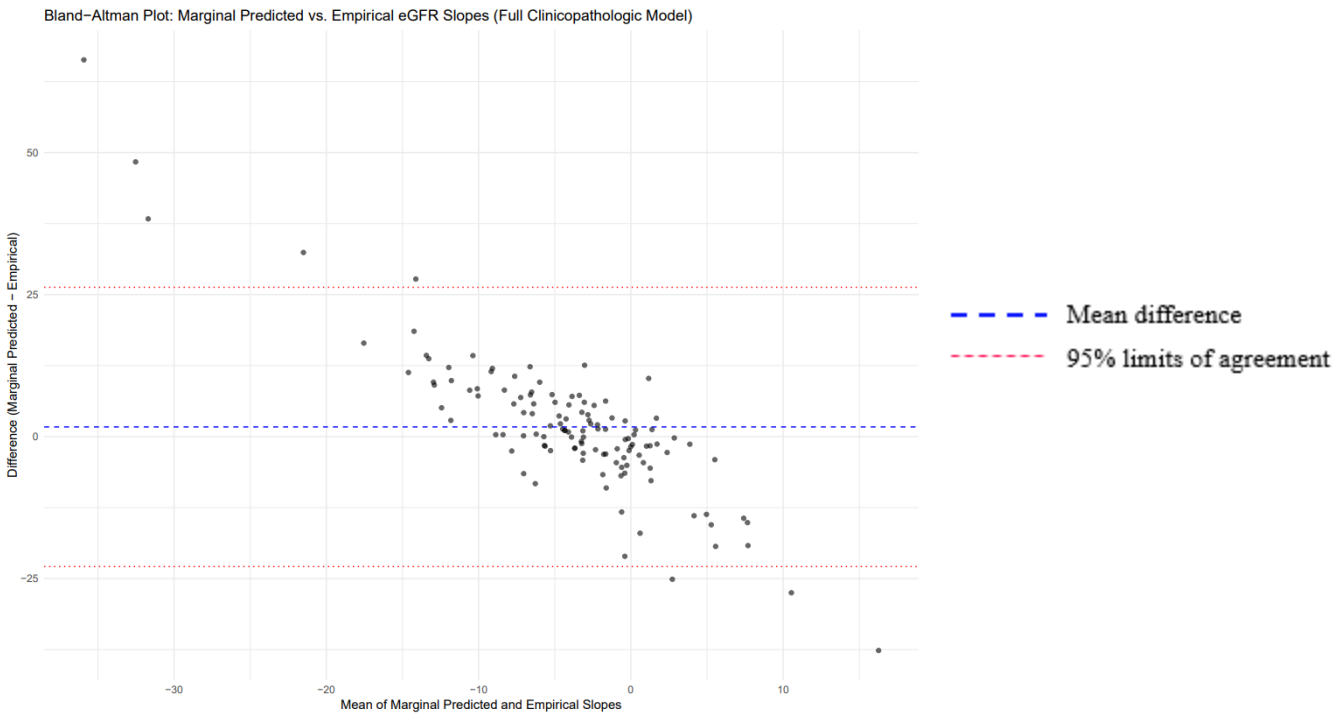

Figure 25. Bland–Altman analysis of marginal predicted versus observed eGFR slopes (Full Clinicopathologic Model)

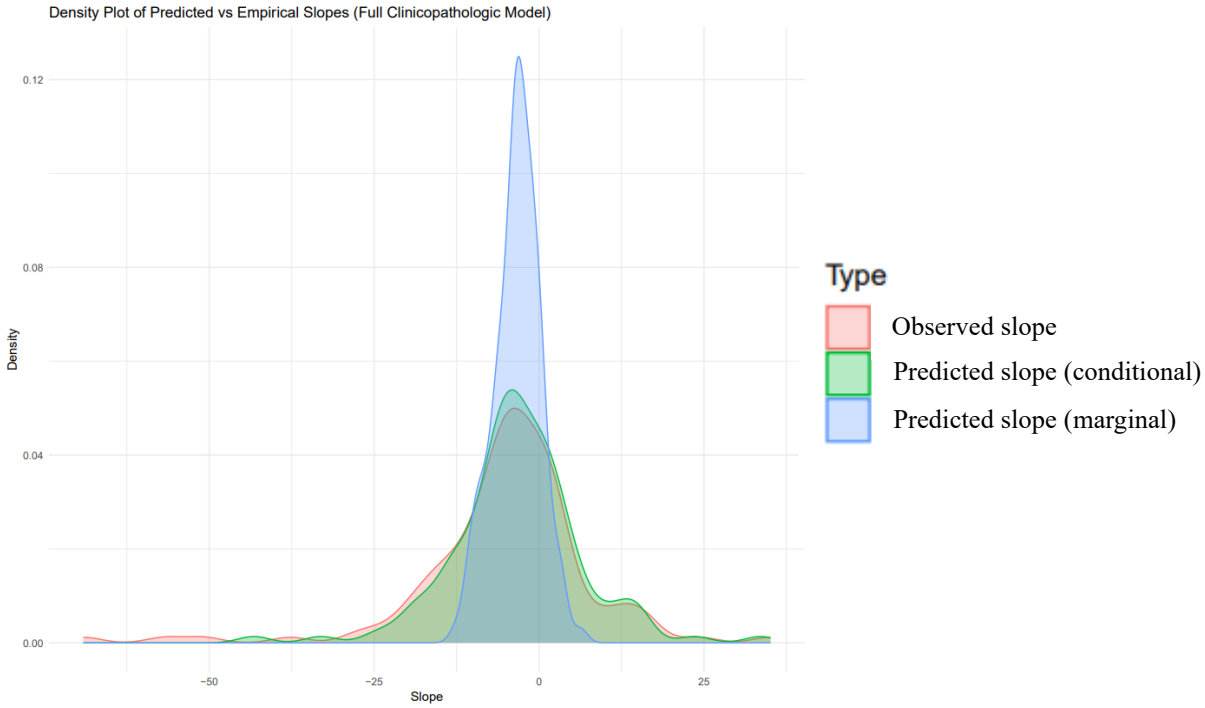

Figure 26. Density plot of conditional and marginal predicted versus observed eGFR slopes from Full Clinicopathologic Model (complete cases)

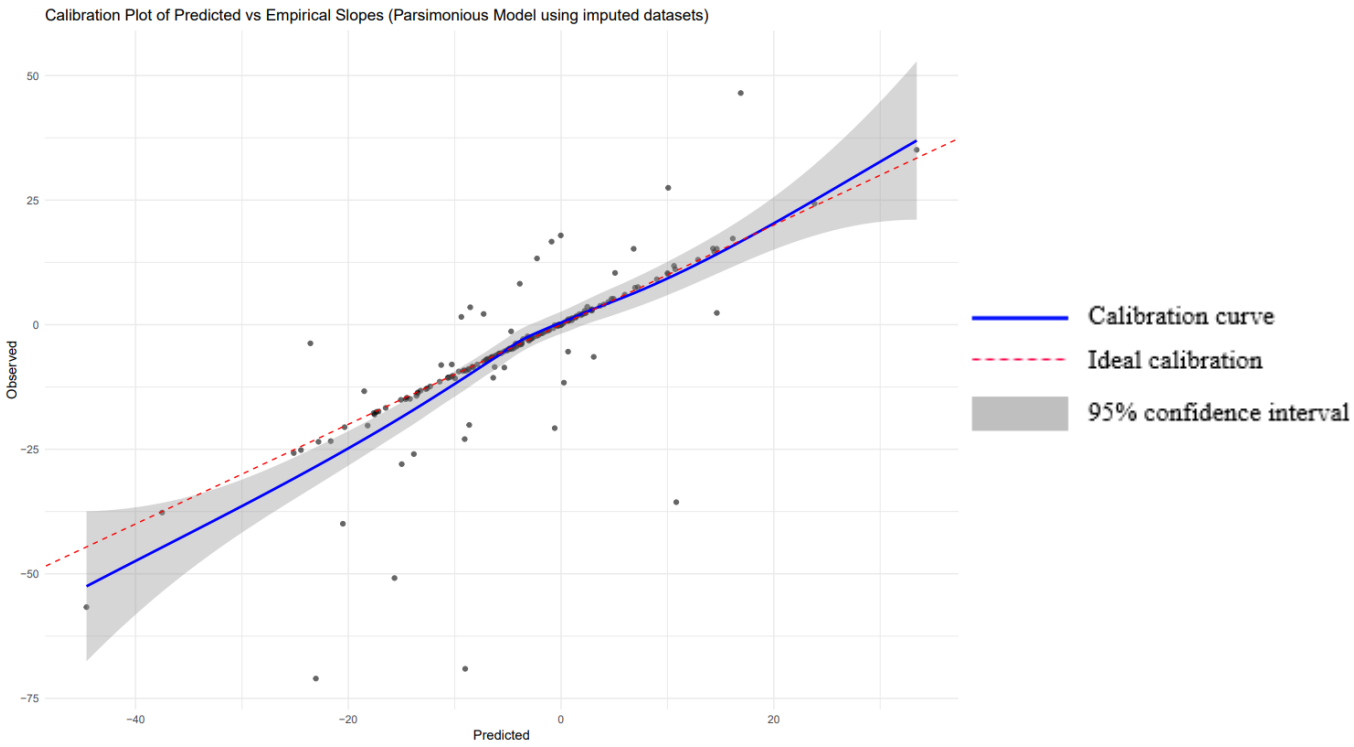

Figure 27. Calibration plot of conditional predicted versus observed eGFR slopes from the Parsimonious Model (imputed datasets)

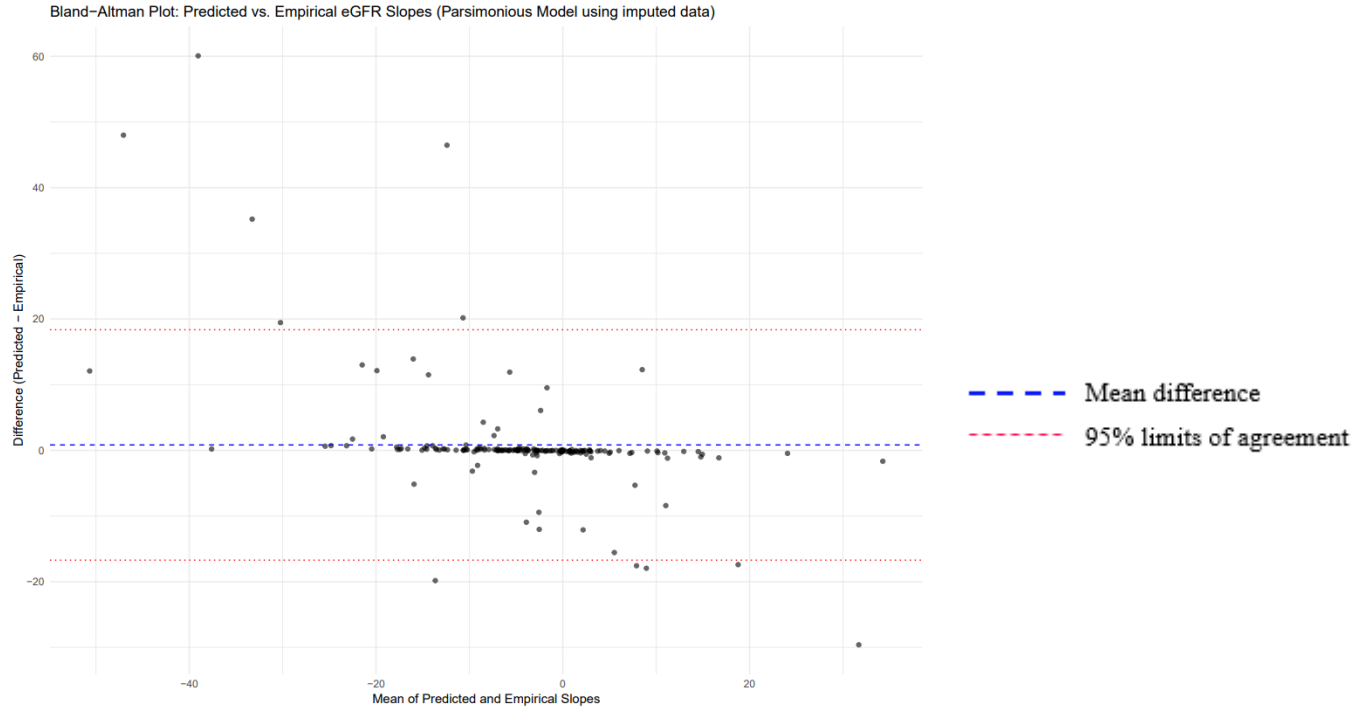

Figure 28. Bland–Altman analysis of conditional predicted versus observed eGFR slopes (Parsimonious Model, imputed datasets)

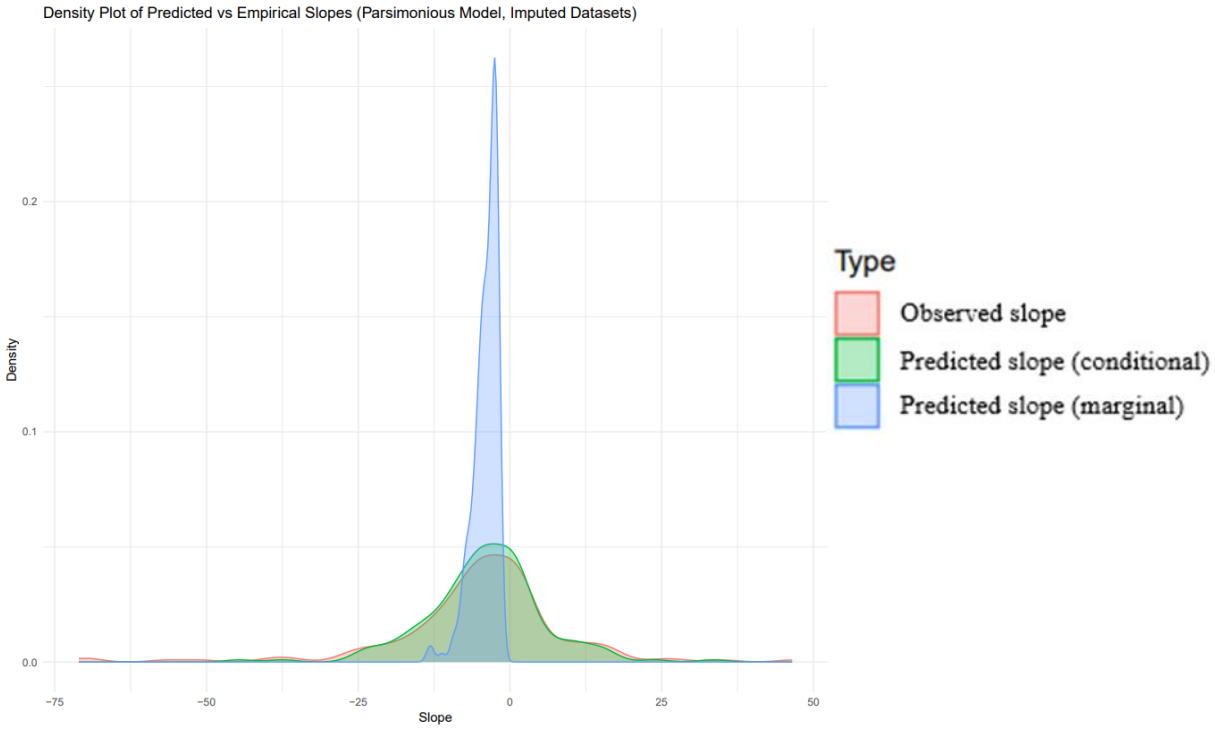

Figure 29. Density plot of conditional and marginal predicted versus observed eGFR slopes from Parsimonious Model (Imputed datasets)

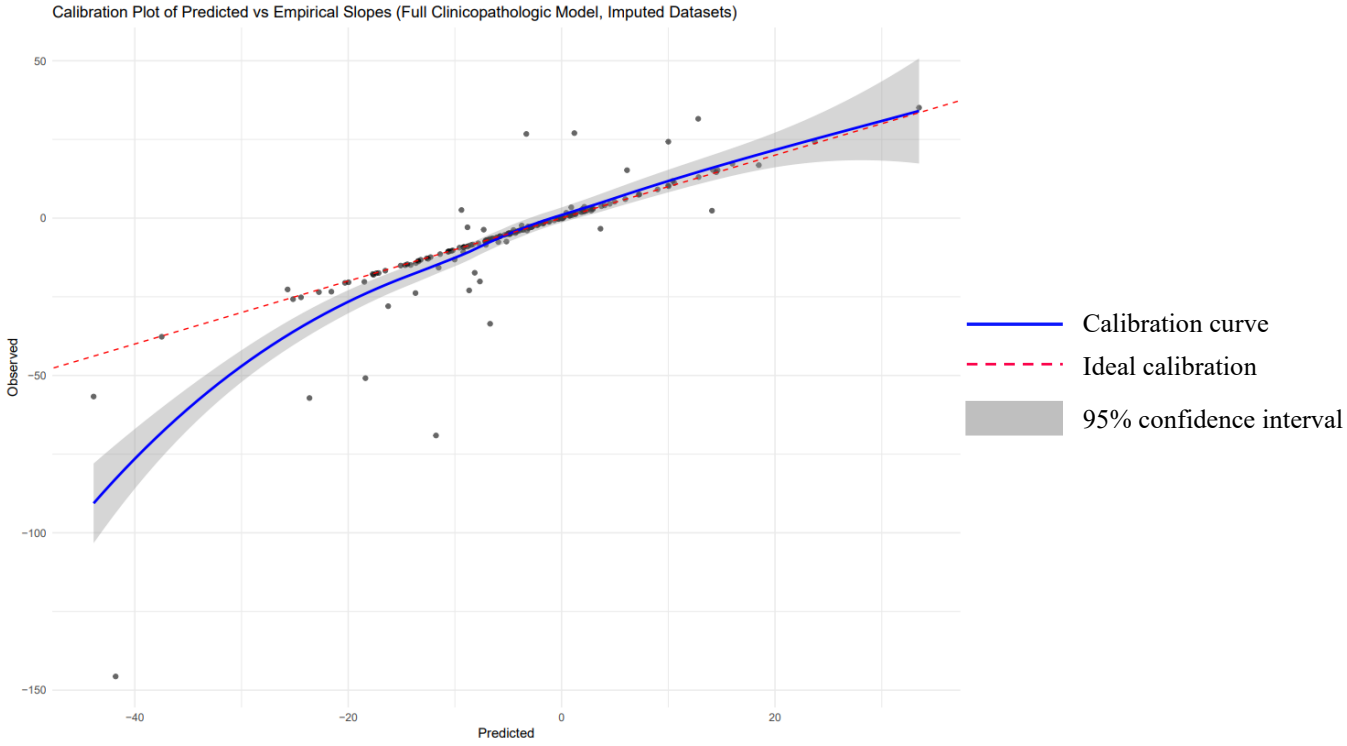

Figure 30. Calibration plot of conditional predicted versus observed eGFR slopes from the Full Clinicopathologic Model (imputed datasets)

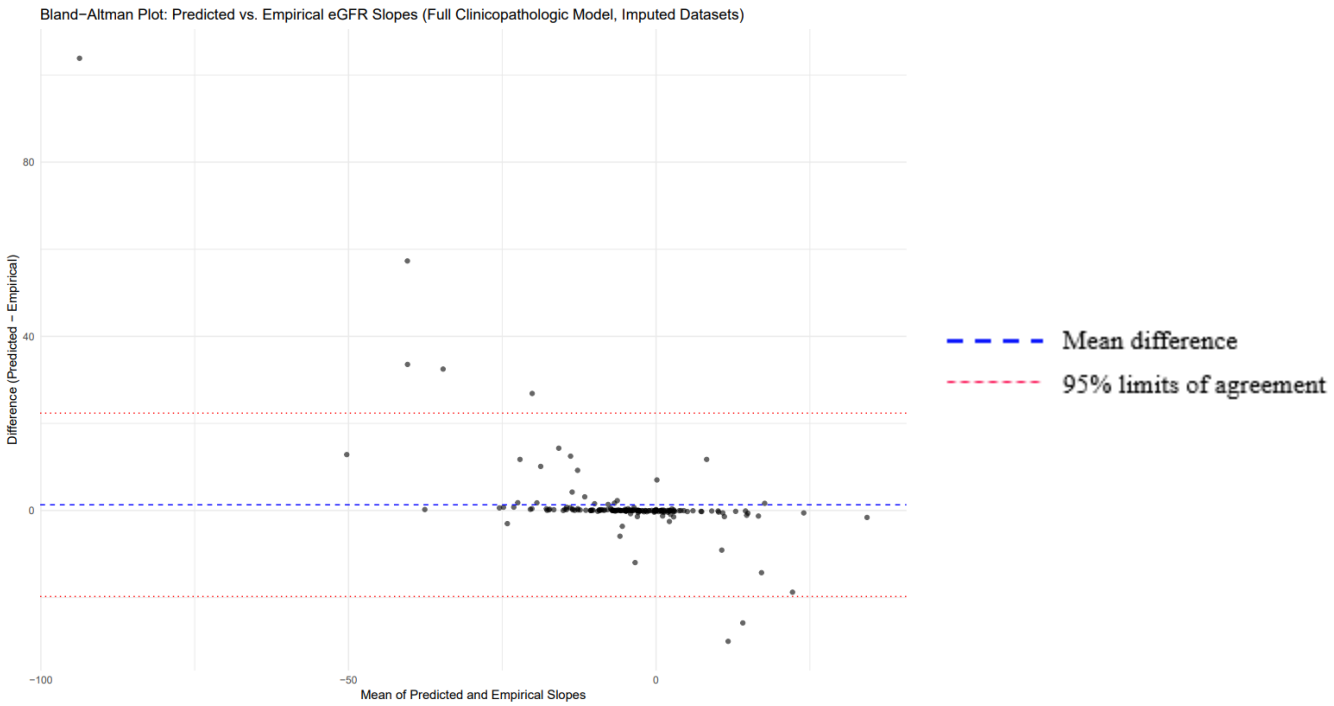

Figure 31. Bland–Altman analysis of conditional predicted versus observed eGFR slopes (Full Clinicopathologic Model, imputed datasets)

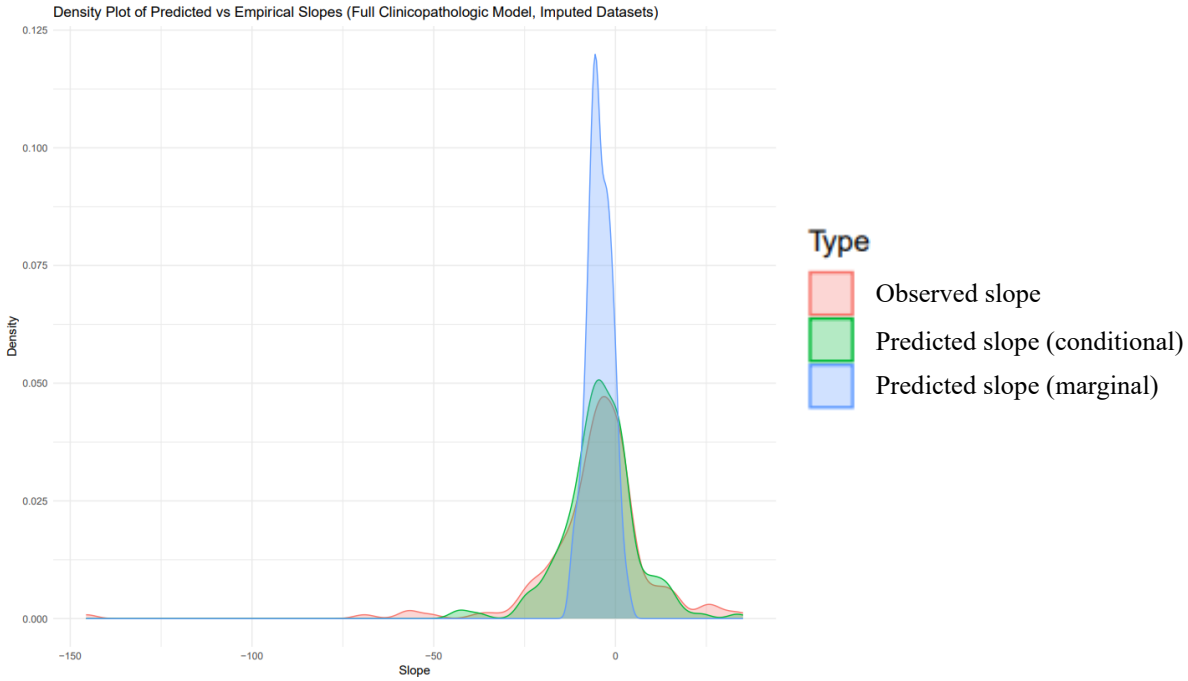

Figure 32. Density plot of conditional and marginal predicted versus observed eGFR slopes from Full Clinicopathologic Model (Imputed datasets)

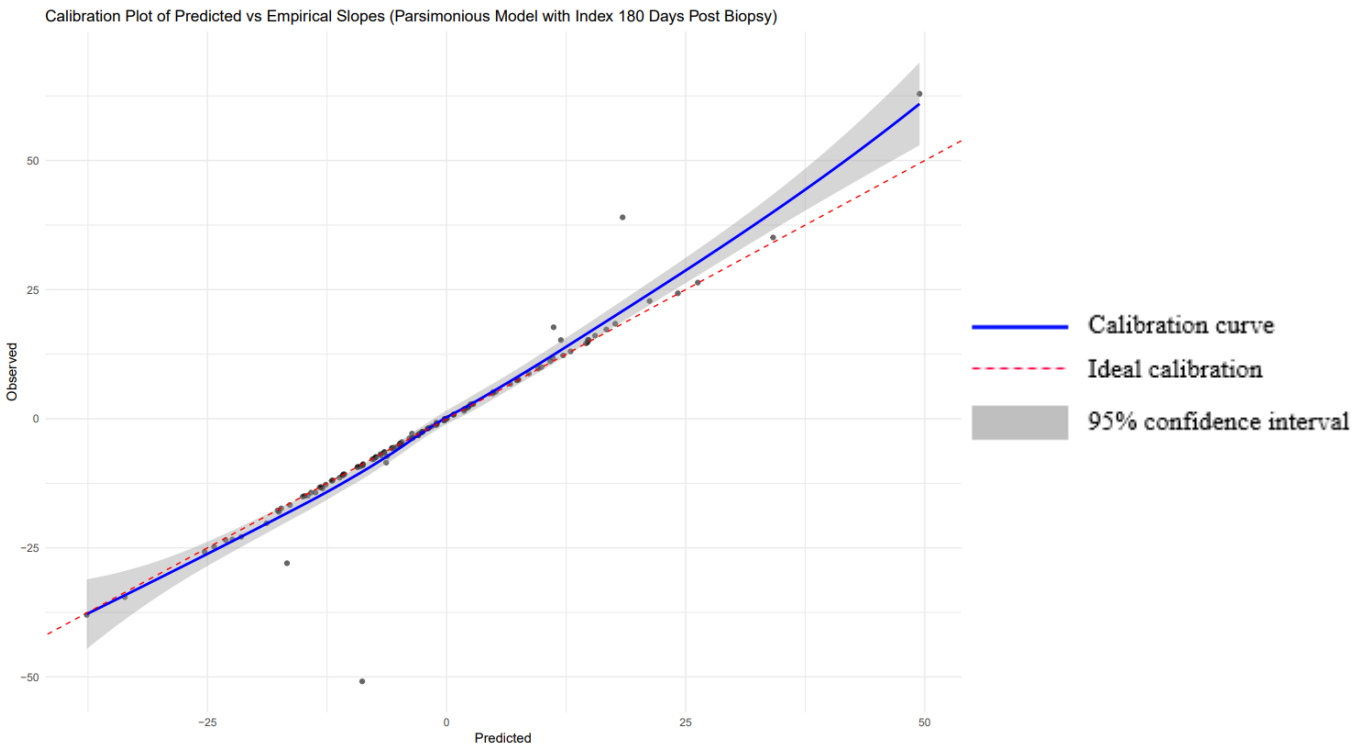

Figure 33. Calibration plot of conditional predicted versus observed eGFR slopes from the Parsimonious Model (index date 180 days post-biopsy)

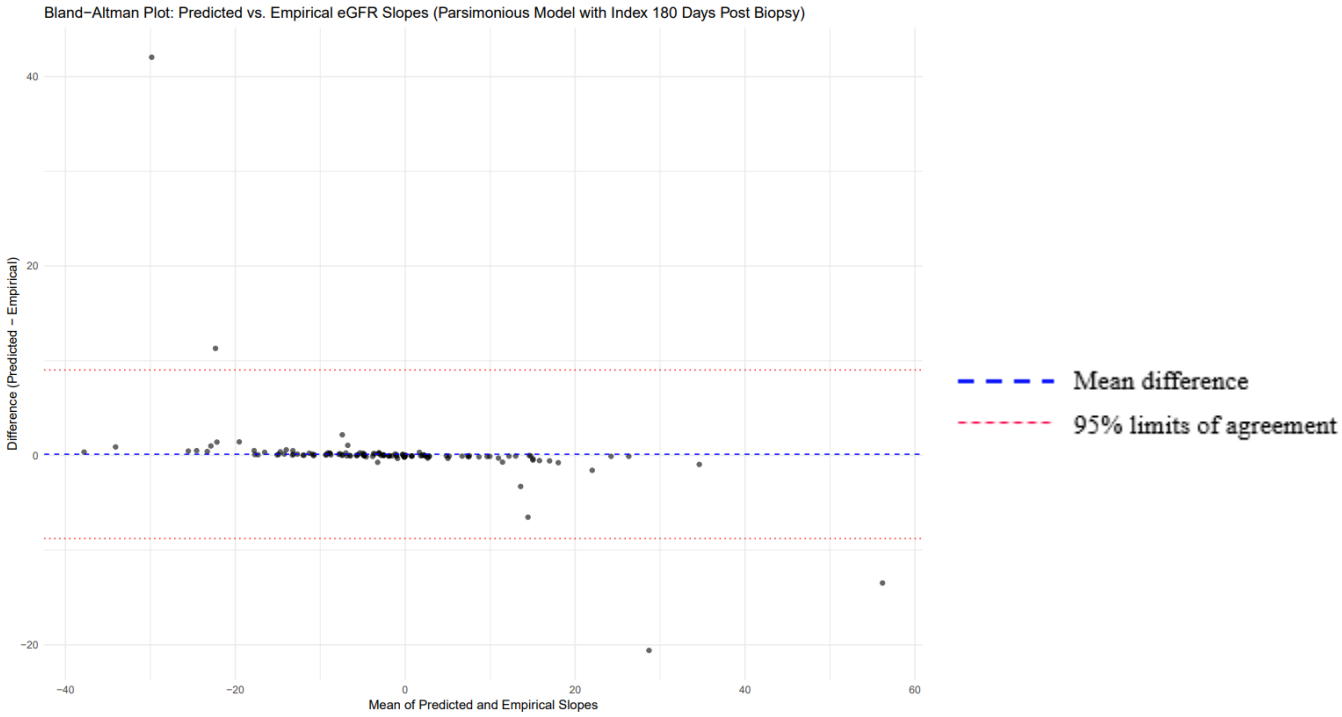

Figure 34. Bland–Altman analysis of conditional predicted versus observed eGFR slopes (Parsimonious Model, index date 180 days post-biopsy)

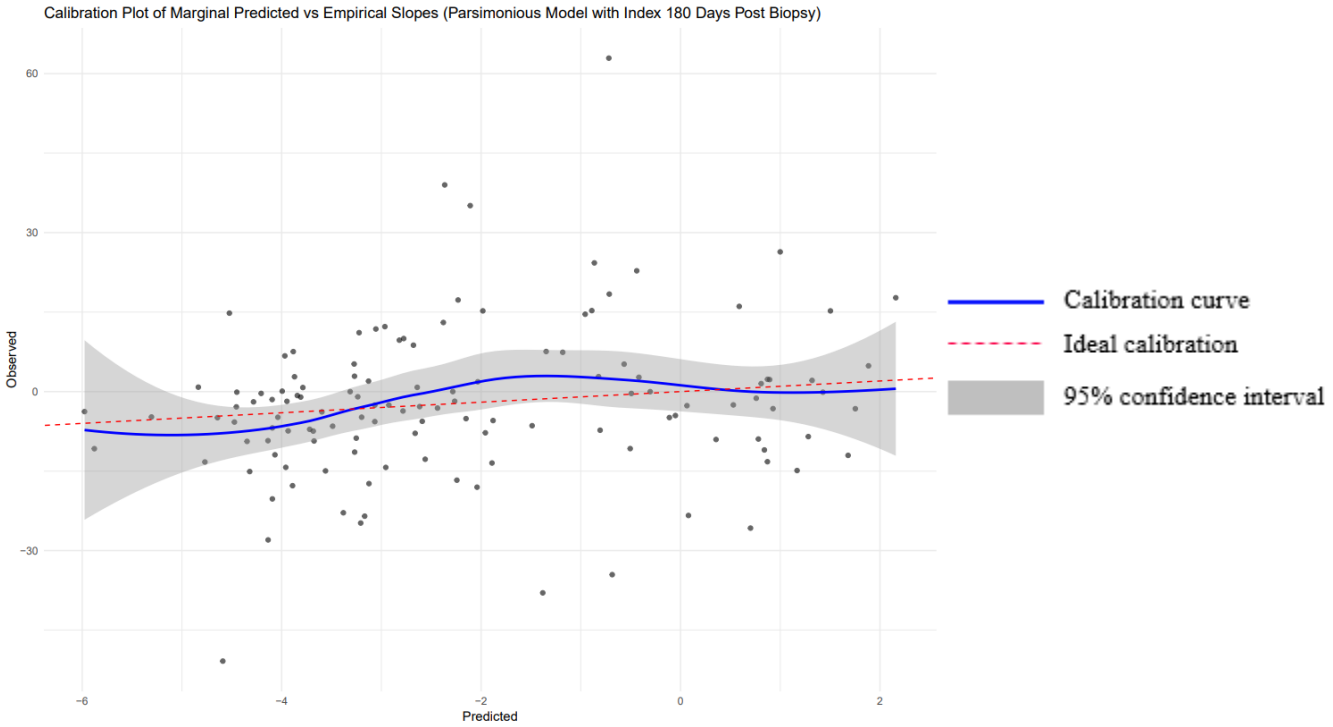

Figure 35. Calibration plot of marginal predicted versus observed eGFR slopes from the Parsimonious Model (index date 180 days post-biopsy)

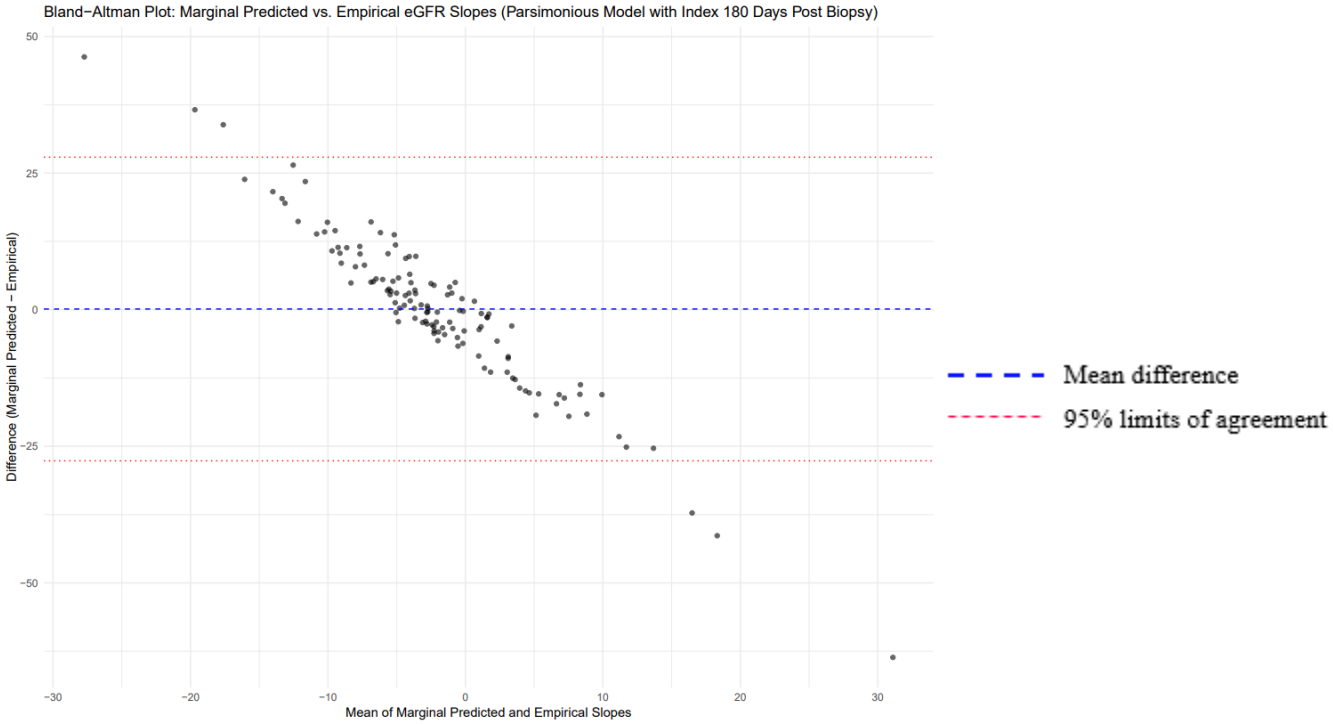

Figure 36. Bland–Altman analysis of marginal predicted versus observed eGFR slopes (Parsimonious Model, index date 180 days post-biopsy)

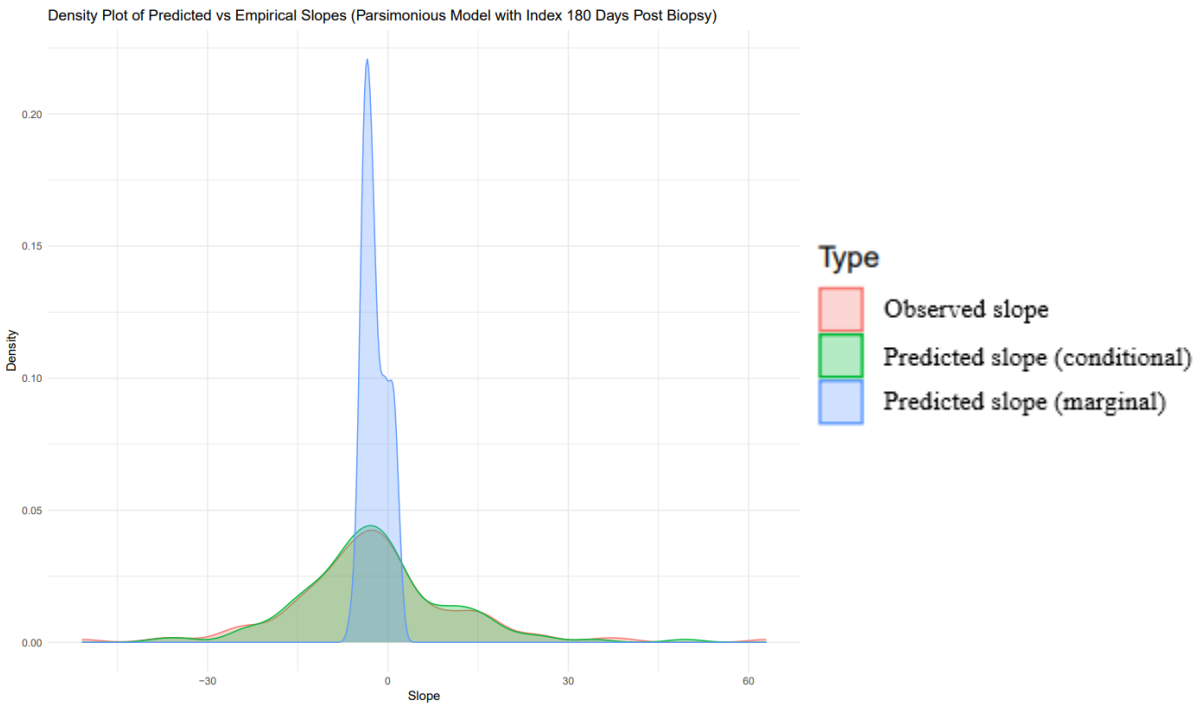

Figure 37. Density plot of conditional and marginal predicted versus observed eGFR slopes from Parsimonious Model With index 180 days post-biopsy

References

1. Barbour SJ, Espino-Hernandez G, Reich HN, et al. The MEST score provides earlier risk prediction in lgA nephropathy. *Kidney Int*. 2016;89(1):167-175. doi:10.1038/ki.2015.322
2. Reich HN, Troyanov S, Scholey JW, Cattran DC. Remission of proteinuria improves prognosis in IgA nephropathy. *J Am Soc Nephrol*. 2007;18(12):3177-3183. doi:10.1681/ASN.2007050526
3. Ai Z, Zhou Q, Huang F, Yang Q, Yu X. Long-term renal outcomes of IgA nephropathy presenting with different levels of proteinuria. *Clin Nephrol*. 2020;94(6):290-296. doi:10.5414/CN110192
4. Rodrigues JC, Haas M, Reich HN. IgA Nephropathy. *Clin J Am Soc Nephrol*. 2017;12(4):677-686. doi:10.2215/CJN.07420716
5. Rovin BH, Adler SG, Barratt J, et al. KDIGO 2021 Clinical Practice Guideline for the Management of Glomerular Diseases. *Kidney Int*. 2021;100(4):S1-S276. doi:10.1016/j.kint.2021.05.021
6. Pitcher D, Braddon F, Hendry B, et al. Long-Term Outcomes in IgA Nephropathy. *Clin J Am Soc Nephrol*. April 2023. doi:10.2215/CJN.0000000000000135
7. Barr B, Harasemiw O, Gibson IW, Tremblay-Savard O, Tangri N. The Development of a Comprehensive Clinicopathologic Registry for Glomerular Diseases Using Natural Language Processing. *Can J Kidney Heal Dis*. 2023;10:20543581231178964. doi:10.1177/20543581231178963
8. Thompson A, Carroll K, A Inker L, et al. Proteinuria Reduction as a Surrogate End Point in Trials of IgA Nephropathy. *Clin J Am Soc Nephrol*. 2019;14(3):469-481. doi:10.2215/CJN.08600718
9. Thompson A, Smith K, Lawrence J. Change in Estimated GFR and Albuminuria as End Points in Clinical Trials: A Viewpoint From the FDA. *Am J kidney Dis Off J Natl Kidney Found*. 2020;75(1):4-5. doi:10.1053/j.ajkd.2019.08.007
10. Barbour SJ, Cattran DC, Espino-Hernandez G, Hladunewich MA, Reich HN. Identifying the ideal metric of proteinuria as a predictor of renal outcome in idiopathic glomerulonephritis. *Kidney Int*. 2015;88(6):1392-1401. doi:10.1038/ki.2015.241
11. Canney M, Gunning HM, Zheng Y, et al. The Risk of Cardiovascular Events in Individuals With Primary Glomerular Diseases. *Am J Kidney Dis*. 2022:1-11. doi:10.1053/j.ajkd.2022.04.005
12. Barbour SJ, Coppo R, Zhang H, et al. Evaluating a New International Risk-Prediction Tool in IgA Nephropathy. *JAMA Intern Med*. 2019;179(7):942-952. doi:10.1001/jamainternmed.2019.0600
13. Tangri N, Stevens LA, Griffith J, et al. A predictive model for progression of chronic kidney disease to kidney failure. *JAMA*. 2011;305(15):1553-1559. doi:10.1001/jama.2011.451
14. Rauen T, Wied S, Fitzner C, et al. After ten years of follow-up, no difference between supportive care plus immunosuppression and supportive care alone in IgA nephropathy. *Kidney Int*. 2020;98(4):1044-1052. doi:10.1016/j.kint.2020.04.046
15. Chadban SJ, Atkins RC. Glomerulonephritis. *Lancet (London, England)*. 2005;365(9473):1797-1806. doi:10.1016/S0140-6736(05)66583-X
16. Mejía-Vilet JM, Ayoub I. The Use of Glucocorticoids in Lupus Nephritis: New Pathways for an Old Drug. *Front Med*. 2021;8:622225. doi:10.3389/fmed.2021.622225

17. Ponticelli C, Escoli R, Moroni G. Does cyclophosphamide still play a role in glomerular diseases? *Autoimmun Rev*. 2018;17(10):1022-1027. doi:10.1016/j.autrev.2018.04.007
18. Steiger S, Ehreiser L, Anders J, Anders H-J. Biological drugs for systemic lupus erythematosus or active lupus nephritis and rates of infectious complications. Evidence from large clinical trials. *Front Immunol*. 2022;13:999704. doi:10.3389/fimmu.2022.999704
19. Rizk D V, Rovin BH, Zhang H, et al. Targeting the Alternative Complement Pathway With Iptacopan to Treat IgA Nephropathy: Design and Rationale of the APPLAUSE-IgAN Study. *Kidney Int reports*. 2023;8(5):968-979. doi:10.1016/j.ekir.2023.01.041
20. Levin A, Ahmed SB, Carrero JJ, et al. Executive summary of the KDIGO 2024 Clinical Practice Guideline for the Evaluation and Management of Chronic Kidney Disease: known knowns and known unknowns. *Kidney Int*. 2024;105(4):684-701. doi:10.1016/j.kint.2023.10.016
21. Pattrapornpisut P, Avila-Casado C, Reich HN. IgA Nephropathy: Core Curriculum 2021. *Am J kidney Dis Off J Natl Kidney Found*. 2021;78(3):429-441. doi:10.1053/j.ajkd.2021.01.024
22. Webster AC, Nagler E V, Morton RL, Masson P. Chronic Kidney Disease. *Lancet (London, England)*. 2017;389(10075):1238-1252. doi:10.1016/S0140-6736(16)32064-5
23. Gomez AT, Kiberd BA, Royston JP, et al. Comorbidity burden at dialysis initiation and mortality: A cohort study. *Can J kidney Heal Dis*. 2015;2:34. doi:10.1186/s40697-015-0068-3
24. Bradbury BD, Fissell RB, Albert JM, et al. Predictors of early mortality among incident US hemodialysis patients in the Dialysis Outcomes and Practice Patterns Study (DOPPS). *Clin J Am Soc Nephrol*. 2007;2(1):89-99. doi:10.2215/CJN.01170905
25. Ferguson TW, Whitlock RH, Bamforth RJ, et al. Cost-Utility of Dialysis in Canada: Hemodialysis, Peritoneal Dialysis, and Nondialysis Treatment of Kidney Failure. *Kidney Med*. 2021;3(1):20-30.e1. doi:10.1016/j.xkme.2020.07.011
26. Suzuki H, Kiryluk K, Novak J, et al. The pathophysiology of IgA nephropathy. *J Am Soc Nephrol*. 2011;22(10):1795-1803. doi:10.1681/ASN.2011050464
27. Gharavi AG, Moldoveanu Z, Wyatt RJ, et al. Aberrant IgA1 glycosylation is inherited in familial and sporadic IgA nephropathy. *J Am Soc Nephrol*. 2008;19(5):1008-1014. doi:10.1681/ASN.2007091052
28. Tomana M, Novak J, Julian BA, Matousovic K, Konecny K, Mestecky J. Circulating immune complexes in IgA nephropathy consist of IgA1 with galactose-deficient hinge region and antiglycan antibodies. *J Clin Invest*. 1999;104(1):73-81. doi:10.1172/JCI5535
29. Barratt J, Lafayette RA, Zhang H, et al. IgA nephropathy: the lectin pathway and implications for targeted therapy. *Kidney Int*. 2023;104(2):254-264. doi:10.1016/j.kint.2023.04.029
30. Schena FP, Nistor I. Epidemiology of IgA Nephropathy: A Global Perspective. *Semin Nephrol*. 2018;38(5):435-442. doi:10.1016/j.semnephrol.2018.05.013
31. Willey CJ, Coppo R, Schaefer F, Mizerska-Wasiak M, Mathur M, Schultz MJ. The incidence and prevalence of IgA nephropathy in Europe. *Nephrol Dial Transplant Off Publ Eur Dial Transpl Assoc - Eur Ren Assoc*. 2023;38(10):2340-2349. doi:10.1093/ndt/gfad082
32. Coppo R, Peruzzi L, Amore A, et al. IgACE: a placebo-controlled, randomized trial of angiotensin-converting enzyme inhibitors in children and young people with IgA

nephropathy and moderate proteinuria. *J Am Soc Nephrol*. 2007;18(6):1880-1888. doi:10.1681/ASN.2006040347
33. Li PK-T, Leung CB, Chow KM, et al. Hong Kong study using valsartan in IgA nephropathy (HKVIN): a double-blind, randomized, placebo-controlled study. *Am J kidney Dis Off J Natl Kidney Found*. 2006;47(5):751-760. doi:10.1053/j.ajkd.2006.01.017
34. Praga M, Gutiérrez E, González E, Morales E, Hernández E. Treatment of IgA nephropathy with ACE inhibitors: a randomized and controlled trial. *J Am Soc Nephrol*. 2003;14(6):1578-1583. doi:10.1097/01.asn.0000068460.37369.dc
35. Wheeler DC, Toto RD, Stefánsson B V, et al. A pre-specified analysis of the DAPA-CKD trial demonstrates the effects of dapagliflozin on major adverse kidney events in patients with IgA nephropathy. *Kidney Int*. 2021;100(1):215-224. doi:10.1016/j.kint.2021.03.033
36. Herrington WG, Staplin N, Wanner C, et al. Empagliflozin in Patients with Chronic Kidney Disease. *N Engl J Med*. 2023;388(2):117-127. doi:10.1056/NEJMoa2204233
37. The Nuffield Department of Population Health Renal Studies Group. Impact of diabetes on the effects of sodium glucose co-transporter-2 inhibitors on kidney outcomes: collaborative meta-analysis of large placebo-controlled trials. *Lancet (London, England)*. 2022;400(10365):1788-1801. doi:10.1016/S0140-6736(22)02074-8
38. Pozzi C, Andrulli S, Del Vecchio L, et al. Corticosteroid effectiveness in IgA nephropathy: long-term results of a randomized, controlled trial. *J Am Soc Nephrol*. 2004;15(1):157-163. doi:10.1097/01.asn.0000103869.08096.4f
39. Manno C, Torres DD, Rossini M, Pesce F, Schena FP. Randomized controlled clinical trial of corticosteroids plus ACE-inhibitors with long-term follow-up in proteinuric IgA nephropathy. *Nephrol Dial Transplant Off Publ Eur Dial Transpl Assoc - Eur Ren Assoc*. 2009;24(12):3694-3701. doi:10.1093/ndt/gfp356
40. Lv J, Zhang H, Chen Y, et al. Combination therapy of prednisone and ACE inhibitor versus ACE-inhibitor therapy alone in patients with IgA nephropathy: a randomized controlled trial. *Am J kidney Dis Off J Natl Kidney Found*. 2009;53(1):26-32. doi:10.1053/j.ajkd.2008.07.029
41. Rauen T, Eitner F, Fitzner C, et al. Intensive Supportive Care plus Immunosuppression in IgA Nephropathy. *N Engl J Med*. 2015;373(23):2225-2236. doi:10.1056/NEJMoa1415463
42. Campbell KN. Corticosteroids Should Be Used to Treat Slowly Progressive IgA Nephropathy: COMMENTARY. *Kidney360*. 2021;2(7):1084-1086. doi:10.34067/KID.0006832020
43. Lv J, Wong MG, Hladunewich MA, et al. Effect of Oral Methylprednisolone on Decline in Kidney Function or Kidney Failure in Patients With IgA Nephropathy: The TESTING Randomized Clinical Trial. *JAMA*. 2022;327(19):1888-1898. doi:10.1001/jama.2022.5368
44. Lafayette R, Kristensen J, Stone A, et al. Efficacy and safety of a targeted-release formulation of budesonide in patients with primary IgA nephropathy (NefIgArd): 2-year results from a randomised phase 3 trial. *Lancet*. 2023;402(10405):859-870. doi:10.1016/S0140-6736(23)01554-4
45. Hou FF, Xie D, Wang J, et al. Effectiveness of Mycophenolate Mofetil Among Patients With Progressive IgA Nephropathy: A Randomized Clinical Trial. *JAMA Netw open*. 2023;6(2):e2254054. doi:10.1001/jamanetworkopen.2022.54054
46. Mathur M, Barratt J, Chacko B, et al. A Phase 2 Trial of Sibeprenlimab in Patients with IgA Nephropathy. *N Engl J Med*. November 2023. doi:10.1056/NEJMoa2305635

47. Berthoux F, Mohey H, Laurent B, Mariat C, Afiani A, Thibaudin L. Predicting the risk for dialysis or death in IgA nephropathy. *J Am Soc Nephrol*. 2011;22(4):752-761. doi:10.1681/ASN.2010040355
48. Wakai K, Kawamura T, Endoh M, et al. A scoring system to predict renal outcome in IgA nephropathy: from a nationwide prospective study. *Nephrol Dial Transplant Off Publ Eur Dial Transpl Assoc - Eur Ren Assoc*. 2006;21(10):2800-2808. doi:10.1093/ndt/gfl342
49. Gutiérrez E, Zamora I, Ballarín JA, et al. Long-term outcomes of IgA nephropathy presenting with minimal or no proteinuria. *J Am Soc Nephrol*. 2012;23(10):1753-1760. doi:10.1681/ASN.2012010063
50. Lee H, Hwang JH, Paik JH, et al. Long-term prognosis of clinically early IgA nephropathy is not always favorable. *BMC Nephrol*. 2014;15:94. doi:10.1186/1471-2369-15-94
51. Lai FM, Szeto CC, Choi PC, et al. Characterization of early IgA nephropathy. *Am J kidney Dis Off J Natl Kidney Found*. 2000;36(4):703-708. doi:10.1053/ajkd.2000.17614
52. Szeto CC, Lai FM, To KF, et al. The natural history of immunoglobulin a nephropathy among patients with hematuria and minimal proteinuria. *Am J Med*. 2001;110(6):434-437. doi:10.1016/s0002-9343(01)00659-3
53. Lafayette R, Kristensen J, Stone A, et al. Efficacy and safety of a targeted-release formulation of budesonide in patients with primary IgA nephropathy (NefIgArd): 2-year results from a randomised phase 3 trial. *Lancet (London, England)*. 2023;402(10405):859-870. doi:10.1016/S0140-6736(23)01554-4
54. Group F-NBW. *BEST (Biomarkers, EndpointS, and Other Tools) Resource*. Silver Spring (MD); 2016.
55. Inker LA, Heerspink HJL, Tighiouart H, et al. Association of Treatment Effects on Early Change in Urine Protein and Treatment Effects on GFR Slope in IgA Nephropathy: An Individual Participant Meta-analysis. *Am J Kidney Dis*. 2021;78(3):340-349.e1. doi:https://doi.org/10.1053/j.ajkd.2021.03.007
56. Vonesh E, Tighiouart H, Ying J, et al. Mixed-effects models for slope-based endpoints in clinical trials of chronic kidney disease. *Stat Med*. 2019;38. doi:10.1002/sim.8282
57. Neuen B, Tighiouart H, Heerspink H, et al. Acute Treatment Effects on GFR in Randomized Clinical Trials of Kidney Disease Progression. *J Am Soc Nephrol*. 2021;33:ASN.2021070948. doi:10.1681/ASN.2021070948
58. Inker LA, Collier W, Greene T, et al. A meta-analysis of GFR slope as a surrogate endpoint for kidney failure. *Nat Med*. 2023;29(7):1867-1876. doi:10.1038/s41591-023-02418-0
59. Barbour SJ, Canney M, Coppo R, et al. Improving treatment decisions using personalized risk assessment from the International IgA Nephropathy Prediction Tool. *Kidney Int*. 2020;98(4):1009-1019. doi:10.1016/j.kint.2020.04.042
60. Radford MGJ, Donadio JVJ, Bergstralh EJ, Grande JP. Predicting renal outcome in IgA nephropathy. *J Am Soc Nephrol*. 1997;8(2):199-207. doi:10.1681/ASN.V82199
61. Geddes CC, Rauta V, Gronhagen-Riska C, et al. A tricontinental view of IgA nephropathy. *Nephrol Dial Transplant Off Publ Eur Dial Transpl Assoc - Eur Ren Assoc*. 2003;18(8):1541-1548. doi:10.1093/ndt/gfg207
62. Frimat L, Briançon S, Hestin D, et al. IgA nephropathy: prognostic classification of end-stage renal failure. L'Association des Néphrologues de l'Est. *Nephrol Dial Transplant Off Publ Eur Dial Transpl Assoc - Eur Ren Assoc*. 1997;12(12):2569-2575. doi:10.1093/ndt/12.12.2569

63. Lv J, Zhang H, Zhou Y, Li G, Zou W, Wang H. Natural history of immunoglobulin A nephropathy and predictive factors of prognosis: a long-term follow up of 204 cases in China. *Nephrology (Carlton)*. 2008;13(3):242-246. doi:10.1111/j.1440-1797.2007.00898.x
64. Bartosik LP, Lajoie G, Sugar L, Cattran DC. Predicting progression in IgA nephropathy. *Am J kidney Dis Off J Natl Kidney Found*. 2001;38(4):728-735. doi:10.1053/ajkd.2001.27689
65. Beukhof JR, Kardaun O, Schaafsma W, et al. Toward individual prognosis of IgA nephropathy. *Kidney Int*. 1986;29(2):549-556. doi:10.1038/ki.1986.33
66. Jongs N, Greene T, Chertow GM, et al. Effect of dapagliflozin on urinary albumin excretion in patients with chronic kidney disease with and without type 2 diabetes: a prespecified analysis from the DAPA-CKD trial. *lancet Diabetes Endocrinol*. 2021;9(11):755-766. doi:10.1016/S2213-8587(21)00243-6
67. Canney M, Barbour SJ, Zheng Y, et al. Quantifying Duration of Proteinuria Remission and Association with Clinical Outcome in IgA Nephropathy. *J Am Soc Nephrol*. 2021;32(2):436-447. doi:10.1681/ASN.2020030349
68. Le W, Liang S, Hu Y, et al. Long-term renal survival and related risk factors in patients with IgA nephropathy: results from a cohort of 1155 cases in a Chinese adult population. *Nephrol Dial Transplant*. 2012;27(4):1479-1485. doi:10.1093/ndt/gfr527
69. Coppo R, Troyanov S, Bellur S, et al. Validation of the Oxford classification of IgA nephropathy in cohorts with different presentations and treatments. *Kidney Int*. 2014;86(4):828-836. doi:10.1038/ki.2014.63
70. Donadio J V, Bergstralh EJ, Grande JP, Rademcher DM. Proteinuria patterns and their association with subsequent end-stage renal disease in IgA nephropathy. *Nephrol Dial Transplant Off Publ Eur Dial Transpl Assoc - Eur Ren Assoc*. 2002;17(7):1197-1203. doi:10.1093/ndt/17.7.1197
71. Woo K-T, Chan C-M, Chin YM, et al. Global evolutionary trend of the prevalence of primary glomerulonephritis over the past three decades. *Nephron Clin Pract*. 2010;116(4):c337-46. doi:10.1159/000319594
72. Yamagata K, Iseki K, Nitta K, et al. Chronic kidney disease perspectives in Japan and the importance of urinalysis screening. *Clin Exp Nephrol*. 2008;12(1):1-8. doi:10.1007/s10157-007-0010-9
73. Kiryluk K, Li Y, Sanna-Cherchi S, et al. Geographic differences in genetic susceptibility to IgA nephropathy: GWAS replication study and geospatial risk analysis. *PLoS Genet*. 2012;8(6):e1002765. doi:10.1371/journal.pgen.1002765
74. Barbour SJ, Cattran DC, Kim SJ, et al. Individuals of Pacific Asian origin with IgA nephropathy have an increased risk of progression to end-stage renal disease. *Kidney Int*. 2013;84(5):1017-1024. doi:10.1038/ki.2013.210
75. Gale DP, Molyneux K, Wimbury D, et al. Galactosylation of IgA1 Is Associated with Common Variation in C1GALT1. *J Am Soc Nephrol*. 2017;28(7):2158-2166. doi:10.1681/ASN.2016091043
76. Yeo SC, Goh SM, Barratt J. Is immunoglobulin A nephropathy different in different ethnic populations? *Nephrology (Carlton)*. 2019;24(9):885-895. doi:10.1111/nep.13592
77. Haas M. Histologic subclassification of IgA nephropathy: a clinicopathologic study of 244 cases. *Am J kidney Dis Off J Natl Kidney Found*. 1997;29(6):829-842. doi:10.1016/s0272-6386(97)90456-x

78. Lee SM, Rao VM, Franklin WA, et al. IgA nephropathy: morphologic predictors of progressive renal disease. *Hum Pathol*. 1982;13(4):314-322. doi:10.1016/s0046-8177(82)80221-9
79. Manno C, Strippoli GFM, D'Altri C, Torres D, Rossini M, Schena FP. A novel simpler histological classification for renal survival in IgA nephropathy: a retrospective study. *Am J kidney Dis Off J Natl Kidney Found*. 2007;49(6):763-775. doi:10.1053/j.ajkd.2007.03.013
80. Roberts ISD, Cook HT, Troyanov S, et al. The Oxford classification of IgA nephropathy: pathology definitions, correlations, and reproducibility. *Kidney Int*. 2009;76(5):546-556. doi:10.1038/ki.2009.168
81. Cattran DC, Coppo R, Cook HT, et al. The Oxford classification of IgA nephropathy: rationale, clinicopathological correlations, and classification. *Kidney Int*. 2009;76(5):534-545. doi:10.1038/ki.2009.243
82. Tesar V, Troyanov S, Bellur S, et al. Corticosteroids in IgA Nephropathy: A Retrospective Analysis from the VALIGA Study. *J Am Soc Nephrol*. 2015;26(9):2248-2258. doi:10.1681/ASN.2014070697
83. Herzenberg AM, Fogo AB, Reich HN, et al. Validation of the Oxford classification of IgA nephropathy. *Kidney Int*. 2011;80(3):310-317. doi:10.1038/ki.2011.126
84. Shi S-F, Wang S-X, Jiang L, et al. Pathologic predictors of renal outcome and therapeutic efficacy in IgA nephropathy: validation of the oxford classification. *Clin J Am Soc Nephrol*. 2011;6(9):2175-2184. doi:10.2215/CJN.11521210
85. Haas M, Verhave JC, Liu Z-H, et al. A Multicenter Study of the Predictive Value of Crescents in IgA Nephropathy. *J Am Soc Nephrol*. 2017;28(2):691-701. doi:10.1681/ASN.2016040433
86. Katafuchi R, Ninomiya T, Nagata M, Mitsuiki K, Hirakata H. Validation study of oxford classification of IgA nephropathy: the significance of extracapillary proliferation. *Clin J Am Soc Nephrol*. 2011;6(12):2806-2813. doi:10.2215/CJN.02890311
87. Trimarchi H, Barratt J, Cattran DC, et al. Oxford Classification of IgA nephropathy 2016: an update from the IgA Nephropathy Classification Working Group. *Kidney Int*. 2017;91(5):1014-1021. doi:10.1016/j.kint.2017.02.003
88. Howie AJ, Lalayiannis AD. Systematic Review of the Oxford Classification of IgA Nephropathy: Reproducibility and Prognostic Value. *Kidney360*. 2023;4(8):1103-1111. doi:10.34067/KID.0000000000000195
89. Xie D, Zhao H, Xu X, et al. Intensity of Macrophage Infiltration in Glomeruli Predicts Response to Immunosuppressive Therapy in Patients with IgA Nephropathy. *J Am Soc Nephrol*. 2021;32(12):3187-3196. doi:10.1681/ASN.2021060815
90. Rovin BH, Barratt J, Heerspink HJL, et al. Efficacy and safety of sparsentan versus irbesartan in patients with IgA nephropathy (PROTECT): 2-year results from a randomised, active-controlled, phase 3 trial. *Lancet*. 2023. doi:https://doi.org/10.1016/S0140-6736(23)02302-4
91. Smith M, Lix LM, Azimaee M, et al. Assessing the quality of administrative data for research: A framework from the manitoba centre for health policy. *J Am Med Informatics Assoc*. 2018;25(3):224-229. doi:10.1093/jamia/ocx078
92. Inker LA, Eneanya ND, Coresh J, et al. New Creatinine- and Cystatin C-Based Equations to Estimate GFR without Race. *N Engl J Med*. 2021;385(19):1737-1749. doi:10.1056/NEJMoa2102953

93. Hogan MC, Reich HN, Nelson PJ, et al. The relatively poor correlation between random and 24-hour urine protein excretion in patients with biopsy-proven glomerular diseases. *Kidney Int*. 2016;90(5):1080-1089. doi:10.1016/j.kint.2016.06.020
94. Smith ER, Cai MMX, McMahon LP, Wright DA, Holt SG. The value of simultaneous measurements of urinary albumin and total protein in proteinuric patients. *Nephrol Dial Transplant Off Publ Eur Dial Transpl Assoc - Eur Ren Assoc*. 2012;27(4):1534-1541. doi:10.1093/ndt/gfr708
95. Ohisa N, Yoshida K, Matsuki R, et al. A comparison of urinary albumin-total protein ratio to phase-contrast microscopic examination of urine sediment for differentiating glomerular and nonglomerular bleeding. *Am J kidney Dis Off J Natl Kidney Found*. 2008;52(2):235-241. doi:10.1053/j.ajkd.2008.04.014
96. Organization WH. Anatomical Therapeutic Chemical (ATC) Classification. https://www.who.int/tools/atc-ddd-toolkit/atc-classification. Accessed October 31, 2024.
97. Lix LM, Ayles J, Bartholomew S, et al. The Canadian Chronic Disease Surveillance System: A model for collaborative surveillance. *Int J Popul data Sci*. 2018;3(3):433. doi:10.23889/ijpds.v3i3.433
98. Little RJA. A Test of Missing Completely at Random for Multivariate Data with Missing Values. *J Am Stat Assoc*. 1988;83(404):1198-1202. doi:10.2307/2290157
99. White IR, Royston P, Wood AM. Multiple imputation using chained equations: Issues and guidance for practice. *Stat Med*. 2011;30(4):377-399. doi:https://doi.org/10.1002/sim.4067
100. Portet S. A primer on model selection using the Akaike Information Criterion. *Infect Dis Model*. 2020;5:111-128. doi:10.1016/j.idm.2019.12.010
101. Schwarz G. Estimating the Dimension of a Model. *Ann Stat*. 1978;6(2):461-464. http://www.jstor.org/stable/2958889.
102. Nakagawa S, Schielzeth H. A general and simple method for obtaining R2 from generalized linear mixed-effects models. *Methods Ecol Evol*. 2013;4(2):133-142. doi:https://doi.org/10.1111/j.2041-210x.2012.00261.x
103. Hodson TO. Root-mean-square error (RMSE) or mean absolute error (MAE): when to use them or not. *Geosci Model Dev*. 2022;15(14):5481-5487. doi:10.5194/gmd-15-5481-2022
104. Bland JM, Altman DG. Statistical methods for assessing agreement between two methods of clinical measurement. *Lancet (London, England)*. 1986;1(8476):307-310.
105. Collins GS, Dhiman P, Ma J, et al. Evaluation of clinical prediction models (part 1): from development to external validation. *BMJ*. 2024;384:e074819. doi:10.1136/bmj-2023-074819
106. Barnett AG, van der Pols JC, Dobson AJ. Regression to the mean: what it is and how to deal with it. *Int J Epidemiol*. 2005;34(1):215-220. doi:10.1093/ije/dyh299
107. Kiryluk K, Sanchez-Rodriguez E, Zhou X-J, et al. Genome-wide association analyses define pathogenic signaling pathways and prioritize drug targets for IgA nephropathy. *Nat Genet*. 2023;55(7):1091-1105. doi:10.1038/s41588-023-01422-x
108. Coppo R. The Gut-Renal Connection in IgA Nephropathy. *Semin Nephrol*. 2018;38(5):504-512. doi:10.1016/j.semnephrol.2018.05.020
109. Chen TJ, Skandalou E, Fritz-Wallace K, et al. Serum proteome analysis detects early molecular signatures of disease progression in IgA nephropathy. *Clin Kidney J*. 2025:sfaf344. doi:10.1093/ckj/sfaf344
110. Yland JJ, Wesselink AK, Lash TL, Fox MP. Misconceptions About the Direction of Bias From Nondifferential Misclassification. *Am J Epidemiol*. 2022;191(8):1485-1495.

doi:10.1093/aje/kwac035
111. McQuarrie EP, Mackinnon B, McNeice V, Fox JG, Geddes CC. The incidence of biopsy-proven IgA nephropathy is associated with multiple socioeconomic deprivation. *Kidney Int*. 2014;85(1):198-203. doi:10.1038/ki.2013.329
112. Canney M, Induruwage D, Sahota A, et al. Socioeconomic position and incidence of glomerular diseases. *Clin J Am Soc Nephrol*. 2020;15(3):367-374. doi:10.2215/CJN.08060719
113. Sisk R, Sperrin M, Peek N, van Smeden M, Martin GP. Imputation and missing indicators for handling missing data in the development and deployment of clinical prediction models: A simulation study. *Stat Methods Med Res*. 2023;32(8):1461-1477. doi:10.1177/09622802231165001
114. Efthimiou O, Seo M, Chalkou K, Debray T, Egger M, Salanti G. Developing clinical prediction models: a step-by-step guide. *BMJ*. 2024;386:e078276. doi:10.1136/bmj-2023-078276
115. Tibshirani R. Regression Shrinkage and Selection via the Lasso. *J R Stat Soc Ser B*. 1996;58(1):267-288. http://www.jstor.org/stable/2346178.
116. Robinson GK. That BLUP is a Good Thing: The Estimation of Random Effects. *Stat Sci*. 1991;6(1):15-32. doi:10.1214/ss/1177011926
117. Gregorich M, Kammer M, Heinzel A, et al. Development and Validation of a Prediction Model for Future Estimated Glomerular Filtration Rate in People With Type 2 Diabetes and Chronic Kidney Disease. *JAMA Netw open*. 2023;6(4):e231870. doi:10.1001/jamanetworkopen.2023.1870
118. Zafari Z, Sin DD, Postma DS, et al. Individualized prediction of lung-function decline in chronic obstructive pulmonary disease. *C Can Med Assoc J = J l'Association medicale Can*. 2016;188(14):1004-1011. doi:10.1503/cmaj.151483
119. Vonesh EF, Greene T, Schluchter MD. Shared parameter models for the joint analysis of longitudinal data and event times. *Stat Med*. 2006;25(1):143-163. doi:10.1002/sim.2249

Supplementary Appendix

Supplementary Figures

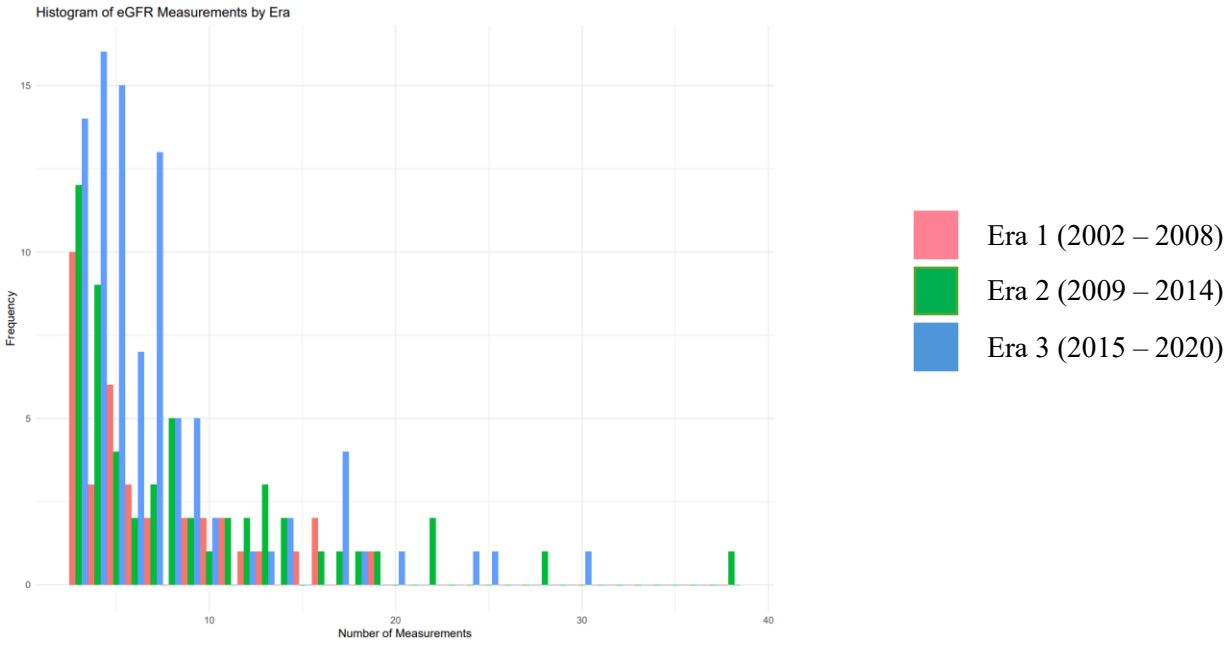

Supplementary Figure 1a. Frequency of eGFR measurements per patient, by era

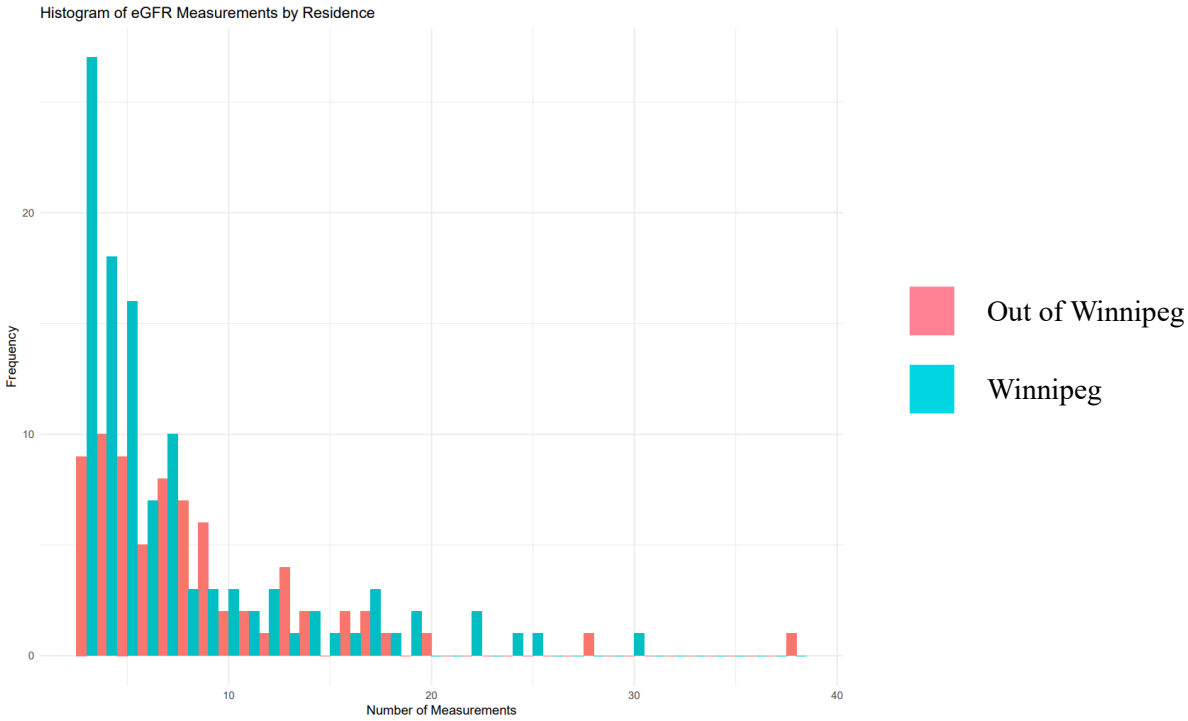

Supplementary Figure 1b. Frequency of eGFR measurements per patient, by residence location

Supplementary Tables

Supplementary Table 1. Data collected in the Manitoba Glomerular Diseases Registry

Data	Type	Possible values / Usual range of values
Personal Health Identification Number	numeric	9-digit number
Last name	text	1 or 2 names
First name	text	1 or 2 names
Date of birth	numeric	DD/MM/YYYY
Age	numeric	Up to 3-digit number
Date biopsy collected / resultreceived	numeric	DD/MM/YYYY
Diagnosis	text	variable
Cores	numeric	1-5
Total glomeruli	numeric	0-50
Sclerosed glomeruli	numeric	0-50
Glomeruli with segmental sclerosis	numeric	0-50
Glomeruli with fibrinoid necrosis	numeric	0-50
Glomeruli with cellular crescents	numeric	0-50
Glomeruli with fibrocellular crescents	numeric	0-50
Glomeruli with fibrous crescents	numeric	0-50
IFTA (interstitial fibrosis and tubular atrophy)	numeric or text	0%-100% or [mild, patchy, moderate, diffuse, significant]
Intimal fibrosis	text	no, yes, mild, moderate, severe
Vasculitis	binary	no, yes
Immunofluorescence	binary	no, yes
IgG	text	trace, 1+. 2+. 3+, +/-
IgA	text	trace, 1+. 2+. 3+, +/-
IgM	text	trace, 1+. 2+. 3+, +/-
AHIg	text	trace, 1+. 2+. 3+, +/-
C3	text	trace, 1+. 2+. 3+, +/-
C1q	text	trace, 1+. 2+. 3+, +/-
Fibrinogen	text	trace, 1+. 2+. 3+, +/-
Kappa	text	trace, 1+. 2+. 3+, +/-
Lambda	text	trace, 1+. 2+. 3+, +/-
Foot Process Effacement (FPE)	text	no, yes, mild, moderate, focal, extensive, diffuse, widespread, severe
Subepithelial deposits	binary	no, yes
Subendothelial deposits	binary	no, yes
Intramembranous deposits	binary	no, yes
Mesangial deposits	binary	no, yes
PLA2R	binary	negative, positive
Oxford M/E/S/T/C	numeric	0, 1, 2
Lupus class	roman num.	I, II, III, IV, V
Lupus AI (activity index)	numeric	0-24
Lupus CI (chronicity index)	numeric	0-12

Supplementary Table 2. List of study databases

Database	Study Years	Data Provider	Data Fields/Variables	Description
Shared Health Diagnostic Services	January 1, 2002 to December 31, 2023	Diagnostic Services, Shared Health	• Scrambled PHIN • Lab Results – Chemistry/Hematology • Date of Collection • Test Description • Test Numeric Results	Laboratory tests and results
Hospital Discharge Abstracts	January 1, 2002 to December 31, 2023	Manitoba Health, Seniors and Active Living	• Scrambled PHIN • Admission Date • Separation Date • Diagnosis Codes • Intervention Codes • Intervention Dates • Length of Stay	Hospital discharge data
Manitoba Health Insurance Registry	January 1, 2002 to December 31, 2023	Manitoba Health, Seniors and Active Living	• Scrambled PHIN • Sex • Date of Birth • Coverage Dates (start/end) • Reason for Coverage Cancellation • Postal Code • Municipality Code	Patient registry and provincial health insurance coverage dates
Medical Health Services Claims	January 1, 2002 to December 31, 2023	Manitoba Health, Seniors and Active Living	• Scrambled PHIN • Date of Service • Tariff Code • Diagnosis Code • Specialty Sub-bloc • Number of Services Provided • Physician type / specialty	Physician claims data
Drug Program Information Network	January 1, 2002 to December 31, 2023	Manitoba Health, Seniors and Active Living	• Scrambled PHIN • Date Prescription Provided • Days Supplied • DIN	Drug prescriptions

			• Dosage (Strength) • ATC Code • Drug Cost Claimed • Drug Cost Paid • Product Description • Product Name	
Manitoba Glomerular Diseases Registry	January 1, 2002 to December 31, 2021	Diagnostic Services, Shared Health	• See Supplementary Table 1	Information on all incident GN biopsies

Supplementary Table 3. Definitions of nephrology visit, dialysis, kidney transplantation, and comorbidities

Variable	Medical Health Services Claims Tariff Codes	Hospital Discharge Abstracts Diagnosis Codes
Nephrology Visit	The first code from the following list: 8595, 8550, 8540 arising from bloc 016	--
Dialysis	2 or more codes from the following list: 9798, 9799, 9801, 9802, 9805, 9806, 9807, 9814, 9819, 9820, 9821, 3792, 3790, 3793, 3794, 3800, 3801, 3803, 3804, 3804, 9610	--
Transplantation	1 tariff code or diagnosis code	
	5883	ICD-9-CM: 556 ICD-10-CA: 1PC85, 1OK85, 556
Hypertension	1 hospital diagnosis or 2 outpatient claims within 2 years	
		ICD-9-CM: 401, 402, 403, 404, 405 ICD-10-CA: I10, I11, I12, I13, I15
Diabetes	1 hospital diagnosis or 2 outpatient claims within 2 years	
		ICD-9-CM: 250 ICD-10-CA: E10, E11, E13, E14

Supplementary Table 4. Anatomical therapeutic chemical (ATC) codes for medications

Medication Type	ATC Codes
Antihypertensives (antiadrenergic agents, diuretics, beta blocking agents, and calcium channel blockers)	C02, C03, C07, C08
Angiotensin-converting enzyme inhibitor / angiotensin receptor blocker (ACEi / ARB)	C09
Statins	C10AA, C10B
Glucocorticoids	H02

Supplementary Table 5. Clinical and pathological variables included as fixed effects

Variable type	Variable	Level of Measurement	Unit	Data source
Demographics	Age	Continuous	Years	Registry
	Sex	Binary	Male-female	Registry
Clinical	Time to biopsy	Continuous	Days	[$]MHSC
Laboratory measurements	Proteinuria	Continuous	grams per day	SHDS^
	Delta-proteinuria	Continuous or categorical	Index:biopsy ratio Index-biopsy Improving/stable/worsening	SHDS
	Index eGFR*	Continuous	mL/min/1.73 m^2	SHDS
	Delta-eGFR	Continuous	Index eGFR – biopsy eGFR	SHDS
Medication prescription	Glucocorticoids	Binary	Yes/no	DPIN[#]
	RAASi[&]	Binary	Yes/no	DPIN
Comorbidities	Hypertension	Binary	Yes/no	MHSC
	Diabetes mellitus	Binary	Yes/no	MHSC
Pathological features	Oxford M	Binary	M1/M0	Registry
	Oxford E	Binary	E1/E0	Registry
	Oxford S	Binary	S1/S0	Registry
	Oxford T	Categorical	T2/T1/T0	Registry
	Oxford C	Categorical	C2/C1/C0	Registry

*eGFR, estimated glomerular filtration rate
[&]RAASi, renin-angiotensin aldosterone system inhibitors
[$]MHSC, Manitoba Health Services Claims
^SHDS, Shared Health Diagnostic Services
[#]DPIN, Drug Program Information Network

Supplementary Table 6. Definition and scoring of the Oxford classification system in IgA nephropathy

Pathological variable	Definition	Scoring system
Mesangial hypercellularity	>4 mesangial cells in any mesangial area of a glomerulus	M0 (<50% of glomeruli showing mesangial hypercellularity M1 (>50% of glomeruli showing mesangial hypercellularity
Endocapillary hypercellularity	Hypercellularity due to increased number of cells within capillary lumina	E0 (no endocapillary hypercellularity) E1 (any glomeruli showing endocapillary hypercellularity)
Segmental sclerosis	Adhesion or sclerosis in part but not the whole glomerular tuft	S0 (absent) S1 (present in any glomeruli)
Tubular atrophy and interstitial fibrosis	Estimated percentage of cortical area showing tubular atrophy or interstitial fibrosis, whichever is greater	T0 0-25% T1 26-50% T2 >50%
Cellular/fibrocellular crescents	Cellular or fibrocellular crescents	C0 (absent) C1 (present in at least one glomerulus) C2 (present in >25% of glomeruli)

Supplementary Table 7. Summary of candidate models for eGFR slope and their covariates

Model	Candidate covariates	Interaction terms (with time)
Parsimonious model	Index eGFR Index Proteinuria Age Sex	Index eGFR Index Proteinuria
Treatment and trajectory model	Model A and Delta-proteinuria Delta-eGFR Time to biopsy Treatment with RAASi Treatment with steroids	Index eGFR Index Proteinuria Treatment with RAASi Treatment with steroids
Full clinical model	Model B and Hypertension Diabetes	Index eGFR Index Proteinuria Treatment with RAASi Treatment with steroids
Full clinicopathologic model	Model C and Oxford S Oxford T Oxford C	Index eGFR Index Proteinuria Treatment with RAASi Treatment with steroids Oxford S Oxford T Oxford C

Supplementary Table 8. Baseline characteristics of patients with IgA nephropathy by era (complete cases)

Characteristic	Overall (n = 137)[1]	2002 to 2008 (n = 27)[1]	2009 to 2014 (n = 46)[1]	2015 to 2020 (n = 64)[1]
Age at cohort entry (years)	41 (30, 54)	35 (25, 47)	44 (36, 57)	41 (31, 56)
Sex				
Male	81 (59%)	18 (67%)	26 (57%)	37 (58%)
Female	56 (41%)	9 (33%)	20 (43%)	27 (42%)
Location of Residence				
Winnipeg	80 (58%)	21 (78%)	29 (63%)	30 (47%)
Outside of Winnipeg	57 (41%)	6 (22%)	17 (37%)	34 (53%)
SES Quintile				
1	46 (34%)	7 (26%)	15 (33%)	24 (38%)
2	29 (21%)	s	10 (22%)	15 (23%)
3	22 (16%)	s	s	12 (19%)
4	28 (20%)	10 (37%)	11 (24%)	7 (11%)
5	12 (8.8%)	s	s	6 (9.4%)
eGFR at cohort entry (mL/min/1.73 m^2)	59 (36, 88)	69 (35, 101)	53 (33, 80)	58 (39, 88)
Proteinuria at cohort entry (g/day)	1.77 (1.09, 2.96)	1.85 (1.23, 3.08)	1.74 (1.05, 3.56)	1.81 (1.20, 2.61)
Index eGFR (mL/min/1.73 m^2)	53 (32, 82)	69 (40, 91)	45 (27, 72)	58 (33, 84)
Index proteinuria (g/day)	1.15 (0.55, 2.28)	0.69 (0.23, 2.24)	1.11 (0.51, 2.16)	1.64 (0.60, 2.56)
Nephrology consult to biopsy (days)	40 (6, 171)	25 (-60, 119)	52 (-7, 262)	36 (14, 154)
Diabetes	22 (16%)	s	8 (17%)	12 (19%)
Hypertension	59 (43%)	6 (22%)	21 (46%)	32 (50%)
RAASi treatment	122 (89%)	26 (96%)	42 (91%)	54 (84%)
Glucocorticoid treatment	41 (30%)	10 (37%)	16 (35%)	15 (23%)
Oxford S				
0	39 (28%)	9 (33%)	16 (35%)	14 (22%)
1	98 (72%)	18 (67%)	30 (65%)	50 (78%)
Oxford T				
0	69 (50%)	18 (67%)	21 (46%)	30 (47%)
1	47 (34%)	s	21 (46%)	17 (27%)
2	21 (15%)	s	4 (8.7%)	17 (27%)
Oxford C (binary)				
0	95 (69%)	16 (59%)	32 (70%)	47 (73%)
1	42 (31%)	11 (41%)	14 (30%)	17 (27%)
Kidney failure status				
No kidney failure	116 (85%)	21 (78%)	39 (85%)	56 (87%)
Kidney failure	21 (15%)	6 (22%)	7 (15%)	8 (13%)
Vital status				
Alive	119 (87%)	s	39 (85%)	57 (89%)
Dead	18 (13%)	s	7 (15%)	7 (11%)

Follow up time (years)	8.3 (5.2, 12.8)	15.7 (14.9, 16.7)	11.1 (9.7, 13.0)	5.7 (4.0, 7.5)

Results are reported as median (Q1, Q3) for continuous variables, and n (%) for categorical variables
SES, socioeconomic status; eGFR, estimated glomerular filtration rate; RAASi, renin-angiotensin-aldosterone system inhibitor; s, suppressed (cell size 5 or less)

Supplementary Table 9. Baseline characteristics of patients with IgA nephropathy by sex (complete cases)

Characteristic	Male (n = 81)	Female (n = 56)
Age at cohort entry (years)	42 (32, 56)	38 (29, 51)
Location of Residence		
Winnipeg	47 (58%)	33 (59%)
Outside of Winnipeg	34 (42%)	23 (41%)
SES Quintile		
1	24 (30%)	22 (39%)
2	16 (20%)	13 (23%)
3	15 (19%)	s
4	17 (21%)	11 (20%)
5	9 (11%)	s
eGFR at cohort entry (mL/min/1.73 m^2)	58 (39, 80)	60 (36, 100)
Proteinuria at cohort entry (g/day)	1.68 (1.03, 2.95)	1.92 (1.34, 3.32)
Index eGFR (mL/min/1.73 m^2)	50 (31, 79)	56 (35, 88)
Index proteinuria (g/day)	1.08 (0.50, 2.02)	1.56 (0.60, 2.90)
Nephrology consult to biopsy (days)	35 (3, 154)	51 (9, 180)
Diabetes	10 (12%)	12 (21%)
Hypertension	35 (43%)	24 (43%)
RAASi treatment	71 (88%)	51 (91%)
Glucocorticoid treatment	22 (27%)	19 (34%)
Oxford S		
0	23 (28%)	16 (29%)
1	58 (72%)	40 (71%)
Oxford T		
0	34 (42%)	35 (63%)
1	33 (41%)	14 (25%)
2	14 (17%)	7 (13%)
Oxford C (binary)		
0	57 (70%)	38 (68%)
1	24 (30%)	18 (32%)
Kidney failure status		
No kidney failure	67 (83%)	49 (87%)
Kidney failure	14 (17%)	7 (13%)
Vital status		
Alive	68 (84%)	51 (91%)
Dead	13 (16%)	5 (8.9%)
Follow up time (years)	8.2 (4.9, 13.9)	8.4 (5.8, 11.9)

Results are reported as median (Q1, Q3) for continuous variables, and n (%) for categorical variables
SES, socioeconomic status; eGFR, estimated glomerular filtration rate; RAASi, renin-angiotensin-aldosterone system inhibitor; s, suppressed (cell size 5 or less)

Supplementary Table 10. Baseline characteristics of patients with IgA nephropathy by kidney failure status over follow up (complete cases)

Characteristic	No kidney failure (n = 116)	Kidney failure (n = 21)
Age at cohort entry (years)	41 (30, 56)	39 (32, 47)
Sex		
Male	67 (58%)	14 (67%)
Female	49 (42%)	7 (33%)
Location of Residence		
Winnipeg	68 (59%)	12 (57%)
Outside of Winnipeg	48 (41%)	9 (43%)
SES Quintile		
1	35 (30%)	s
2	27 (23%)	s
3	18 (16%)	s
4	25 (22%)	s
5	11 (9.5%)	s
eGFR at cohort entry (mL/min/1.73 m^2)	63 (41, 91)	36 (23, 47)
Proteinuria at cohort entry (g/day)	1.74 (1.07, 2.61)	2.50 (1.33, 3.84)
Index eGFR (mL/min/1.73 m^2)	60 (40, 86)	17 (11, 27)
Index proteinuria (g/day)	0.92 (0.46, 1.86)	2.67 (2.18, 3.38)
Nephrology consult to biopsy (days)	41 (8, 148)	22 (-60, 287)
Diabetes	20 (17%)	s
Hypertension	49 (42%)	10 (48%)
RAASi treatment	106 (91%)	16 (76%)
Glucocorticoid treatment	33 (28%)	8 (38%)
Oxford S		
0	37 (32%)	s
1	79 (68%)	s
Oxford T		
0	64 (55%)	s
1	37 (32%)	10 (48%)
2	15 (13%)	s
Oxford C (binary)		
0	84 (72%)	11 (52%)
1	32 (28%)	10 (48%)
Vital status		
Alive	104 (90%)	15 (71%)
Dead	12 (10%)	6 (29%)
Follow up time (years)	8.3 (5.1, 12.6)	8.3 (5.8, 14.9)

Results are reported as median (Q1, Q3) for continuous variables, and n (%) for categorical variables
SES, socioeconomic status; eGFR, estimated glomerular filtration rate; RAASi, renin-angiotensin-aldosterone system inhibitor; s, suppressed (cell size 5 or less)

Supplementary Table 11. Baseline characteristics of patients with IgA nephropathy by CKD stage at cohort entry (complete cases)

Characteristic	CKD 1 (n = 37)	CKD 2 (n = 44)	CKD 3 (n = 60)	CKD 4 (n = 22)
Age at cohort entry (years)	29 (23, 37)	41 (30, 48)	45 (37, 55)	57 (43, 64)
Sex				
Male	16 (43%)	30 (68%)	37 (62%)	12 (55%)
Female	21 (57%)	14 (32%)	23 (38%)	10 (45%)
Location of Residence				
Winnipeg	23 (62%)	25 (57%)	37 (62%)	12 (55%)
Outside of Winnipeg	14 (38%)	19 (43%)	23 (38%)	10 (45%)
SES Quintile				
1	16 (43%)	13 (30%)	18 (30%)	9 (41%)
2	9 (24%)	10 (23%)	9 (15%)	s
3	s	10 (23%)	12 (20%)	s
4	s	s	11 (18%)	s
5	s	s	10 (17%)	s
eGFR at cohort entry (mL/min/1.73 m^2)	108 (100, 116)	76 (65, 82)	44 (35, 48)	23 (21, 26)
Proteinuria at cohort entry (g/day)	1.86 (0.97, 2.41)	1.66 (1.02, 2.31)	1.75 (1.08, 3.09)	1.61 (1.16, 3.69)
Index eGFR (mL/min/1.73 m^2)	108 (87, 117)	67 (60, 74)	38 (29, 50)	21 (14, 35)
Index proteinuria (g/day)	1.06 (0.50, 2.22)	1.49 (0.66, 2.05)	1.48 (0.63, 2.44)	0.55 (0.38, 2.20)
Nephrology consult to biopsy (days)	98 (27, 354)	89 (15, 247)	41 (1, 162)	23 (6, 119)
Diabetes	s	7 (16%)	15 (25%)	s
Hypertension	10 (27%)	15 (34%)	36 (60%)	16 (73%)
RAASi treatment	33 (89%)	40 (91%)	57 (95%)	15 (68%)
Glucocorticoid treatment	9 (24%)	9 (20%)	14 (23%)	11 (50%)
Oxford S				
0	7 (19%)	13 (30%)	16 (27%)	s
1	30 (81%)	31 (70%)	44 (73%)	s
Oxford T				
0	s	s	16 (27%)	6 (27%)
1	s	12 (30%)	31 (52%)	7 (32%)
2	s	s	13 (22%)	9 (41%)
Oxford C (binary)				
0	27 (73%)	34 (77%)	45 (75%)	15 (68%)
1	10 (27%)	10 (23%)	15 (25%)	7 (32%)
Kidney failure status				
No kidney failure	36 (97%)	s	44 (73%)	12 (55%)
Kidney failure	1 (2.7%)	s	16 (27%)	10 (45%)
Vital status				
Alive	s	s	53 (88%)	14 (64%)
Dead	s	s	7 (12%)	8 (36%)

Follow up time (years)	8.4 (6.2, 13.6)	7.8 (4.7, 10.8)	7.3 (4.9, 10.7)	8.1 (4.0, 12.0)

Results are reported as median (Q1, Q3) for continuous variables, and n (%) for categorical variables
SES, socioeconomic status; eGFR, estimated glomerular filtration rate; RAASi, renin-angiotensin-aldosterone system inhibitor; s, suppressed (cell size 5 or less)

Supplementary Table 12. Baseline characteristics of patients with IgA nephropathy by location of residence at cohort entry (complete cases)

Characteristic	Out of Winnipeg (n = 73)	Winnipeg (n = 108)
Age at cohort entry (years)	41 (31, 58)	42 (31, 52)
Sex		
Male	43 (59%)	58 (54%)
Female	30 (41%)	50 (46%)
SES Quintile		
1	32 (44%)	30 (28%)
2	13 (18%)	23 (21%)
3	9 (12%)	21 (19%)
4	9 (12%)	27 (25%)
5	10 (14%)	7 (6.5%)
eGFR at cohort entry (mL/min/1.73 m^2)	58 (31, 84)	58 (37, 87)
Proteinuria at cohort entry (g/day)	1.62 (1.03, 2.86)	1.76 (1.10, 2.95)
Index eGFR (mL/min/1.73 m^2)	54 (31, 82)	50 (31, 81)
Index proteinuria (g/day)	1.15 (0.50, 2.02)	1.23 (0.55, 2.44)
Nephrology consult to biopsy (days)	50 (8, 255)	48 (8, 191)
Diabetes	12 (16%)	19 (18%)
Hypertension	34 (47%)	49 (45%)
RAASi treatment	62 (85%)	98 (91%)
Glucocorticoid treatment	18 (25%)	28 (26%)
Oxford S		
0	16 (22%)	34 (31%)
1	57 (78%)	74 (69%)
Oxford T		
0	37 (51%)	57 (53%)
1	21 (29%)	36 (33%)
2	15 (21%)	15 (14%)
Oxford C (binary)		
0	52 (71%)	80 (74%)
1	21 (29%)	28 (26%)
Kidney failure status		
No kidney failure	60 (82%)	88 (81%)
Kidney failure	13 (18%)	20 (19%)
Vital status		
Alive	58 (79%)	97 (90%)
Dead	15 (21%)	11 (10%)
Follow up time (years)	7.4 (4.5, 9.9)	9.1 (5.7, 13.8)

Results are reported as median (Q1, Q3) for continuous variables, and n (%) for categorical variables
SES, socioeconomic status; eGFR, estimated glomerular filtration rate; RAASi, renin-angiotensin-aldosterone system inhibitor; s, suppressed (cell size 5 or less)

Supplementary Table 13. Baseline characteristics of patients with IgA nephropathy by SES quintile at cohort entry (complete cases)

Characteristic	1 (n = 62)	2 (n = 36)	3 (n = 30)	4 (n = 36)	5 (n = 17)
Age at cohort entry (years)	39 (29, 52)	44 (32, 58)	42 (34, 54)	46 (33, 54)	39 (29, 57)
Sex					
Male	29 (47%)	18 (50%)	19 (63%)	22 (61%)	s
Female	33 (53%)	18 (50%)	11 (37%)	14 (39%)	s
Location of Residence					
Winnipeg	32 (52%)	13 (36%)	9 (30%)	9 (25%)	10 (59%)
Outside of Winnipeg	30 (48%)	23 (64%)	21 (70%)	27 (75%)	7 (41%)
eGFR at cohort entry (mL/min/1.73 m^2)	59 (31, 91)	66 (43, 91)	58 (45, 80)	47 (30, 79)	43 (33, 62)
Proteinuria at cohort entry (g/day)	1.92 (1.17, 3.32)	1.84 (1.10, 2.63)	1.57 (1.06, 2.26)	1.75 (0.87, 4.39)	1.48 (0.97, 1.95)
Index eGFR (mL/min/1.73 m^2)	52 (25, 86)	50 (32, 92)	58 (30, 71)	62 (34, 80)	41 (32, 77)
Index proteinuria (g/day)	1.48 (0.55, 2.67)	1.63 (0.74, 2.24)	1.10 (0.45, 2.09)	0.66 (0.29, 2.05)	1.36 (0.60, 1.67)
Nephrology consult to biopsy (days)	38 (9, 175)	48 (3, 421)	96 (13, 214)	52 (8, 312)	41 (-4, 171)
Diabetes	13 (21%)	7 (19%)	15 (25%)	s	s
Hypertension	32 (52%)	13 (36%)	15 (50%)	15 (42%)	8 (47%)
RAASi treatment	51 (82%)	32 (89%)	26 (87%)	35 (97%)	16 (94%)
Glucocorticoid treatment	18 (29%)	7 (19%)	s	12 (33%)	s
Oxford S					
0	15 (24%)	15 (42%)	8 (27%)	9 (25%)	s
1	47 (76%)	21 (58%)	22 (73%)	27 (75%)	s
Oxford T					
0	34 (55%)	21 (58%)	16 (53%)	18 (50%)	s
1	14 (23%)	s	s	s	s
2	14 (23%)	s	s	s	s
Oxford C (binary)					
0	47 (76%)	25 (69%)	21 (70%)	24 (67%)	s
1	15 (24%)	11 (31%)	9 (30%)	12 (33%)	s
Kidney failure status					
No kidney failure	45 (73%)	s	24 (80%)	s	s
Kidney failure	17 (27%)	s	6 (20%)	s	s
Vital status					
Alive	52 (84%)	29 (81%)	s	s	s
Dead	10 (16%)	7 (19%)	s	s	s
Follow up time (years)	7.6 (5.2, 10.6)	7.8 (4.4, 11.2)	8.0 (5.7, 13.9)	11.0 (5.5, 15.4)	8.4 (5.7, 12.7)

Results are reported as median (Q1, Q3) for continuous variables, and n (%) for categorical variables
SES, socioeconomic status; eGFR, estimated glomerular filtration rate; RAASi, renin-angiotensin-aldosterone system inhibitor; s, suppressed (cell size 5 or less)

Supplementary Table 14. Baseline characteristics of patients with IgA nephropathy by number of eGFR measurements per patient

Characteristic	≥3 Measurements (n = 181)[1]	2 Measurements (n = 60)[1]
Age at cohort entry (years)	41 (31, 54)	44 (34, 52)
Sex		
Male	101 (56%)	37 (62%)
Female	80 (44%)	23 (38%)
Location of Residence		
Winnipeg	108 (60%)	41 (68%)
Outside of Winnipeg	73 (40%)	19 (32%)
SES Quintile		
1	62 (34%)	26 (43%)
2	36 (20%)	11 (18%)
3	30 (17%)	7 (12%)
4	36 (20%)	8 (13%)
5	17 (9.4%)	8 (13%)
eGFR at cohort entry (mL/min/1.73 m^2)	58 (35, 86)	48 (32, 71)
Missing	13 (7.2%)	7 (12%)
Proteinuria at cohort entry (g/day)	1.73 (1.06, 2.95)	1.70 (0.88, 2.71)
Missing	14 (7.7 %)	9 (15%)
Index eGFR (mL/min/1.73 m^2)	51 (31, 81)	40 (20, 82)
Missing	26 (14%)	27 (45%)
Index proteinuria (g/day)	1.19 (0.53, 2.27)	0.83 (0.37, 1.57)
Missing	33 (18%)	16 (27%)
Nephrology consult to biopsy (days)	49 (8, 210)	51 (13, 382)
Diabetes	31 (17%)	9 (15%)
Hypertension	83 (46%)	31 (52%)
RAASi treatment	160 (88%)	46 (77%)
Glucocorticoid treatment	46 (25%)	8 (13%)
Oxford S		
0	50 (28%)	26 (43%)
1	131 (72%)	34 (57%)
Oxford T		
0	94 (52%)	32 (53%)
1	57 (31%)	9 (15%)
2	30 (17%)	19 (32%)
Oxford C (binary)		
0	132 (73%)	51 (85%)
1	49 (27%)	9 (15%)
Kidney failure status		
No kidney failure	148 (82%)	48 (80%)
Kidney failure	33 (18%)	12 (20%)
Vital status		
Alive	155 (86%)	54 (90%)
Dead	26 (14%)	6 (10%)
Follow up time (years)	8.2 (5.2, 12.6)	7.1 (4.0, 10.6)

Results are reported as median (Q1, Q3) for continuous variables, and n (%) for categorical variables

SES, socioeconomic status; eGFR, estimated glomerular filtration rate; RAASi, renin-angiotensin-aldosterone system inhibitor; s, suppressed (cell size 5 or less)